UTILIZING *C. ELEGANS* AS A NEUROLOGICAL MODEL TO CHARACTERIZE KCNL-2, AN SK CHANNEL HOMOLOGUE

by

Cavita Kitty Chotoo

BA, Hood College, 2005

Submitted to the Graduate Faculty of

School of Medicine in partial fulfillment

of the requirements for the degree of

Doctor of Philosophy

University of Pittsburgh

2013

UNIVERSITY OF PITTSBURGH

SCHOOL OF MEDICINE

This thesis was presented

by

Cavita Kitty Chotoo

It was defended on

March 26, 2013

and approved by

Peter Drain, Ph.D., Associate Professor, Cell Biology

Alfred L. Fisher, M.D., Ph.D., Assistant Professor, Division of Geriatric Medicine

Thomas Kleyman, M.D., Professor, Department of Medicine, Renal-Electrolyte Division

Committee Chair: Yang Hong, Ph.D., Assistant Professor, Cell Biology

Dissertation Advisor: Daniel C. Devor, Ph.D., Professor, Cell Biology

UTILIZING *C. ELEGANS* AS A NEUROLOGICAL MODEL TO CHARACTERIZE KCNL-2, AN SK CHANNEL HOMOLOGUE

Cavita Kitty Chotoo, BA, PhD

University of Pittsburgh, 2013

In the mammalian nervous system, SK channels function to regulate neuronal excitability through the generation of a component of the afterhyperpolarization that follows action potentials. In humans, irregular action potential firing frequency underlies diseases such as ataxia, epilepsy, schizophrenia and Parkinson's disease. Mouse models have been used to define the role of SK channels in diseases of the CNS, but the anatomical complexity of the mammalian nervous system and the existence of numerous redundant mechanisms to compensate for the loss of any protein limit the study of SK channels in this system. I therefore sought to characterize an SK channel homologue, KCNL-2, in *C. elegans*, a genetically tractable system in which the lineage of individual neurons have been mapped from their early developmental stages. KCNL-2 shares ~35% identity with the human SK2 and SK3 channels, with the greatest degree of conservation occurring in the six transmembrane domains, the pore motif and the calmodulin binding domain. The KCNL-2 gene was amplified from the WRM063DE08 fosmid and was fused to GFP at the amino and carboxy termini. Widefield and confocal fluorescence imaging of transgenic animals that expressed these constructs showed that KCNL-2 localizes to neurons of the nerve ring, pharyngeal nervous system, ventral nerve cord, dorsal cord, processes innervating the vulva, the ventral type-C neurons, mechanosensory neurons and in the lumbar ganglia. The complexity of the KCNL-2 gene was also demonstrated as the isoforms of KCNL-2 are differentially expressed due to varying promoter regions. Through phenotypic analysis of a

KCNL-2 null strain and of transgenic lines that overexpress the channel, I demonstrated that KCNL-2 plays a role in the regulation of the rate of egg-laying. The KCNL-2 null strain was found to be mildly egg-laying defective while the transgenic lines that overexpress KCNL-2 showed a strong hyperactive egg-laying phenotype. I propose that overexpression of KCNL-2 hyperpolarizes unidentified neurons that inhibit egg-laying and subsequently causes a hyperactive egg-laying phenotype. With the ability to drive the expression of proteins in specific neuronal circuits, I propose that *C. elegans* is a sophisticated neurological model organism to study the biochemical, biophysical and physiological functions of SK channels.

TABLE OF CONTENTS

LIST OF TABLES

LIST OF FIGURES

PREFACE

When I first came to the University of Pittsburgh I still had a lot to learn about research and my place in research. Unlike many other students, I had not determined my field of interest. I thank my advisor Dr. Daniel C. Devor for accepting me in his lab despite this lack of initial direction. With your training and the independence you inspired, I was able to develop a unique project. One of the things that I appreciate the most is that you encouraged me from the very first day to be innovative and fearless with experiments regardless of the result. Your lab was the first place where I could envision myself for years to come because it felt like a home away from home. Shortly after joining Dan's lab, I was introduced to Dr. Cliff J. Luke who was my co-mentor and who also became a friend over the years. Despite my initial awkwardness, you did everything in your power to help me blend into your lab and you were available at all times to answer questions about my project to questions about my car. With the mentorship of both Dan and Cliff, the project evolved into what it currently is.

I thank Dr. Gary A. Silverman for allowing me to be in his lab for so many years. Despite being a "visitor" in his lab, he integrated me into lab meetings, invited me to every celebration, allowed me to access the lab's confidential network and data and to carry out experiments at all hours of the day and night. At no time did I ever feel like less of a lab member. I truly had complete access to all resources of the Silverman lab. Dr. Stephen Pak has also been very kind and has always taken the time to explain scientific concepts to me and to

help me with anything that I needed. Thanks to Mark Miedel, Kyle Holden, and Nate Graf for their constant support.

I have had a phenomenal thesis committee. Thanks to Dr. Drain, Dr. Hong, Dr. Fisher, Dr. Kleyman, and my mentors Cliff and Dan who not only mentored me throughout this degree, but took it upon themselves to recommend post-doctoral positions that would allow me to grow both personally and professionally. In addition to suggesting labs for me to interview with, they secured me positions by offering and providing letters and phone calls of recommendations.

I have had the support of my dear friends Anu, Kritika and Corina throughout this entire process. We lived through this degree together and we became family throughout these years. There isn't enough space here to say how much I love and appreciate you. Our bonds will last for a lifetime. I have been blessed with a large and crazy family who knows no boundary. I have to especially thank my eldest sister Nirmala Ramadhin who stood by me for the past few years and gave me a strength and structure that I didn't even know I was missing. Your children and husband are so lucky to have you and I could not have made it without you. And last but definitely not least, I thank my mother and father who have given me my spirituality in addition to giving me their world. Because of my faith in God, I was able to remember the meaning of life and the importance of maintaining a balance between spirituality, family and a career.

1.0 INTRODUCTION

1.1 OVERVIEW

The human genome encodes 78 potassium (K^+) channels which are expressed in both excitable and non-excitable cells. K^+ channels are multimers and through structural differences in their α-subunits, association with auxiliary β-subunits and hetero-oligomerization, there are a seemingly infinite number of K^+ channels with unique biophysical properties. In excitable cells, such as neurons and muscle cells, K^+ channels serve to fine-tune their electrical properties. As a result of this ubiquitous function, mutations of various K^+ channels are associated with human channelopathies. In mammals, four KCNN genes encode the small conductance calcium-activated K^+ (SK) channels, SK1-4. In the central nervous system (CNS), the SK channels function to generate a component of the afterhyperpolarization (AHP) that follows action potentials. The AHP is the rate-limiting step in controlling pacemaker activity. Disruption of this pacemaker activity in neurons of the CNS is linked to numerous neurological disorders including episodic ataxia, epilepsy and schizophrenia. SK channel functions have been studied extensively in mammalian mouse models, but the use of these models are limited since mice have a very complex nervous system and generation of mutant strains is costly and time-consuming. Four SK channel homologues, KCNL-1, -2, -3 and -4, are encoded by the *Caenorhabditis elegans* genome. *C. elegans* is a relatively simple model organism that is

genetically and molecularly tractable due to its fully sequenced genome. In this dissertation, I provided a neurological model system to study the biological functions of the KCNL-2 protein. I investigated the tissue expression pattern of KCNL-2 and showed that this protein is expressed in the nervous system of *C. elegans*. Additionally, I investigated the phenotypes of a KCNL-2 null strain and of transgenic lines that overexpress KCNL-2 and showed that through its expression in the nervous system, KCNL-2 functions to regulate the rate of egg-laying. The entire nervous system of *C. elegans* has been mapped from the embryo to the adult stage and the functions of individual neurons are continuously being investigated. My investigation of KCNL-2 contributes to the growing literature that seeks to find parallels between conserved mechanisms that exist in the neurons of mammals and the nervous system of this invertebrate. This thesis supports the hypothesis that an SK channel homologue plays a conserved role in regulating the excitability of neurons in *C. elegans* thereby making it an ideal model system to study protein function.

1.2 IONIC REGULATION OF CELLULAR EXCITABILITY

The cell membrane potential is the driving force for transport of nutrients, ions and water into and out of cells. The maintenance of the membrane potential is essential for all cellular processes. One of the factors that determines the electrical gradient across the cell membrane is its permeability to K^+ and Na^+ which is regulated by ion channels (Hodgkin and Huxley, 1952). The intracellular concentration of K^+ is ~20 fold higher than the extracellular concentration, thereby creating an outwardly directed K^+ gradient. Another factor that determines the resting membrane potential of cells is the Na^+-K^+-ATPase pump which actively transports Na^+ out of the

cell while concomitantly moving K^+ into the cell (Koefoed-Johnsen and Ussing, 1958). Therefore, the two factors that determine the membrane potential are the cell membrane permeability to K^+ and Na^+ and the activity of the Na^+-K^+-ATPase pump.

Between 1935 and 1952, the forefathers of membrane permeability established the "ionic theory of membrane excitation" (Hille, 2001). Electrical signals such as action potentials were shown to occur as a result of currents generated by the movement of ions across the membrane. The fundamental properties of action potentials were being defined where it was first proposed that action potentials are propagated by the generation of local circuits across and along the axonal cell membrane and it was shown that the membrane conductance is increased approximately 40-fold during an action potential (Hille, 2001). An action potential could be described in two phases: an early transient inward current followed by a sustained outward current. The early transient current was identified as a Na^+ current (I_{Na}) since the reversal potential occurred at approximately +60 mV, characteristic of Na^+ ions, and the late current was identified as a K^+ current (I_K) since the reversal potential was more negative than -60 mV, characteristic of K^+ ions (Hodgkin and Huxley, 1952). Therefore, Hodgkin and Huxley identified the two ionic currents in action potentials as I_{Na} and I_K (Hodgkin and Huxley, 1952). In summary, an action potential can be described as a depolarization of the axonal membrane due to I_{Na} generated by voltage-gated sodium channels (VGSCs), followed by a repolarization and an AHP due to I_K generated by various sub-families of K^+ channels described in greater detail hereafter. The repolarization and AHP would later be shown to limit the action potential firing frequency, disruption of which causes multiple diseases of the CNS.

1.3 K^+ CHANNEL FAMILIES IN MAMMALS

K^+ channels are K^+-selective conduits in cell membranes formed by the assembly of two or more protein subunits. K^+ channels play a crucial role in maintaining the resting membrane potential of cells and through this seemingly basic task, K^+ channels function to repolarize or hyperpolarize the membrane potential of neurons after an action potential is generated. Additionally, K^+ channels have diverse functions in non-excitable cells such as regulation of insulin release from pancreatic β-cells to activation of T lymphocytes in the immune system (Ashcroft and Rorsman, 1989; Chandy et al., 1984; Ghanshani et al., 2000).

In humans, the K^+ channel gene family consists of 78 members (Wulff et al., 2009). Using a genetic approach, the *Shaker* channel in *Drosophila melanogaster* was first identified due to a leg-shaking phenotype of mutants on exposure to ether (Papazian et al., 1987). Papazian and colleagues isolated genomic DNA from the *Shaker* locus and showed that the gene encoded a voltage-dependent K^+ channel where loss-of-function mutations reduced a K^+ current in the *Drosophila* pupal muscles (Papazian et al., 1987). The *Shab*, *Shaw* and *Shal* sequences in *Drosophila*, voltage-gated K^+ channels of the same family as the *Shaker* channel, were subsequently deduced by using a *Shaker* oligonucleotide probe to identify corresponding cDNA clones (Butler et al., 1989). In both *C. elegans* and *Drosophila*, K^+ channels are structurally conserved (Littleton and Ganetzky, 2000; Wei et al., 1996). Based on the mechanisms of activation and on the primary sequence of the individual subunits that assemble to form a functional K^+ channel, these channels can be classified into four families: voltage-gated K^+ channels (K_v), calcium-activated K^+ channels (K_{Ca}), inwardly rectifying K^+ channels (K_{ir}), and leak K^+ channels (Wulff et al., 2009). Figure 1.1 shows the classification of K^+ channels according to their structure and function (Salkoff et al., 2005).

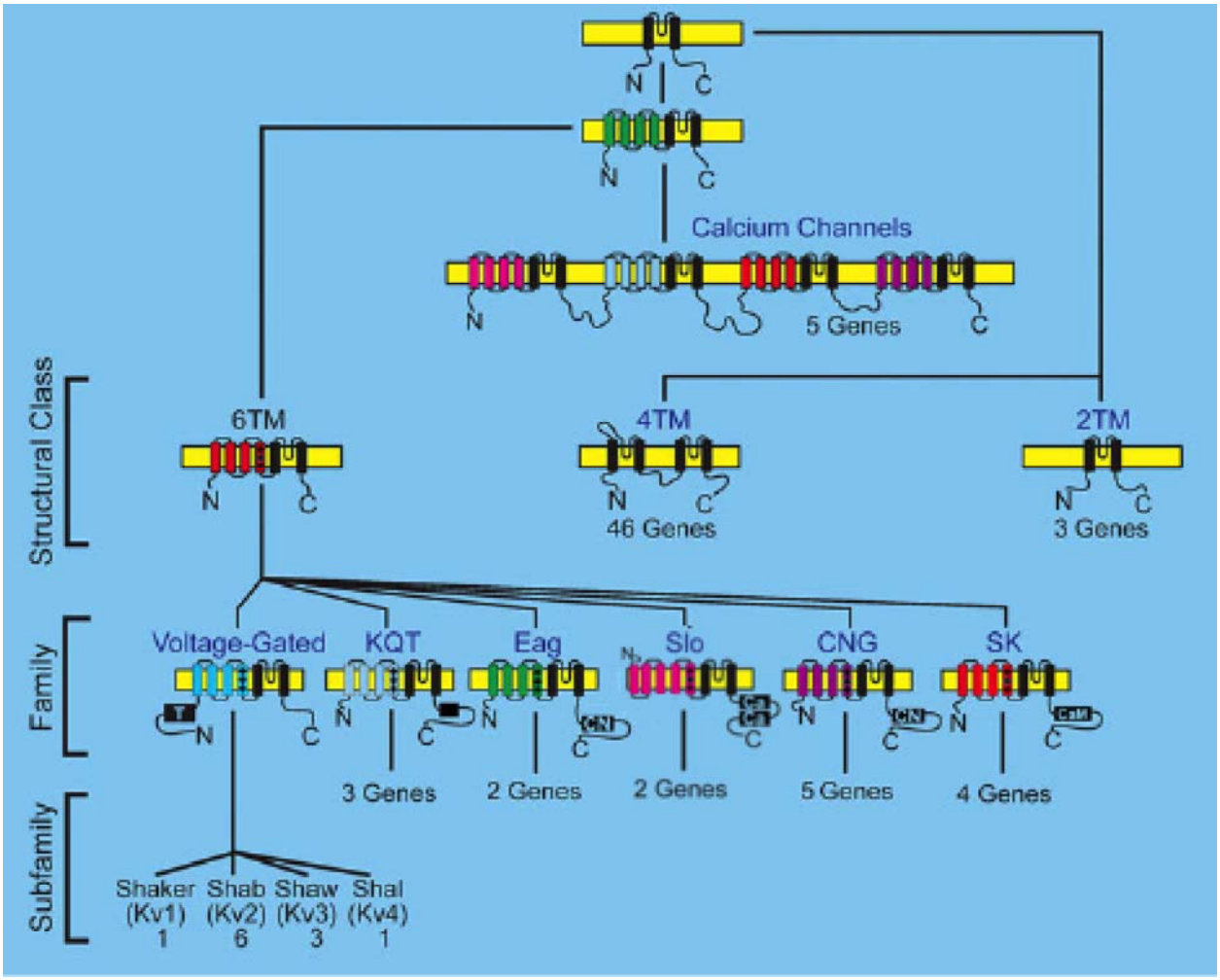

Figure 1.1. Diagram of K^+ Channel Families and Subfamilies in *C. elegans*.
The three structural classes of K^+ channels are defined by their component α-subunits, having six, four, or two transmembrane (TM) segments. The structural class of the 6TM family of K^+ channels is further divided into six conserved gene families. Reprinted with permission from Salkoff, L., Potassium channels in *C. elegans* (December 30, 2005), *Wormbook*, ed. The *C. elegans* Research Community, WormBook, doi/10.1895/wormbook.1.42.1, http://www.wormbook.org.

1.3.1 Structural Classification of K^+ Channels

The K^+ channel gene family forms a large and diverse group of ion channels. All K^+ channels have the following features in common: they have a central pore that allows the passage of K^+ ions through the channels and they undergo conformational changes that allow the channel to switch between open and closed states (Hille, 2001). As shown by Figure 1.2, K^+ channels can be broadly categorized into three structural families based on the primary sequence of the individual subunits that assemble to form the channel: 6 transmembrane domain (TMD), 4 TMD & 2 TMD-containing α subunits (Shieh et al., 2000). Among the members of the 6-TMD family are the K_v channels and the K_{Ca} channels. The subunits of the 2-pore K^+ channels have 4 TMDs and those of the K_{ir} channels have 2 TMDs. While these three families describe the general backbone of K^+ channel subunits, there are structural deviations that contribute to the unique gating properties of each channel. Additionally, K^+ channels can be homotetramers or heterotetramers, which further contributes to the unique biophysical properties of individual channels.

The pore or P-loop of K^+ channels has a signature sequence, the G(Y/F)G motif, that confers K^+-selectivity to the channel (Heginbotham et al., 1992; Heginbotham et al., 1994). Assembly of four P-loops allows for the formation of a functional K^+-selective pore. Therefore, the members of the 6-TMD and the 2-TMD families of K^+ channels are tetramers since they are composed of four α subunits with each subunit containing a single P-loop (Figure 1.2). Alternatively, the two-pore (2P) K^+ channels contain two subunits, but similarly form a central K^+-selective pore like the channels described previously (Figure 1.2). The GYG motif occurs in the S5-S6 linker of the 6-TMD subfamily or between the two transmembrane segments of the 2-TMD subfamily (Shieh et al., 2000). In the 4-TMD channels, the P-loops occur between the first

and second pairs of TMDs. As shown by Figure 1.1, the hierarchy and structure of K^+ channels is conserved across various species and more specifically in mammals and in *C. elegans* as is discussed in greater detail below.

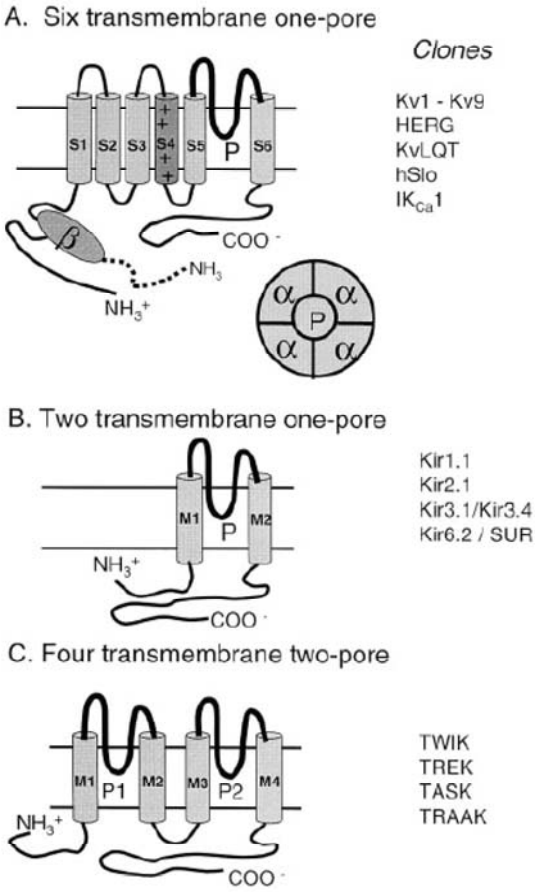

Figure 1.2. Schematic Representation of the Structural Classification of K^+ Channel Subunits.
A) Members of the K_v channels are tetramers composed of 6-TMD α subunits. Each α subunit contains a P-motif between S5 and S6 with a voltage sensor located in the S4 TMD. Some of the K_v channels associate with an auxiliary β-subunit. The inset shows the general assembly of tetrameric K^+ channels. B) The K_{ir} channels contain four 2-TMD (M1 and M2) α-subunits with a P-loop between the two TM segments. C) This represents a class of the K^+ channels that has four TMDs with two P-loops in each α subunit. Reprinted with permission from Shieh, C., *Pharmacol Rev*, vol. 52, pg. 559. Copyright 2000 by the American Society for Pharmacology and Experimental Therapeutics.

1.3.2 Voltage-Gated K^+ (K_v1-4) Channels

The α-subunits of the K_v channels contain 6 TMDs, a K^+-selective pore and intracellular amino and carboxy termini (Heinemann and Hehl, 2001). In mammals, the K_v-1, -2, -3 and -4 channels are synonymous with the *Drosophila* K^+ channel genes named the *Shaker*, *Shab*, *Shaw* and *Shal* subfamilies, respectively (Jan and Jan, 1997). These channels can be homo- or heterotetramers, but only members within a subfamily can co-assemble to form a functional channel. K_v channels are expressed in excitable cells such as neurons of the CNS, skeletal muscle, cardiac myocytes, and vascular smooth muscle cells (Wulff et al., 2009). Their expression is also prominent in other cells such as T and B cells, macrophages and pancreatic β-cells (Wulff et al., 2009).

The fourth TMD (S4) of K_v channels contains a series of positively charged amino acid residues that forms a pertinent part of the voltage-sensing domain, displacement of which produces a gating current (Papazian et al., 1991). These positively charged residues in the S4 domain initiate conformational changes upon depolarization that allows gating of the channel (Papazian et al., 1991). A membrane depolarization of only +4mV results in a large increase in conductance incurred by conformational changes of ion channels in the plasma membrane (Papazian and Bezanilla, 1997). Experimental strategies that include intragenic suppression have been used to resolve the structure of the *Shaker* K^+ channel. The voltage-sensing domain is largely composed of acidic residues in the S2 and S3 TM segments and the basic residues of S4 (Tiwari-Woodruff et al., 2000; Tiwari-Woodruff et al., 1997). Electrostatic interactions between these residues are required for protein folding and assembly and maintaining protein-stability. For example, mutation of K374 (S4), D316 (S3), or E283 (S2) leads to rapid degradation of *Shaker* channels. In the *Shaker* K^+ channel, several voltage-sensing residues of the S4 segment (R365, R368, R371) traverse the plasma membrane during voltage-dependent activation

(Aggarwal and Mackinnon, 1996). Mutation of R368 and R371 of S4 and E293 of S2 alters the gating properties of the channel. Some of these residues are conserved in Slo1 and K_{Ca} channels where their functions vary from channel gating to channel biogenesis as discussed in greater detail below (Gao et al., 2008; Ma et al., 2006).

As mentioned previously, an action potential can be described as an early transient inward current caused by the opening of VGSCs followed by a sustained outward current caused mainly by the loss of K^+ ions through voltage-dependent K^+ channels. To propagate a wave of action potentials, K^+ channels are essential to returning the polarized membrane potential to the resting membrane potential. The K_v1-4 channels are rapidly activating, delayed-rectifier channels; that is, subsequent to depolarization, there is a delay prior to channel opening (Hille, 2001). These channels are important in neurons with short action potentials since they determine the interspike interval through their high K^+ permeability (Hille, 2001). K_v channels function to regulate the excitability of unmyelinated axons, motor neurons, and vertebrate fast skeletal muscle (Hille, 2001).

The tissue expression of these channels is very diverse and mutations are associated with channelopathies. For example, K_v1.1 is expressed in the CNS and the kidney of humans where missense mutations cause episodic ataxia and primary hypomagnesaemia, respectively (Glaudemans et al., 2009; Zuberi, 1999). Mutations in K_v3.3 and K_v4.2 cause spinocerebellar ataxia and temporal lobe epilepsy, respectively (Singh et al., 2006; Waters et al., 2006). As a result, K_v channels are the subjects of many pharmacological and clinical studies as a means to treat associated diseases.

The auxiliary or β-subunits selectively associate with and modify K_v channel properties, but they are not mandatory for K_v channel function (Heinemann and Hehl, 2001). They are

expressed in both excitable and non-excitable cells and their functions may include modification of surface expression, gating or channel assembly (Deutsch, 2002). The β-subunits that associate with K_v channels belong to the $K_v\beta$(1-3), KChAP, KCNE(1-3), KCR1, KChIP(1-4), Slo β(1-4) and Frequenin subfamilies (Coetzee and Rudy, 2006). Only a specific subfamily of β-subunits can interact with a subfamily of α-subunits. Their functions are diverse and include changing the inactivation kinetics, voltage-dependence of activation, and acting as molecular chaperones of K_v channels (Coetzee and Rudy, 2006). Mutations of these auxiliary subunits can be associated with channelopathies. Mutations in KCNE1 & KCNE2 are linked to long QT syndrome, while mutations in KCNE3 are associated with hypokalemic periodic paralysis (Dias Da Silva et al., 2002; Seebohm et al., 2008; Splawski et al., 2000). $K_v\beta$1 mediates inactivation of K_v1.1-1.4 channels and disruption of $K_v\beta$1 by a regulatory protein, LGI1, is associated with temporal lobe epilepsy (Schulte et al., 2006).

1.3.3 KCNQ (K_v7) K^+ Channels

The KCNQ1-5 (K_v7.1-7.5) channels are members of the K_v7 subfamily of K^+ channels (Wulff et al., 2009). KCNQ channels are homo- or heterotetramers with each α-subunit containing six TMDs, intracellular amino and carboxy termini, and a single P-loop. In neurons, they are partly activated at the resting membrane potential and they function in its maintenance (Hille, 2001). The KCNQ channels are slow delayed rectifiers that are activated at potentials greater than -60 mV and function to repolarize the membrane potential after the generation of an action potential (Hille, 2001). The gating properties of these channels are modified by the KCNE1-3 auxiliary subunits, which have a single transmembrane domain (also known as MiRP1-3) (Wulff et al., 2009). Interaction of KCNQ1 with KCNE1 enhances current amplitudes and slows activation,

while KCNE3 assembles with KCNQ1 and leads to the formation of constitutively open channels (Jentsch, 2000). In contrast, KCNE3 markedly inhibits KCNQ4 currents (Jentsch, 2000).

KCNQ1 is expressed in cardiac muscle and is modulated by the KCNE1-3 auxiliary subunits (Wulff et al., 2009). Loss-of-function mutations in KCNQ1 or KCNE1 prolong cardiac action potentials by causing a delay in cardiac repolarization and long QT syndrome (LQTS), while its expression and function in the inner ear to secrete K^+ in the endolymph causes Jervell and Lange-Nielson syndrome when mutated (Jentsch, 2000; Wulff et al., 2009). Gain-of-function mutations have an opposing effect where the hyperactive channels shorten the cardiac action potentials and lead to disorders such as short QT syndrome and atrial fibrillation (Wulff et al., 2009). In intestinal crypt cells, KCNE3 assembles with KCNQ1 to recycle K^+ ions at the basolateral membrane, which ultimately provides the impetus for chloride secretion (Jentsch 2000). In the CNS and PNS, loss-of-function mutations in KCNQ2 and KCNQ3 underlie benign familial neonatal convulsion (Wulff et al., 2009). KCNQ4 is expressed in the auditory nervous system and in outer hair cells where a loss-of-function mutation that produces a dominant negative effect is linked to autosomal dominant deafness-2 (Wulff et al., 2009). KCNQ5 is expressed in the CNS, skeletal muscle and vascular smooth muscle cells; however there are no reported links to diseases (Wei et al., 2005; Wulff et al., 2009). KCNQ1 channels are pharmaceutical targets for the treatment of atrial arrhythmias and LQTS, while KCNQ2/3 channels are targets for the treatment of epilepsy and pain (Wulff et al., 2009). Mutations in the KCNQ channels are directly linked to the described diseases and therefore they remain a promising target for treatment of the associated diseases.

1.3.4 The Ether-A-Go-Go K^+ Channel Family

The ether-a-go-go (EAG) gene family encodes the EAG (Kv10.1, 10.2), ERG (Kv11.1-11.3) and ELK (K_v12.1-12.3) channels (Asher et al., 2010). Members of the EAG gene family belong to the 6-TMD subfamily of K^+ channels, are voltage-dependent and are delayed rectifier K^+ channels (Hille, 2001). The EAG channels were first identified in *Drosophila* as a result of a rhythmic leg-shaking phenotype displayed in *eag* mutants on exposure to ether (Warmke et al., 1991). In *eag* mutant *Drosophila* larvae, the motor nerve fibers exhibit an increase in neuronal excitability (Ganetzky and Wu, 1983). Both EAG1 and EAG2 are expressed in the CNS, but EAG2 is also expressed in other peripheral tissues where its functions remain unknown (Wulff et al., 2009). EAG1 is upregulated in tumor cell lines and inhibitors of this channel are being explored as a therapeutic target to decrease tumor cell proliferation (Wulff et al., 2009).

ERG channels are inwardly rectifying K^+ channels and human ERG (HERG) channels are expressed in the heart, CNS, endocrine cells, smooth muscle fibers of the gastrointestinal tract and lymphocytes (Schwarz and Bauer, 2004; Wulff et al., 2009). In smooth muscle cells, they function to maintain the resting membrane potential (Schwarz and Bauer, 2004). HERG channels underlie the delayed rectifier K^+ current in ventricular myocytes. Similar to KCNQ1, HERG channels function to repolarize the membrane potential after the generation of a cardiac action potential (Schwarz and Bauer, 2004; Wulff et al., 2009). HERG channels are blocked by dofetilide, an antiarrhythmic drug, which acts to prolong cardiac action potentials (Trudeau et al., 1995). However, both antiarrhythmic drugs and loss-of-function mutations of HERG can reduce cardiac repolarization and induce LQTS type 2, ventricular fibrillation and sudden death (Sanguinetti et al., 1996; Wulff et al., 2009).

1.3.5 Inward Rectifier K^+ (K_{ir}) Channels

The α-subunits of inward rectifier K^+ (K_{ir}) channels consist of 2 TMDs (M1 and M2), a P-loop, cytoplasmic amino and carboxy termini and they can be homo- or heterotetrameric channels. In some cases K_{ir} channels can associate with auxiliary subunits which modify their gating properties. K_{ir} channels received their name based on their gating properties to conduct larger inward currents at membrane potentials negative to the K^+ equilibrium potential than outward currents at more positive membrane potentials (Lu, 2004). The inward rectification is attributed in part to the fact that cations such as magnesium or polyamines block the pore of the channel on the cytoplasmic side of the cell membrane and therefore prevents the exit of K^+ ions from the cell interior (Hibino et al., 2010). Because K_{ir} channels lack the S4 voltage-sensing domain, they are insensitive to membrane voltage.

In vertebrates, the K_{ir} channels are encoded by the K_{ir}1-6 genes. The K_{ir}1.1 channel was the first member of this family of channels to be cloned and it was first referred to as the rat outer medullary K^+ (ROMK) channel (Hibino et al., 2010). The activity of K_{ir}1.1 is modulated by intracellular pH and mutations that alter the pH-sensitivity of K_{ir}1.1 cause Bartter's syndrome (Schulte et al., 1999). K_{ir}1.1 is expressed in the epithelial cells of the nephron where they facilitate the re-uptake of NaCl via the Na^+-K^+-$2Cl^-$ co-transporter and in secretion of K^+ into the urine (Hibino et al., 2010). Two other functional groups of K_{ir} channels are those that are G protein-gated (K_{ir}3.X) and those that are ATP-sensitive (K_{ir}6) (Ito et al., 1992). K_{ir} channels are expressed in cardiac myocytes, neurons, osteoclasts, endothelial cells, glial cells and epithelial cells (Hibino et al., 2010). In neurons, their key function is to maintain the resting membrane potential and hence to regulate the excitability of these cells (Hibino et al., 2010). In cardiac myocytes, they function to set the resting membrane potential, generate the plateau phase of the

action potential and induce rapid repolarization (Hibino et al., 2010). In vascular smooth muscle cells, they maintain the resting membrane potential at a negative value, which allows calcium influx, secretion of vasoactive factors and ultimately allows for vasodilation (Hibino et al., 2010). K_{ATP} channels function to inhibit insulin-release from hyperpolarized pancreatic β-cells when the blood glucose level becomes low (Hille, 2001). K_{ATP} channels associate with four sulfonylurea receptor (SUR) subunits and drugs that target these subunits to inhibit K_{ATP} channels act to enhance insulin secretion in diabetes patients (Hille, 2001).

1.3.6 KCNK K^+ Channels

There are 14 genes that encode KCNK channels in humans (Coetzee and Rudy, 2006). KCNK channels are unique in their structure since they have four TMDs and two pore motifs, each P loop being located between the first and second pairs of the TMDs. Most human KCNK channels are open rectifiers since they allow the passage of K^+ ions down its concentration gradient and are not voltage-dependent. However, both KCNK2 and KCNK3 are open rectifiers and exhibit voltage-dependence due to intracellular divalent cations that block the channel pore. KCNK channels underlie leak currents that maintain hyperpolarized membrane potentials when activated or permit depolarization when closed (Goldstein et al., 2001). KCNK2 is expressed in the CNS and KCNK3 is expressed in cardiac myocytes where they contribute to native cardiac currents and to the duration of myocardial contraction (Goldstein et al., 2001). These channels are clinically important since their currents are increased by volatile anesthetics and therefore these channels are targets for anesthetics such as halothane. Despite the studies that have contributed to our understanding of KCNK channels, much remains to be investigated about

these channels since expression of KCNK1, 7, 8 and 12 in cells do not result in the formation of functional channels (Goldstein et al., 2001).

1.3.7 Large-Conductance Calcium-Activated K^+ (BK) Channels

There are two families of calcium-activated K^+ (K_{Ca}) channels in mammals: large conductance (BK, Slo or MaxiK) and small conductance (SK/IK). This section will describe BK channels only and IK1 and SK channels will be discussed in greater detail in section 1.4. BK channels are encoded by the KCNM gene family in humans and as shown by Figure 1.3, they deviate structurally from the 6-TMD family of K^+ channels in that the amino terminus of the α-subunit is extracellular, there is an additional TM segment (S0) that precedes the S1-S6 TMDs, a pore motif between S5 and S6, and an intracellular carboxy terminus that has four hydrophobic domains (S7-S10) (Berkefeld et al., 2010). The carboxy terminus contains two regulating conductance of K^+ (RCK) domains and a signature Ca^{2+} bowl (Berkefeld et al., 2010). Similar to members of the 6-TMD K^+ channels, they are tetramers that can interact with β-subunits. BK channels have a large unitary conductance of 100-200 pS. The series of positively-charged amino acid residues in the S4 domain confers voltage-sensitivity to the channel, while the Ca^{2+} bowl determines the calcium-sensitivity of the channel (Ghatta et al., 2006). In the presence of an intracellular Ca^{2+} concentration greater than 10 μM, the voltage-dependent activation is shifted towards hyperpolarized membrane potentials (Berkefeld et al., 2010). BK channels are weakly voltage-dependent relative to K_v channels and accordingly, they do not have the full complement of voltage-sensing residues present in K_v channels (Ma et al., 2006). For example, there are five charged residues in the S4 domain of Slo1, of which only one contributes to the gating charge (Ma et al., 2006). The R213 residue in the S4 domain of Slo1, analogous to R371

in *Shaker*, acts as a voltage-sensor and contributes to gating (Ma et al., 2006). Alternatively, four of seven positively charged residues in the S4 domain of Shaker have been shown to be important as voltage-sensing residues. Interestingly, the charged residues R207 and R210, conserved with R365 and R368 in Shaker, are non-voltage sensing. Both charge neutralization and charge reversal of R207 and R210 stabilize the activated state of Slo1, supporting the participation of these residues in the formation of salt bridges that are important for assembly of the channel, however, their interacting residues remain unknown (Ma et al., 2006). Most charged residues in S1-S4 are non-voltage sensing, but they are evolutionarily conserved in K_v, BK and SK channels and function in stabilizing channel structure and function (Aggarwal and Mackinnon, 1996; Gao et al., 2008; Ma et al., 2006). These differences likely determine the disparity in voltage-sensitivity between Slo1 and K_v channels.

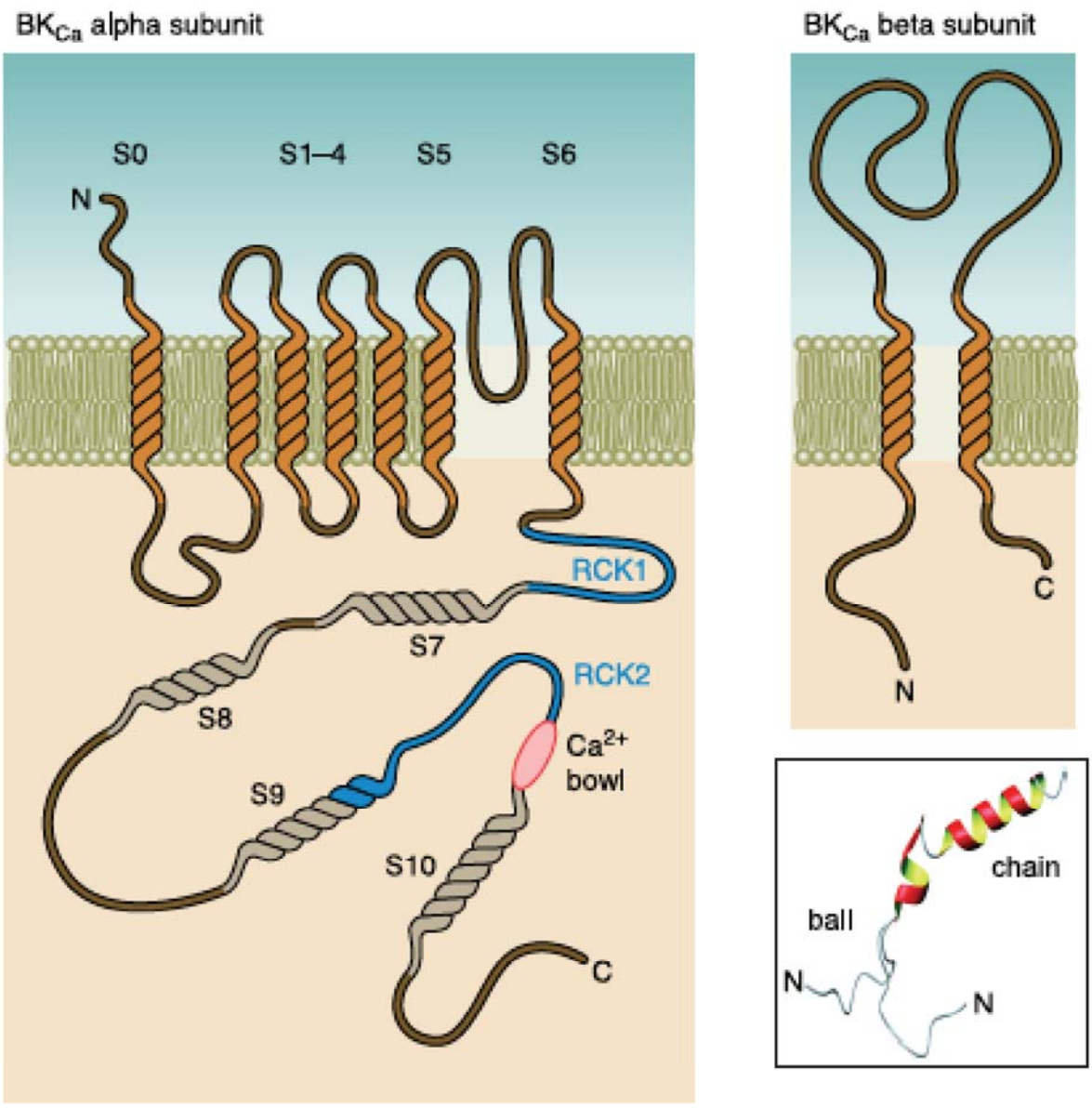

Figure 1.3. The BK β Subunits Shape the Properties of BK Channels.
A) Membrane topology of BKα and BKβ. *Inset*: Structure of the NH2-terminal "ball-and-chain" domain of BKβ2 as derived from solution NMR. Reprinted with permission from Berkefeld, H. *Physiol. Rev*, vol. 90, pg. 1440. Copyright 2010 by the American Physiological Society.

BK channels associate with the auxiliary β-subunits encoded by the KCNMB1-4 genes (Berkefeld et al., 2010). The structural topology of the β-subunits consists of intracellular amino and carboxy termini and 2 TMDs separated by an extracellular loop (Figure 1.3). The β-subunits affect channel gating by altering activation and deactivation kinetics, inactivation and permeation of the associated BK channels (Berkefeld et al., 2010). Furthermore, the β-subunits can affect trafficking and cell-surface expression of BK channels.

BK channels are expressed in many tissue types such as neurons, pancreas, cochlear hair cells, and smooth muscle cells of blood vessels, airway, uterus, gastrointestinal tract and bladder (Ghatta et al., 2006). BK channels are pertinent in maintaining vascular tone where they function to hyperpolarize vascular smooth muscle cells, which leads to closure of voltage-dependent calcium channels, a decrease in intracellular calcium concentration and vasodilation (Ghatta et al., 2006). Therefore loss of BK-signaling underlies hypertension and associated diseases. BK channel activators are being investigated as a means to treat vascular dysfunction that results in hypertension and coronary heart disease. The β1-subunit has been shown to increase the calcium-sensitivity of BK channels and drugs that target this subunit are also of clinical interest to alleviate diseases of the circulatory system. BK channels also function to maintain the urinary bladder smooth muscle tone (Ghatta et al., 2006). Loss of the hyperpolarization effect in the urinary bladder that underlies BK channel function causes overactive or excitable urinary bladder smooth muscles, which is linked to urinary incontinence. Therefore, BK channel activators are also of clinical interest for the treatment of bladder instability.

1.4 SMALL-CONDUCTANCE CALCIUM-ACTIVATED K^+ (SK) CHANNELS

The small-conductance ($K_{Ca}2.1$/SK1, $K_{Ca}2.2$/SK2, $K_{Ca}2.3$/SK3) and intermediate-conductance Ca^{2+}-activated K^+ ($K_{Ca}3.1$/SK4/IK1) channels are encoded by the KCNN gene family. Adelman and colleagues revealed the molecular identity of $K_{Ca}2.1$-2.3 by isolating full-length clones that encoded human SK1 (hSK1), rat SK2 (rSK2) and rat SK3 (rSK3), while a partial clone of rSK1 was isolated (Kohler et al., 1996). $K_{Ca}3.1$ was first identified and cloned from human placental and pancreatic libraries (Ishii et al., 1997; Joiner et al., 1997). Alignment of the peptide sequences of $K_{Ca}2.1$, $K_{Ca}2.2$, and $K_{Ca}2.3$ shows that these proteins are 60% identical, whereas $K_{Ca}3.1$ shares only ~40% identity with $K_{Ca}2.1$-2.3 (Figure 1.4). There are seven highly hydrophobic regions in the human SK channels that correspond to the six TMDs and a K^+ -selective pore region (Joiner et al., 1997). All four channels are structurally similar and the hydrophobic motifs are conserved among the channels (Joiner et al., 1997; Kohler et al., 1996).

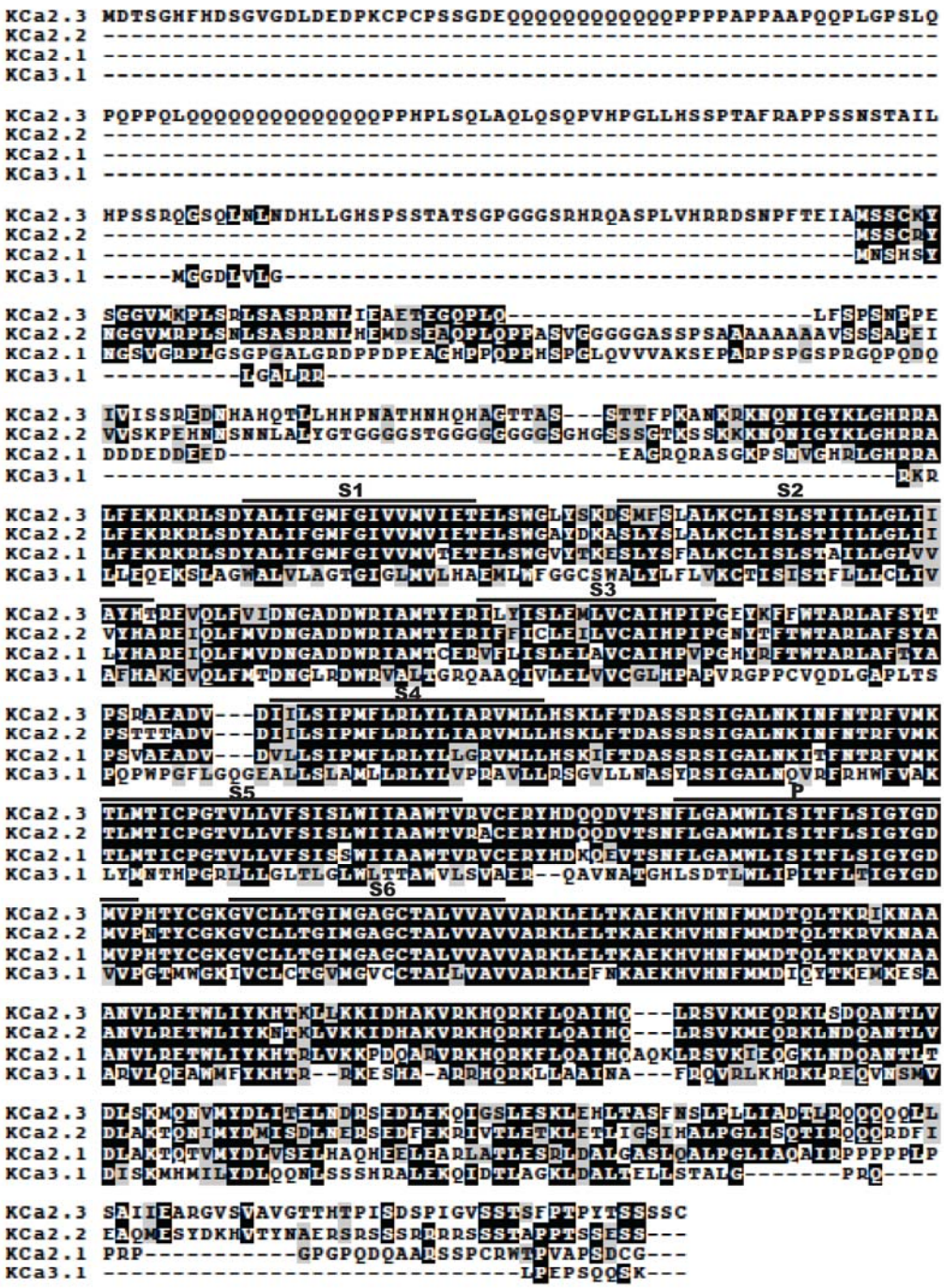

Figure 1.4. Amino Acid Sequence Alignment of Human K_{Ca}2.1, K_{Ca}2.2, K_{Ca}2.3 and K_{Ca}3.1. Lines are drawn above the transmembrane domains S1-S6 and the pore motif (P). Shading denotes identical residues among channels. The Genbank accession numbers for KCa2.1, KCa2.2, KCa2.3, and KCa3.1 are NP_002239, NP_067627, NP_002240 and NP_002241, respectively.

The $K_{Ca}2.x$ channels were found to be highly expressed in the CNS of rat (Kohler et al., 1996). Two of the most distinct characteristics of SK channels are their sensitivity to intracellular Ca^{2+} concentration and their voltage-independence. The $K_{0.5}$ of rSK2 and hSK1 by Ca^{2+} from excised patches of *Xenopus* oocytes was 0.63±0.23 μM and 0.70±0.06 μM, respectively (Kohler et al., 1996). The $K_{Ca}2.1$-2.3 channels were shown to have a mean single channel conductance of ~10 pS (Kohler et al., 1996). The $K_{Ca}2.x$ subfamily is also inhibited by the bee venom toxin apamin giving rise to inhibition constants (K_i) of ~10 nM, ~63 pM and ~1 nM for $K_{Ca}2.1$, $K_{Ca}2.2$ and $K_{Ca}2.3$, respectively (Ishii et al., 1997; Kohler et al., 1996). The distinct pharmacological profiles of the $K_{Ca}2.x$ channels are often used to study and distinguish their functions *in vitro* and *in vivo*.

$K_{Ca}3.1$ is strictly found in peripheral tissues such as the placenta, lungs, pancreas, T cells, colon, smooth muscle and the PNS (Ishii et al., 1997; Joiner et al., 1997). Like the $K_{Ca}2.x$ channels, $K_{Ca}3.1$ channels are activated by intracellular calcium ($K_{0.5}$ of ~300 nM free calcium) and are voltage-independent (Ishii et al., 1997; Joiner et al., 1997). Recordings from excised macropatches from *Xenopus* oocytes showed that $K_{Ca}3.1$ channels are inwardly rectifying and have a unitary conductance of ~40 pS between -60 to -100 mV (Ishii et al., 1997). Additionally, these channels have an outward conductance of between 5-12 pS (Ishii et al., 1997). $K_{Ca}3.1$ channels are apamin and d-tubocurarine-insensitive, but are inhibited by picomolar concentrations of charybdotoxin (K_i=2.5 nM) and clotrimazole (K_i=24.8 nM) (Ishii et al., 1997). Several compounds, including 1-ethyl-2-benzimidazolinone (1-EBIO) and NS309, have been shown to activate both IK1 and SK2 channels (Strobaek et al., 2004; Syme et al., 2000). The $K_{0.5}$ for activation of hIK1 by 1-EBIO is 84 μM and its mechanism of activation is to increase the open probability of the channel (Syme et al., 2000).

1.4.1 Calcium-Sensitivity and Voltage-Independence of SK Channels

The structure of SK channels is important in determining its biophysical properties. Upon cloning and identifying SK channels, several groups showed that these channels were uniquely calcium-sensitive and voltage-independent. However, the mechanisms by which the intracellular calcium concentration controlled channel-gating remained unknown (Ishii et al., 1997; Joiner et al., 1997; Kohler et al., 1996). Analysis of the primary sequence of SK1-3 channels did not show the presence of the known calcium-binding domains; that is, the EF hand motif, C2 domain or calcium bowl were absent in these channels (Xia et al., 1998). Through a series of elegant experiments, Adelman and colleagues showed that the proximal carboxy terminus of SK1-3 is constitutively bound to calmodulin, which imparts calcium-sensitivity to SK channels and allows channel-gating (Xia et al., 1998). CaM contains four EF hand motifs; the first and second motifs occur in the globular amino terminal domain and the third and fourth occur in the carboxy terminal domain (Babu et al., 1985). Mutation of all four aspartic acid residues in the first position of each EF hand motif in calmodulin when co-expressed with SK2 in *Xenopus* oocytes resulted in a greater than 50-fold reduction in the current amplitude (Xia et al., 1998). Similarly, the first 62 amino acid residues of the carboxy terminus of IK1 were found to be essential for binding to calmodulin (Fanger et al., 1999). Therefore, SK1-4 channels were found to be solely dependent on intracellular calcium concentration for activation.

Several groups went on to define the interaction of CaM with SK channels in greater detail. Using yeast two-hybrid assays, it was shown that the constitutive binding of CaM to the SK2 CaMBD was Ca^{2+}-independent (Keen et al., 1999). That is, upon mutation of the aspartic acid residues in the EF hands of CaM that are known to be required for Ca^{2+}-binding the channel continued to bind CaM (Keen et al., 1999). Additionally, Maylie and colleagues showed that

while the C-terminal EF hands of CaM is exclusively required for binding the CaMBD, the EF hands 1 and 2 of the N-terminal are required for Ca^{2+}-dependent gating of the channel (Keen et al., 1999). The crystal structure of the CaMBD of rat SK2 bound to CaM was later determined by Adelman and colleagues (Schumacher et al., 2001). Each CaMBD forms an elongated dimer, where the two α helices are aligned with each other and connected by a loop. Additionally, two CaMBDs dimerize and are organized in an antiparallel manner (Schumacher et al., 2001). CaM was shown to bind either end of the CaMBD dimer and in agreement with previous studies the Ca^{2+}-coordinating residues in the N-lobe were shown to be essential for gating, while those of the C-lobe can be mutated without having any effect on SK gating (Keen et al., 1999; Schumacher et al., 2001). Overall, the model proposed by Adelman and colleagues suggests that the CaMBD/CaM complex exists as a monomer in the absence of Ca^{2+} and dimerizes in the presence of Ca^{2+} (Schumacher et al., 2001). This conformational change is transmitted to the S6 TMD and causes the channel to open, thereby explaining the Ca^{2+}-dependent activation of SK channels.

Despite being voltage-independent, several charged residues that have been shown to be important for protein folding and gating in K_v channels are conserved in SK channels. In $K_{Ca}3.1$ channels, there are two conserved residues in the S4 domain, R160 and R166, and one conserved residue in the S3 domain, E112 (Gao et al., 2008). These residues are akin to R368, K374 and D316 in the *Shaker* K^+ channel, respectively (Gao et al., 2008). Mutation of the analogous residues abolishes expression of the $K_{Ca}3.1$ channel and resulted in decreased $K_{Ca}2.3$ expression, which is restored by proteasome inhibition with lactacystin. Mutation of R266 in $K_{Ca}2.2$ (homologous to R166 in $K_{Ca}3.1$) also abolished expression of the channel, which was subsequently restored by lactacystin treatment. While previous studies have demonstrated that

charge reversal mutations in S2, S3 and S4 were able to restore expression of K_v channels, similar charge reversal mutations in $K_{Ca}3.1$ did not restore expression of the mutant channels, suggesting a divergence in the function of these salt bridges in K_{Ca} channels and K_v channels. Ultimately, these conserved residues function similarly in K_{Ca} and K_v channels in protein folding since mutation of these residues result in rapid degradation.

1.4.2 Physiological Functions of SK Channels in the Nervous System

The AHP that follows an action potential functions to limit the excitability of neurons. There are three kinetic components of the AHP: the fast (fAHP), medium (mAHP) and slow (sAHP) components (Adelman et al., 2012). Various K^+ channels underlie each component. For example, BK channels contribute to the fast and medium AHP (Adelman et al., 2012). A component of the medium AHP was also shown to be apamin-sensitive, while the slow AHP is apamin-insensitive (Bond et al., 2004). Figure 1.5 shows the fast and medium AHPs that follow an action potential train in CA1 pyramidal neurons (Stocker et al., 2004). SK channels are widely distributed throughout the CNS and have been reported to underlie the medium component of the AHP. Through voltage-clamp recordings in hippocampal slices from SK knock-out mice, Adelman and colleagues showed that application of apamin blocks an early component of the AHP in wild type (WT), SK1- and SK3-knockout mice, while SK2-knockout mice did not exhibit an apamin-sensitive component of the medium AHP (Bond et al., 2004). Therefore, this data provided evidence that SK2 channels underlie the medium component of the AHP (Bond et al., 2004; Gerlach et al., 2004). SK channel function is implicated in controlling firing patterns of neurons of the amygdala, hippocampal pyramidal neurons, dopaminergic (DA) midbrain neurons, Purkinje cells, and the deep cerebellar nuclei (DCN), in addition to numerous

other neurons. Disruption of the precision of pacemaker activity in Purkinje cells, hippocampal pyramidal neurons and DA neurons have been linked to episodic ataxia type 2, epilepsy, Parkinson's disease and schizophrenia (Pedarzani and Stocker, 2008).

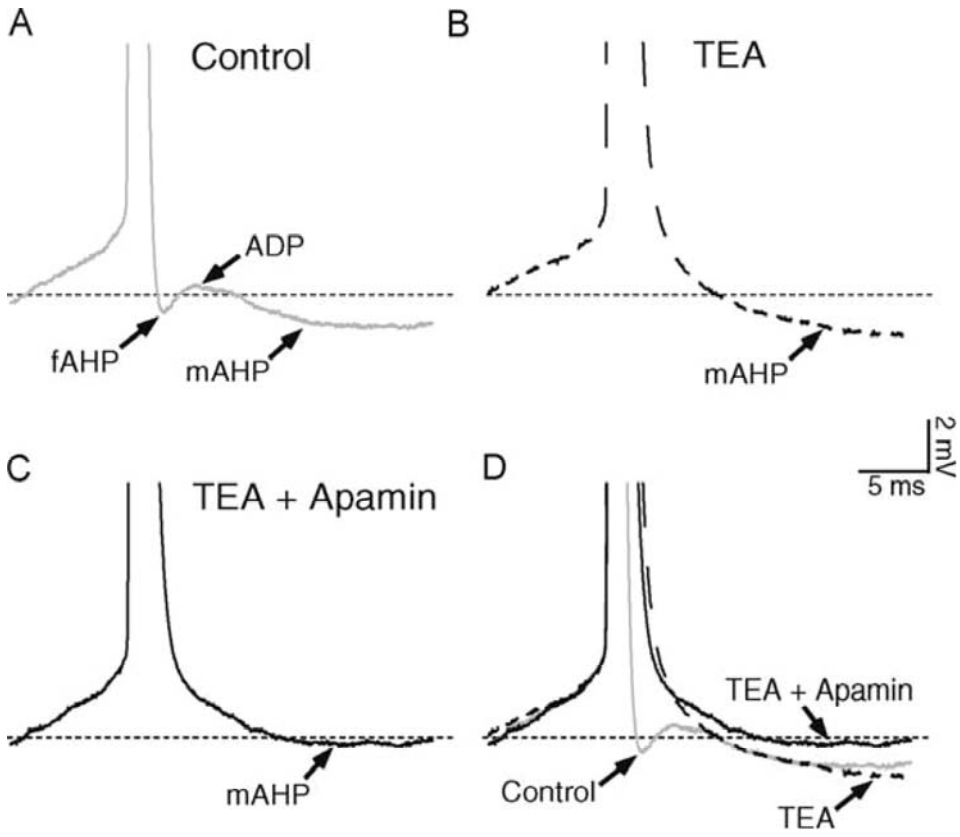

Figure 1.5. After-potentials Following the First Spike in a Train in a CA1 Pyramidal Neuron.
A) Under control conditions, the action potential (truncated) is followed by a fAHP, an afterdepolarization (ADP) and a mAHP. B) Application of tetraethylammonium (TEA, 1 mM) causes spike broadening and suppresses fAHP, while the mAHP persists. C) Subsequent addition of apamin (50 nM) leads to a strong suppression of mAHP following the single spike. D) The traces in A, B and C are shown superimposed to highlight the changes in the after-potentials caused by TEA and apamin. The cell had a membrane resting potential of −55 mV, and the depolarising current pulse was 70 pA and 800 ms long. Reprinted with permission from Stocker, M. *Toxicon*, vol. 43, pg. 934. Copyright 2004 by Elsevier.

In hippocampal CA1 pyramidal neurons, SK2 channels colocalize with *N*-methyl-D-aspartate receptors (NMDARs) and voltage-gated calcium channels (Lin et al., 2008; Ngo-Anh et al., 2005). While apamin application to cultured hippocampal neurons increase the average excitatory postsynaptic potential (EPSP), blocking NMDARs reversed and prevented this increase in EPSP amplitude, suggesting a functional coupling of SK2 and NMDARs (Ngo-Anh et al., 2005). Calcium-entry through NMDARs and R-type calcium channels in dendritic spines activate SK channels, which hyperpolarize the membrane potential, inhibit calcium-entry into the neuron and ultimately limits the amplitude of synaptic potentials (Ngo-Anh et al., 2005). Additionally, it was shown that long-term potentiation (LTP) leads to a PKA-dependent endocytosis of SK2 from the postsynaptic densities in dendritic spines (Lin et al., 2008). This feedback loop is physiologically relevant as changes in synaptic plasticity are essential in learning and memory (Ngo-Anh et al., 2005).

In DA neurons of the substantia nigra (SN), SK3 channels were shown by RT-PCR and immunolabeling to be the dominant SK isoform that is expressed (Wolfart et al., 2001). SK channels were pharmacologically shown to control pacemaker frequency and precision in the DA SN neurons. Application of d-tubocurarine (dTC) to mouse midbrain slices inhibits SK channel activity and resulted in an increased pacemaker frequency, while application of 1-EBIO increased the duration and amplitude of the AHP and decreased pacemaker frequency (Wolfart et al., 2001). Additionally, through inhibition with dTC and apamin, SK channels were shown to be vital for maintenance of spiking precision in the DA SN neurons. The electrical excitability of DA neurons is vital as they are involved in the etiology of schizophrenia and Parkinson's disease (Wolfart et al., 2001).

The studies described above have shown that SK1-3 channels give rise to a component of the AHP and studies of various mouse models have shown that alteration of SK channel function is linked to diseases of the CNS. A 3,441 bp genomic deletion in the KCNN2 gene causes the *frissonant* (*fri*) phenotype, which is characterized by severe motor behavior dysfunction (Szatanik et al., 2008). This mutation, which disrupts the first and second coding exons of the KCNN2 gene, results in the formation of two abnormal transcripts in the brain of heterozygous and homozygous mice. The *fri* mutation was shown to result in irregular neuronal firing in type B medial vestibular nucleus (MVN) neurons in homozygous mice due to the suppression of the slow, apamin-sensitive component of the AHP (Szatanik et al., 2008). This model once again shows that SK2 channels function to generate a component of the AHP in MVN neurons and that elimination of the AHP results in severe neurological phenotypes. Interestingly, overt behavioral deficits were not reported for an alternative knockout mouse model for the KCNN2 gene (Bond et al., 2004). This could be due to the different genetic backgrounds of the mouse models or to the fact that the underlying mutations in the KCNN2 gene in both mouse models could result in entirely different gene products that may differentially affect the function of other SK channels in the CNS.

A mouse model for cerebellar ataxia was developed where SK channel function was disrupted in the CNS (Shakkottai et al., 2004). The Purkinje neurons of the cerebellum provide inhibitory signals to the deep cerebellar nuclei (DCN) and this neuronal pathway is responsible for coordination of movement (Shakkottai et al., 2004). Disruption of Purkinje neuronal function therefore causes DCN hyperexcitability which can impair motor performance. Cerebellar ataxia is characterized by incoordination of movement, instability of posture and tremors. Tomita and colleagues described a truncated SK3 transcript, SK3-1B-GFP, where the amino terminus and

the first TMD are deleted and the protein translation begins eight amino acids upstream of the second TMD (Tomita et al., 2003). This transcript does not result in the formation of functional channels when expressed but has a dominant negative effect that suppresses the function of all SK channels. In this mouse model for cerebellar ataxia, SK3-1B-GFP was expressed under a neuron-specific promoter in mice (Shakkottai et al., 2004). Two mouse lines that expressed this construct only in the DCN of the cerebellum and in other regions of the CNS were investigated and they showed phenotypes that included defective motor learning, impaired balance and grip strength, and gait ataxia (Shakkottai et al., 2004). The molecular mechanism that underlay these symptoms of cerebellar ataxia was shown to be the increased firing frequency of the DCN neurons as a result of the loss of SK channel function and the loss of the AHP generated by SK channels. This study ultimately showed the relevance of SK channels in regulating the firing frequency of the DCN, but it has not been shown to be the main cause of this disease due to the existence of redundant mechanisms in mammals. However, this model provides an alternative mechanism that brings about symptoms of this disease and hence provides alternative treatment strategies for cerebellar ataxia.

SK channel function in the CNS remains a central interest to investigators as a therapeutic target to regulate neuronal pacemaker activity for the treatment of various neurological disorders. For example, blocking SK channel activity in midbrain DA neurons has been suggested as a treatment for Parkinson's disease since this will stimulate dopamine-release (Faber and Sah, 2007). However, the expression of SK1-3 in a broad spectrum of neurons of the CNS and the lack of drug specificity leads to multiple side effects in mouse models in addition to alleviating specific symptoms and therefore, these topics remain to be further investigated.

1.4.3 Physiological Functions of SK Channels in Muscle

The role of SK channels in regulating the excitability of muscle cells is also well documented. In a transgenic mouse model, SK3 expression was regulated by a tetracycline-based genetic switch so that SK3 expression was constitutively overexpressed ~3-fold higher in homozygous transgenic (SK3 T/T) mice than in wild-type mice or was abolished by dietary doxycycline (dox) administration (Bond et al., 2000). In myotube cultures prepared from SK3 T/T mice in the presence of dox, the AHP was eliminated, while cultures from WT and SK3 T/T mice without dox showed a prominent and apamin-sensitive AHP. SK3 T/T mice showed respiratory defects in response to hypoxic challenge; that is, overexpression of SK3 channels resulted in apneic episodes in response to hypoxia. Additionally, SK3 T/T mice showed parturition defects where the pups blocked the birth canal during delivery and both progeny and parent mice died. Parturition defects were proposed to be due to overexpression of SK3 and hence enhanced hyperpolarization of the circular and longitudinal layers of the uterine smooth muscle, while the respiratory defects were proposed to be due to disruption in bursting patterns in inspiratory neurons. Based on this study, drugs that target SK3 were suggested as potential therapeutic targets for sleep apnea or sudden infant death syndrome (Bond et al., 2000). A more recent report showed that SK1-3 channels are expressed in the rat myometrium, where SK2 channel expression was regulated during pregnancy (Noble et al., 2010). SK2 expression was shown to decrease as gestation progressed, but the expression level increased again during labor (Noble et al., 2010). Application of apamin was shown to increase the force of phasic contractions in 21 day pregnant rat myometrium and therefore, this study suggests that SK2 may also play a role in regulating uterine contractility during pregnancy (Noble et al., 2010).

SK2 and SK3 channels play important roles in regulating non-voiding contractions of the bladder, which is important for the overall health and function of the bladder in micturition (Herrera et al., 2003; Thorneloe et al., 2008). SK3 is expressed in the urothelium and in urinary bladder smooth muscle (UBSM) cells, while SK2 expression is limited to UBSM cells alone (Herrera et al., 2003; Thorneloe et al., 2008). The function of SK3 in UBSM contractility was investigated in the SK3 transgenic mouse model described by Adelman and colleagues (Bond et al., 2000). In this mouse model, it was shown that suppression of SK3 in SK3T/T mice increased the frequency of phasic contractions *in vitro* and resulted in bladder overactivity *in vivo*, while it was shown that SK3T/T mice that overexpress SK3 have a bladder capacity that is two-fold higher than WT mice (Bond et al., 2000). SK3 was also shown to be expressed in the urothelium where it plays an additional role in regulating the contractility of the bladder (Herrera et al., 2003). Additionally, through the application of apamin to UBSM strips, it was shown that SK2 contributes to urinary bladder phasic contractions (Thorneloe et al., 2008). Therefore, modulating SK channel function remains an option for treating bladder overactivity.

1.4.4 Physiological Functions of SK Channels in the Circulatory System

A major determinant of vascular tone is intracellular calcium concentration. In vascular smooth muscle cells (VSMCs), there is an elegant feedback mechanism where an increase in intracellular calcium concentration promotes the opening of Ca^{2+}-activated K^+ channels which hyperpolarizes the membrane (Ledoux et al., 2006). This hyperpolarization in turn promotes the closure of voltage-dependent calcium channels (VDCC), which causes a decrease in intracellular calcium concentration and therefore leads to vasodilation (Ledoux et al., 2006). Alternatively, an increase in intracellular calcium concentration in endothelial cells stimulates the release of

endothelium-derived relaxing factors, which is communicated to adjacent VSMCs and leads to vasodilation. While SK channels are expressed in endothelial cells, they are not expressed in VSMCs, with the exception of IK1 which is only expressed in proliferating myocytes (Ledoux et al., 2006).

It has been shown that SK3 channels are expressed in the endothelial cells of resistance arteries where they play an important role in maintaining arterial tone and blood pressure (Taylor et al., 2003). Membrane potential measurements in endothelial cells of SK3 T/T mice were tonically hyperpolarized relative to SK3 T/T mice treated with dox and this hyperpolarization was shown to be communicated to VSMCs (Taylor et al., 2003). Suppressing SK3 expression in resistance arteries of SK3 T/T mice led to a sustained constriction and increased arterial tone, which resulted in a significant increase in systolic and diastolic blood pressure. Untreated SK3 T/T mice showed decreased arterial tone in response to increases in intravascular pressure. The proposed model suggests that activation of SK3 hyperpolarizes the membrane potential of endothelial cells which is communicated to neighboring VSMCs (Taylor et al., 2003). Hyperpolarization of VSMCs causes VDCCs to close, which subsequently leads to a decrease in intracellular calcium concentration and vasodilation (Taylor et al., 2003).

Various studies have proposed that endothelial SK3 and IK1 underlie the endothelium-derived hyperpolarizing factor (EDHF) response, which as yet remains an unidentified factor or signaling pathway (Brahler et al., 2009; Taylor et al., 2003). Kohler and colleagues showed that measurements of smooth muscle membrane potentials in carotid arteries isolated from WT mice in response to acetylcholine showed a hyperpolarization of the resting membrane potential, while suppression of SK3 and IK1 expression significantly attenuated the hyperpolarization response (Brahler et al., 2009). Additionally, application of ACh resulted in a robust EDHF-like

vasodilation in WT mice, which was absent in IK1-/-/SK3 T/T + dox mice (Brahler et al., 2009). Unlike IK1 channels, SK3 was also shown to be crucial for wall shear-stress induced dilation and SK3/IK1-deficient mice demonstrated an increased blood pressure (Brahler et al., 2009). This study suggests that SK channels are a significant factor in the EDHF regulation of vascular tone. Figure 1.6 shows the proposed function of SK3 and IK1 in the EDHF-induced vasodilation (Kohler and Hoyer, 2007).

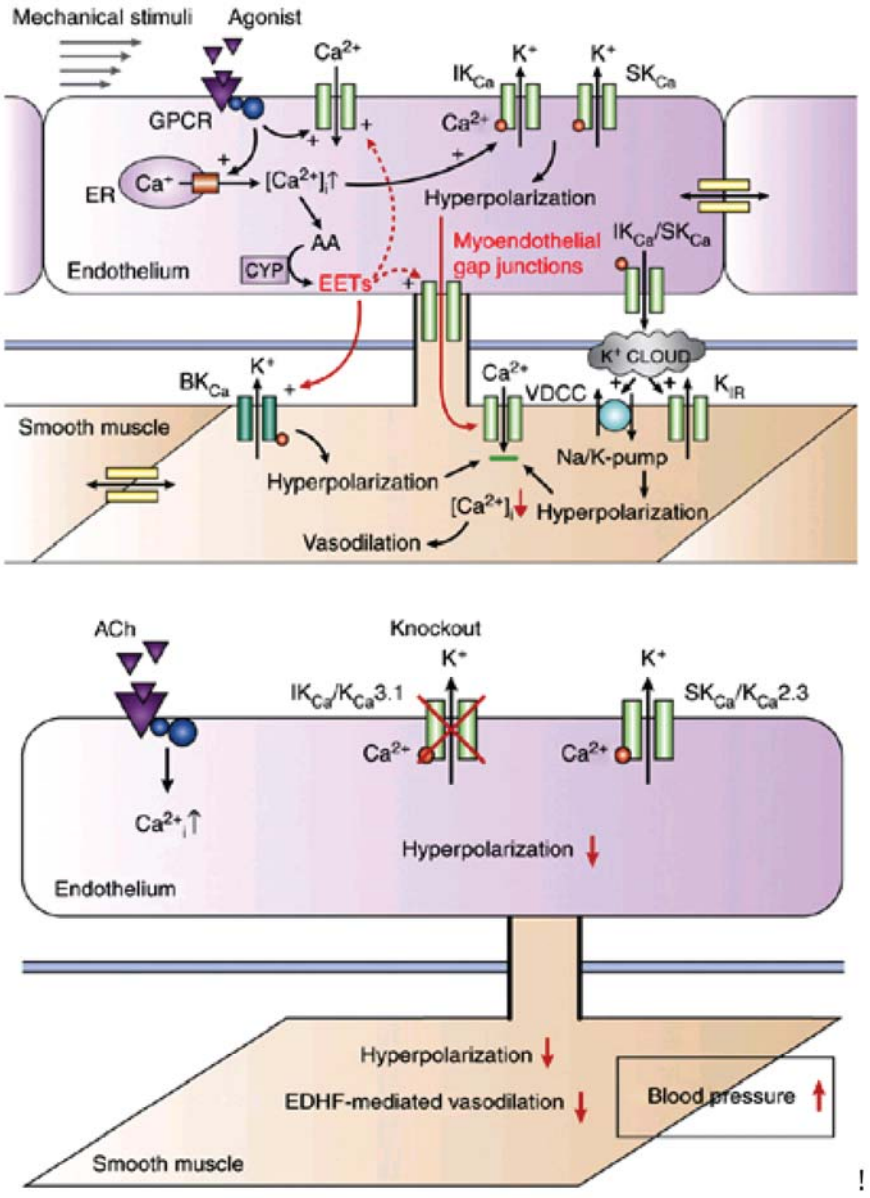

Figure 1.6. Putative EDHF Signaling Pathways Related to Endothelial and Smooth Muscle Ion-Channel Opening.
Impaired endothelial and smooth muscle hyperpolarization in $IK_{Ca}/K_{Ca}3.1$ KO mice leads to defective EDHF-mediated vasodilation and elevated systemic blood pressure. AA, arachidonic acid; ACh, acetylcholine; CYP, cytochrome P450 epoxygenase; EET, epoxyeicosatrienoic acid. Reprinted with permission from Kohler, R. & Hoyer, J. *Kidney Int.*, vol. 72, pg. 149. Copyright 2007 by Nature Publishing Group.

1.5 *C. ELEGANS* AS A MODEL SYSTEM TO STUDY PROTEIN FUNCTION

Through sequencing of cosmid, yeast artificial chromosome (YAC) and fosmid clones, the full sequence of the *C. elegans* genome became available in 1998 where greater than 19,000 genes were predicted to be encoded by the 97-Megabase genome (Consortium, 1998). Although the genome size of *C. elegans* is approximately 2.5% of that of the human genome, which allows for a genetically tractable system, the number of protein coding genes is similar to that of mammals (Salkoff et al., 1998). The use of *C. elegans* as a model system to study protein function is advantageous due to its genetic tractability. Since 99.9% of the *C. elegans* population is hermaphroditic, mutations are easily maintained between generations. The remaining 0.1% population of males is formed by chromosome X nondisjunction (XO) and therefore the male abundance can be increased by heat-shock. These males can then be mated with hermaphrodites so that strains can carry multiple mutations in the genome. Additionally, microinjection of DNA into the distal arm of the gonad allows a fraction of the germ cells to be transformed and to carry the DNA as extrachromosomal arrays (Mello et al., 1991). In this way, transmitting transgenic lines can be propagated and the transgenes can then be integrated into the genome of the organism through gamma irradiation (Mello and Fire, 1995).

The *C. elegans* adult hermaphrodite has a simple body plan which is composed of 959 somatic cells. These cells are divided into the epithelial, nervous, muscular, excretory, coelomocyte, alimentary and reproductive systems (Altun and Hall, 2008). The *C. elegans* body consists of an outer tube or body wall that is made of the cuticle, hypodermis, excretory system, neurons, and muscles (Altun and Hall, 2008). The outer tube is separated from an inner tube that is composed of the pharynx, intestine and gonad by a pseudocoelomic space (Altun and Hall, 2008). The epithelial system consists of the hypodermis which secretes a collagenous cuticle

that lines the pharynx and rectum (Altun and Hall, 2008). The nervous system of the hermaphrodite is composed of 302 neurons and has been reconstructed in its entirety by the use of electron micrographs (White et al., 1986b). From these studies, the developmental origin of every neuron and their synapses were determined (White et al., 1986b). This organism remains viable with severe defects in the nervous system, therefore making it feasible to study numerous mutations of proteins that lead to severe phenotypes (Avery and Horvitz, 1989). Most of the neuronal processes run along the ventral nerve cord (VNC), the dorsal cord (DC) or project to the nerve ring (NR). The muscular system is composed of the striated body wall muscles and non-striated muscles in the pharynx, intestine, anus, and gonad. The coelomocyte system consists of three pairs of scavenger cells in the pseudocoelomic cavity. The alimentary system is made up of the pharynx, 20 cells arranged in pairs along the body length that form a central lumen and the enteric muscles (Altun and Hall, 2008). And finally, the reproductive system consists of the gonad, the germ line and the egg-laying apparatus (Altun and Hall, 2008).

Reverse genetic studies through double-stranded RNA-mediated gene interference (RNAi) is a practical tool for *C. elegans* researchers. Exposure of the organisms to dsRNA causes degradation of the target mRNAs (Fire et al., 1998). Three methods commonly used to induce knockdown are RNAi by injections, soaking in bacteria or by feeding them bacteria engineered to produce dsRNA (Fire et al., 1998; Kamath et al., 2001; Tabara, 1998). SID-1 is a transmembrane protein that allows the cellular uptake of dsRNA and is ubiquitously expressed in all organ systems of *C. elegans* except the nervous system (Calixto et al., 2010). Neurons are refractory to RNAi because of their lack of expression of SID-1 under normal conditions (Calixto et al., 2010). Various strains have been engineered that are more susceptible to RNAi in the nervous system, however they may present alternative disadvantages as discussed elsewhere.

Therefore, with the exception of neurons, RNAi in other organ systems have proven to be effective in elucidating the functions of numerous proteins and in outlining various biological processes.

Embryogenesis in the *C. elegans* life cycle begins with the stage of proliferation where a single cell divides until gastrulation and organogenesis. Post-embryonic development of a *C. elegans* embryo occurs through four larval stages (L1-L4) prior to reaching the adult stage (Sulston et al., 1983). During the L3 though L4 stages, the gonadal sheaths, the spermathecae and the uterus are formed (Altun and Hall, 2008). At the L3/L4 molt, the germ cells differentiate into mature sperm. During the L4 stage gonadogenesis is completed and at the L4/adult molt spermatogenesis halts and the oocytes are generated (Altun and Hall, 2008). The vulva and the egg-laying apparatus, which include the ventral type C (VC) neurons, the hermaphrodite-specific neurons (HSNs) and the sex muscles, is fully formed at the L4/adult molt (Altun and Hall, 2008). *C. elegans* has a life-cycle of ~3 days, and once formed, the adult hermaphrodite is fertile for ~4 days and has a life span of ~2-3 weeks. Therefore, *C. elegans* can be an optimal model organism due to its genetic tractability, its simple anatomy, its thoroughly defined nervous system, and its short life cycle which allows for mass culture under laboratory conditions.

1.5.1 K^+ Channels in *C. elegans*

The *C. elegans* genome-sequencing project has provided us with a complete library of K^+ channels from a single organism. This genome encodes 70 K^+ channel genes and upon sequence analysis of these K^+ channels, it was revealed that the hierarchy of K^+ channels in this invertebrate is conserved with those found in vertebrates (Figure 1.1) (Bargmann, 1998; Salkoff et al., 1998). Additionally, screens for overt phenotypes in *C. elegans* have allowed the

characterization of mutations in various K^+ channel genes. These mutations have often times been shown to occur in conserved structural domains of the channel across the phylogeny of organisms and therefore study of these mutations can yield information about the role of conserved amino acids in channel structure and their physiological roles (Salkoff et al., 1998). If proven to hold true, conservation of structure, biophysical properties, and functions of specific K^+ channels in *C. elegans* makes it an ideal model organism to study K^+ channels in the context of an *in vivo* system. The conservation of K^+ channel gene families in *C. elegans* as they relate to their mammalian counterparts is discussed in greater detail in the following sections.

1.5.2 Voltage-Gated K^+ Channels in *C. elegans*

In humans, there are 40 genes that encode K_v channels and in *C. elegans* there are eleven genes that encode K_v channel homologues (Salkoff et al., 2005). A *Shaw*-type K^+ channel in *C. elegans*, EGL-36, was shown to be 58% identical to the Drosophila *Shaw2* channel, where the greatest degree of conservation occurred in the N-terminal domains involved in tetramer assembly, the six TMDs and the pore motif (Elkes et al., 1997). An *egl-36::gfp* reporter construct was shown to be expressed in the nervous system and in the egg-laying, anal depressor, sphincter and anterior head muscles of *C. elegans* (Elkes et al., 1997; Johnstone et al., 1997). Gain-of-function mutations in EGL-36 (*egl-36(gf)*) led to an egg-laying defective (Egl) phenotype where the organisms did not expel their eggs efficiently, while a dominant negative mutation in the *egl-36(gf)* background restored egg-laying and also produced an egg-laying constitutive phenotype (Egl-C) where the mutant organisms retained fewer eggs *in utero* and laid eggs that were in the early embryonic developmental stages (Elkes et al., 1997; Johnstone et al., 1997). Additionally, *egl-36(gf)* mutants show a decrease in percent expulsions relative to the N2

and dominant negative mutants (Elkes et al., 1997; Johnstone et al., 1997). While behavioral defects were observed with gain-of-function mutations and dominant negative mutations in EGL-36, loss-of-function mutations in EGL-36 did not result in differences in egg-laying or defecation from wild type organisms (Johnstone et al., 1997). Despite its expression in the ventral type C neurons of the egg-laying neurons, EGL-36 was shown to regulate the rate of egg-laying through its expression in the vulval muscles (Elkes et al., 1997). Expression of an EGL-36 cDNA in COS cells resulted in outward K^+ currents that activated at 30 mV & did not demonstrate voltage-dependent inactivation, while the gain-of-function mutations produced large negative shifts in voltage-dependence of activation (Elkes et al., 1997; Johnstone et al., 1997). These properties are characteristic of mouse $K_v3.1$ channels. It was proposed that the *egl-36(gf)* mutations caused defects in egg-laying and defecation by decreasing the excitability of the associated muscles in which they were expressed (Elkes et al., 1997; Johnstone et al., 1997). In these studies, the two gain-of-function mutations, P435S and E138K, are highly conserved with the mammalian homologues and therefore, this system offers the opportunity to gain further insight into how mutations in this channel affect gating.

Another K_v channel that has been studied extensively in *C. elegans* is the EXP-2 channel which was identified in a screen for defective defecation behavior (Thomas, 1990). The primary sequence of EXP-2 has greatest identity with K_v channels and contains 6 TMDs, an S4 domain with six positively charged amino acids, a tetramerization domain in the N-terminus, and two consensus sites for N-glycosylation in the S1-S2 linker (Fleischhauer et al., 2000). EXP-2 bears 35-43% identity with other K_v channels, with the greatest homology being with $K_v2.1$ (Fleischhauer et al., 2000).

An *exp-2::GFP* fusion construct was shown to be expressed in the nerve ring, amphid neurons, phasmid neurons and in the pharyngeal and intestinal muscles (Davis et al., 1999). EXP-2 mutants showed defective defecation behavior, hyperactive head movements, and pharyngeal contractions, but most importantly the EXP-2 channel became of interest due to its function in determining the shape and duration of pharyngeal action potentials, a function that is similar to HERG channels in the rapid repolarization of cardiac action potentials (Davis et al., 1999).

Loss-of-function mutations in EXP-2 resulted in broad action potentials and slow pharyngeal pumping, while mutants that carried the exp-2 gain-of-function mutation (*exp-2(gf/+)*) as heterozygotes displayed narrow action potentials and fast and shallow pharyngeal pumping (Davis et al., 1999). The gain-of-function mutation resulted from a C480Y change and when expressed in *Xenopus laevis* oocytes, this mutation resulted in large inward currents which increased at more negative holding potentials relative to the wild type EXP-2 currents (Davis et al., 1999). Therefore, this study also identified a novel mutation in a K_v channel that favored the open conformation of this channel. The pharyngeal action potentials are comparable to mammalian cardiac action potentials which have characteristic magnitudes, durations and shapes, and since the pharynx has contractile properties that are governed by K^+ channels similar to those expressed in the mammalian heart it remains a model to study the role of K^+ channels in regulating the excitability of the mammalian heart (Shtonda and Avery, 2005).

In mammals, KCNEs or MinK-related peptides (MiRPs) are auxiliary β-subunits of K_v channels. In *C. elegans*, there are four KCNE-related genes, MPS-1 through MPS-4 (Bianchi et al., 2003; Park and Sesti, 2007). MPS-1 is a single transmembrane protein that is 20% identical and 59% homologous to human MiRP1 (Bianchi et al., 2003). KVS-1 is a K_v4.2 homologue that

is a putative interacting subunit of MPS-1 in *C. elegans* (Bianchi et al., 2003). Both MPS-1 and KVS-1 have neuronal expression profiles and show an overlapping expression profile in the amphid head neurons. RNAi of MPS-1 or KVS-1 induced defects in nose-touch sensation, chemotaxis to lysine and biotin and osmotic avoidance, suggesting that both subunits may function together in the ADF, ASG, ASE, and ASH amphid neurons (Bianchi et al., 2003). RNAi of KVS-1 suppressed MPS-1 expression in neurons in which both proteins colocalized and vice versa, suggesting that stable expression of either protein is dependent on the other (Bianchi et al., 2003). Whole cell measurements of CHO cells transfected with KVS-1 cDNA showed that it is a voltage-gated, K^+ selective channel activated by depolarization ($V_{0.5}$=44.6±1.8 mV). Co-expression of KVS-1 and MPS-1 created a hyperpolarized shift in the voltage-dependence of activation ($V_{0.5}$=32.6±1.2 mV). Additionally, MPS-1 increased the rate of inactivation of KVS-1 and altered the inhibition kinetics of KVS-1 by 4-aminopyridine (4-AP). Therefore, MPS-1 showed conserved functions with human MiRP-1 in altering the biophysical properties of a K_v channel and this study provided evidence that these two subunits function together to regulate neuronal excitability in *C. elegans*.

KCNEs are expressed in the heart where mutations in KCNE1 and KCNE2 cause congenital and acquired long QT syndrome (Park and Sesti, 2007). As described previously, EXP-2 repolarizes the pharyngeal membrane and terminates pharyngeal action potentials (Davis et al., 1999). MPS-4 colocalizes with EXP-2 in the pharyngeal muscle. RNAi of MPS-4 causes the expression levels of EXP-2 to decrease significantly, suggesting that this β-subunit assembles with EXP-2 (Park and Sesti, 2007). Recordings of the electrical activity from the pharynx of wild type organisms are regular, while knockout of MPS-4 and EXP-2 lead to prolonged action potentials, delayed after-depolarization and irregular pharyngeal rhythm (Park and Sesti, 2007).

Given the conserved electrical properties of the pharynx and the roles of MPS-4 and EXP-2 in the pharynx, *C. elegans* is being utilized by this and other groups to study KCNE- and K_V-mediated arrhythmia susceptibility and pharmacology (Park and Sesti, 2007).

1.5.3 KCNQ-Like K^+ Channels in *C. elegans*

The human genome encodes five KCNQ genes, while in *C. elegans* there are three genes that encode KCNQ-like channels, KQT1-3 (Salkoff et al., 2005). Primary sequence alignments of KQT1-3 showed a 70% identity in the core of the channel which encodes the S1-S6 transmembrane segments and a region of the carboxy terminus that is implicated in tetramer assembly (Wei et al., 2005). Translation fusion constructs with GFP showed that KQT-1 is expressed in the pharyngeal muscle, mechanosensory and unidentified head neurons (Wei et al., 2005). KQT-2 was expressed in the intestinal cells and KQT-3 was expressed in mechanosensory and chemosensory amphid and phasmid neurons (Wei et al., 2005). Salkoff and colleagues showed that KQT-1 and KQT-3 had a comparable half-maximal conductance, pharmacology and regulation to mammalian KCNQ channels when expressed in *Xenopus* oocytes (Wei et al., 2005). That is, both channels were inhibited by linopridine, a KCNQ-specific inhibitor in mammals, and regulation of both channels occurred when co-expressed with the M1 muscarinic receptor and upon application of a muscarinic agonist, oxotremine (Wei et al., 2005). Therefore, both KQT and KCNQ channels encode M-currents. No measurements of KQT-2 were made since this channel was not expressed in oocytes. The conserved biophysical and pharmacological properties of these KQT channels make *C. elegans* an appropriate system to study the effects of channel inhibitors and openers since KCNQ channels are pharmacological

targets for treatment of diseases such as long QT syndrome, atrial fibrillation, and benign familial neonatal convulsion (Wulff et al., 2009).

1.5.4 The Ether-A-Go-Go K^+ Channels in *C. elegans*

In humans, the EAG gene family is composed of three channels, EAG, ERG and ELK, while *C. elegans* has two EAG-like K^+ channel homologues, EGL-2 and UNC-103 (Salkoff et al., 2005). EGL-2 is highly homologous to Drosophila and mouse EAG proteins with greater than 75% identity in the S1-S6 transmembrane segments, the pore loop and the cyclic nucleotide binding domain (Weinshenker et al., 1999). An *egl-2::gfp* fusion construct showed expression in the intestinal muscles and multiple chemosensory neurons including the AWC neurons. A gain of function mutation in EGL-2, *egl-2(gf)*, inhibits egg-laying and enteric muscle contraction, causes defects in chemotaxis to isoamyl alcohol and benzaldehyde and results in anterior mechanosensory defects (Weinshenker et al., 1999). The *egl-2(gf)* mutation occurs as a result of an A478V mutation in the S6 TMD which causes a negative shift in the voltage dependence of activation (Weinshenker et al., 1999). Thomas and colleagues proposed that *egl-2(gf)* caused the described behavioral defects by reducing the excitability of the enteric muscles, the AWC (amphid wing cells) neurons and the ALM (anterior lateral microtubule cell) mechanosensory neurons, respectively (Weinshenker et al., 1999). These phenotypes are rescued by treatment with imipramine, which inhibits both wild type and *egl-2(gf)* currents. Interestingly, imipramine is a tricyclic antidepressant which has clinical side effects such as cardiac arrhythmia, constipation and sexual dysfunction (Weinshenker et al., 1999). Additionally, imipramine has been shown to decrease tumor cell proliferation *in vivo*, which is clinically important since EAG1 is expressed in up to 70% of tumor cell lines (Wulff et al., 2009). This study was the first

to show that an EAG channel orthologue is a molecular target of tricyclic drugs that may underlie some of the side effects of imipramine treatment. In this case, *C. elegans* was proven to be an exceptional model to investigate the pharmacology and clinical relevance of a K^+ channel.

In humans, HERG is a cardiac K^+ channel and mutations of HERG are known to induce acquired long QT syndrome (aLQTS), while modulators of HERG function may also contribute to the development of this disease. A study by Balser and colleagues used *C. elegans* as a model system to identify modulators of a HERG orthologue, UNC-103 (Petersen et al., 2004). The transmembrane domains and pore region of UNC-103 has 70% identity with HERG. When driven under the *unc-103* promoter, GFP was expressed in the body-wall muscles, egg-laying muscles, pharyngeal muscles, and the nervous system (Petersen et al., 2004). A mutation in UNC-103, UNC-103(A334T), results in severe defects in locomotion based on a liquid thrashing assay and severe pharyngeal pumping defects represented by a 40-fold increase in pause lengths in between contractions (Petersen et al., 2004). Treatment of *unc-103(500)* mutant worms with D-sotalol, a known HERG-inhibitor, partially rescued the thrashing defect, but had no effect on the pharyngeal pumping defect (Petersen et al., 2004). On the other hand, *unc-103* RNAi partially rescued the locomotion defect and more strongly rescued the pharyngeal pumping defect by decreasing the average pause length by approximately 2.5-fold (Petersen et al., 2004). Since UNC-103 could not be expressed in heterologous expression systems, the analogous mutation to UNC-103(A334T), HERG(A653T), was analyzed by voltage-clamp protocols in *Xenopus* oocytes (Petersen et al., 2004). HERG(A653T) induced a 22-mV hyperpolarized shift in $V_{0.5}$ and therefore the analogous mutation in UNC-103 could potentially reduce the excitability of tissues in which it is expressed if it has similar biophysical properties to the human counterpart (Petersen et al., 2004). In an RNAi screen to identify potential K^+ channel modifiers,

KCR1 and mec-14, a *Drosophila* hyperkinetic homologue, were identified (Petersen et al., 2004). Both subunits interact with the rat EAG-homologue and HERG (Kupershmidt et al., 2003; Wilson, 1998). KCR1 RNAi decreased the pharyngeal pumping defect of *unc-103(n500)* mutants by 42%, while mec-14 RNAi rescued the pumping defects in *+/n500* heterozygous worms only (Petersen et al., 2004). As mentioned previously, various drug-treatment in humans can inhibit HERG as a side effect and induce aLQTS. KCR1 was shown to be protective as it significantly decreased the rate of dofetilide block of HERG when co-expressed in CHO cells (Petersen et al., 2004). Therefore this study identified a novel modifier of HERG channels and a candidate gene target for alleviating the risk of aLQTS.

1.5.5 BK Channels in *C. elegans*

In *C. elegans*, there is a SLO-1 and a SLO-2 orthologue, while in humans there is one Slo- or MaxiK-encoding gene (Berkefeld et al., 2010; Salkoff et al., 2005). Mutants in SLO-1 were identified in a genetic screen to identify proteins that relieved behavioral lethargy of *unc-64* hypomorphic syntaxin mutants that do not release neurotransmitters efficiently (Wang et al., 2001). As a result of this screen, SLO-1 was implicated in the regulation of neurotransmitter release. There are three splice variants of SLO-1 and the major structural domains of these splice variants are conserved; that is, the seven TMDs, the pore motif, the four hydrophobic domains in the carboxy terminus, and the calcium bowl are conserved (Wang et al., 2001). The *C. elegans* SLO-1 channel is 58.6% identical to the human SLO-1. Patch clamp analysis of the SLO-1a and -b cDNA transcripts in *Xenopus* oocytes showed that channel gating was dependent on intracellular calcium concentration and on membrane depolarization (Wang et al., 2001). The single channel conductance was ~250pS and therefore the biophysical properties of the *C.*

elegans SLO-1 are comparable to those of mammalian BK channels (Wang et al., 2001). Loss-of-function mutations of *C. elegans slo-1*, as determined by electrophysiological measurements, were found to rescue *unc-64* locomotion velocity, resistance to aldicarb and inhibitory post-synaptic potentials (IPSPs) in the pharynx (Wang et al., 2001). Through immunolabeling, the SLO-1 channel was found to be expressed in the nerve ring, nerve cords, the body wall and vulval muscles (Wang et al., 2001). Driving expression of *slo-1a* under a neuron-specic promoter, *snb-1*, reverted the rescue of loss of function of *slo-1* in the unc-64 background, while expression of *slo-1* under a muscle-specific promoter, *myo-3*, had no effect (Wang et al., 2001). Therefore Salkoff and colleagues concluded that SLO-1 potentially acts presynaptically in neurons to limit neurotransmitter release (Wang et al., 2001). Additionally, measurements of evoked excitatory postsynaptic currents (EPSCs) in the body wall muscle cells showed that the quantal content was increased in *slo-1* mutants relative to wild type organisms, supporting the hypothesis that neurotransmitter release was increased in these mutants (Wang et al., 2001).

SLO-2 is 41% identical to rSlack, a rat SLO-2 orthologue and the amino terminus and the core of the channel encoding the S1-S6 TMDs are conserved (Yuan et al., 2000). However, topological discrepancies are observed since the C-terminus has only two hydrophobic segments and a non-conserved linker region (Yuan et al., 2000). Whereas the mammalian SLO-2 channel is sensitive to voltage, intracellular sodium and intracellular calcium concentrations, *C. elegans* SLO-2 is activated by depolarization and is sensitive to intracellular calcium and chloride ions (Yuan et al., 2000; Yuan et al., 2003). Patch clamp analysis of *C. elegans* SLO-2 when expressed in *Xenopus* oocytes revealed that the channels were inactive in the absence of calcium or chloride and that increasing the concentrations of either ion created significant left shift in V_{50} (Yuan et al., 2000). The SLO-2 channels were shown to be outward rectifiers and the voltage

dependence was independent of $[Cl^-]_i$ and $[Ca^{2+}]_i$ (Yuan et al., 2000). A noteworthy difference between the sequence of mSLO-1 and *C. elegans* SLO-2 is the absence of a string of aspartate residues in the putative calcium bowl of mSLO-1 (Yuan et al., 2000). Instead, this motif contains a series of positively charged residues and when neutralized, the channel's sensitivity to chloride was markedly decreased as determined by the decreased slope in V_{50} (Yuan et al., 2000). This study identified a novel SLO channel in *C. elegans* and lends information with regards to the structural motifs involved in sensing intracellular factors that determines the channel's activity and physiological effects.

1.6 REGULATION OF THE RATE OF EGG-LAYING IN *C. ELEGANS*

The egg-laying apparatus consists of two HSNs and six VC neurons which innervate the sixteen egg-laying muscles (White et al., 1986b). Through the release of the neurotransmitter serotonin the HSNs stimulate contraction of the egg-laying muscles which leads to expulsion of eggs out of the vulva (Desai and Horvitz, 1989). However, the role of the VC neurons remains disputed as they have been shown to have dual functions of inhibition and stimulation of egg-laying (Bany et al., 2003; Kim et al., 2001; Zhang et al., 2008). Defects in the egg-laying apparatus often result in an egg-laying defective (Egl) or hyperactive egg-laying (Egl-C) phenotype.

The egg-laying neurons of *C. elegans* have been used extensively to dissect the functions and signaling pathways of G proteins. The G protein signaling pathway is composed of heterotrimeric G proteins that relay signals from the plasma membrane intracellularly through interaction with their G protein-coupled receptors (GPCRs). The G_0 alpha subunit ($G_\alpha 0$) is expressed in the nervous system of the worm, including the HSNs and VCs, and the egg-laying

muscles (Mendel et al., 1995). The gene that encodes $G_{\alpha}0$ was termed *goa-1* and loss-of-function mutations in *goa-1* yield Egl-C mutants, while a constitutively active *goa-1* mutation yield animals that are severely Egl (Mendel et al., 1995). $G_{\alpha}0$ in *C. elegans* was shown to have both defective egg-laying muscles and HSNs leading to these phenotypes (Mendel et al., 1995). In *C. elegans*, EGL-10 was shown to encode a protein that has a regulator of G protein signaling (RGS) domain (Koelle and Horvitz, 1996). EGL-10 has been shown to be expressed in the nervous system of the worm and in the body wall muscles and more specifically, it was shown to be expressed in the HSNs (Koelle and Horvitz, 1996). Loss-of-function mutations in EGL-10 caused an Egl phenotype, while overexpression causes an Egl-C phenotype (Koelle and Horvitz, 1996). Another component in this pathway is the EGL-47 receptor, a putative GPCR that is expressed in the HSNs (Moresco and Koelle, 2004). Activation of EGL-47 in the HSNs inhibit egg-laying, suggesting that it functions in the same pathway as GOA-1 to inhibit egg-laying (Moresco and Koelle, 2004). Alternatively, EGL-30 is a *C. elegans* homolog of $G_{\alpha}q$ where loss-of-function mutations result in a strong Egl phenotype and overexpression causes a strong Egl-C phenotype (Brundage et al., 1996). Therefore within these neuromuscular junctions, the G proteins $G_{\alpha}q$ and $G_{\alpha}0$ have been shown to have opposing effects on egg-laying, where stimulation of egg-laying occurs through $G_{\alpha}q$ while inhibition of egg-laying occurs through $G_{\alpha}0$ (Moresco and Koelle, 2004).

Bany and colleagues discovered gross morphological defects in the VC neurons of several hyperactive egg-laying mutants (Bany et al., 2003). The VC neurons act to inhibit egg-laying through the neurotransmitter acetylcholine (Bany et al., 2003). In *egl-1(n986)* mutants and in *lin-39(n709)* mutants, the HSNs and the VC neurons undergo premature cell death, respectively. In *egl-1(n986)* mutants the VCs remain largely inactive, while in *lin-39(n709)*

mutants the HSNs become hyperactive, supporting an interdependence between these two subsets of neurons (Zhang et al., 2008). Calcium transients in both sets of neurons are coupled to egg-laying events, suggesting that the HSNs and the VCs act synergistically to control the rate of egg-laying events in *C. elegans* (Zhang et al., 2008).

In addition to the VC neurons, the posterior touch receptor (PLM) neurons and the PVNR neuron forms chemical synapses with the HSNs (White et al., 1986b). Inhibition of egg-laying occurs through the ALM and PLM touch receptor neurons which alter the activity of the HSNs (Sawin, 1996; Zhang et al., 2008). Additionally, neuropeptides released by the BAG neurons have been shown to inhibit egg-laying by stimulating EGL-6 which is expressed in the HSNs (Ringstad and Horvitz, 2008). Therefore, there are multiple neurons that function to regulate the rate of egg-laying.

1.7 SUMMARY OF INTRODUCTION AND RESEARCH GOALS

With an underlying function to regulate the excitability of cells in which they are expressed, K_{Ca} channels play a role in the regulation of pacemaker activity of neurons in the CNS by generating a component of the AHP that follows action potentials. Overt mutations of K^+ channels can be classified as gain-of-function or loss-of-function, but loss-of-function mutations can also exert a dominant negative effect on K^+ channels within the same family. SK channels have been studied extensively in mouse models. Voltage clamp recordings in hippocampal pyramidal neurons of SK_{Ca} knockout mice revealed a role for $K_{Ca}2.2$ in the generation of the medium AHP, while these channels were shown to generate the slow AHP in the MVN neurons in $K_{Ca}2.2$ knockout mice (Bond et al., 2004; Szatanik et al., 2008). The use of pharmacological inhibitors and

activators of SK_{Ca} channels in mice have demonstrated a role for these channels in controlling spiking precision and pacemaker frequency in DA neurons of the SN thereby linking SK channels to Parkinson's disease and Schizophrenia (Wolfart et al., 2001). Another mouse model in which there was a genomic deletion that disrupted the first two exons of the KCNN2 gene demonstrated severe motor behavior defects (Szatanik et al., 2008). And finally, expression of a truncated $K_{Ca}2.3$ transcript in the nervous system of mice led to phenotypes reminiscent of cerebellar ataxia (Shakkottai et al., 2004).

The use of mouse models has therefore been an invaluable tool to study the neurophysiological functions of SK channels. Despite the knowledge that has been gained using the described mouse models, the mammalian nervous system remains complex, manipulation of which is costly and time-consuming. My goal in this dissertation was to develop a system using *C. elegans* as a model organism to study the physiological functions of an SK channel homologue, KCNL-2. The advantages of using this model organism have been discussed in detail above, but most importantly strategies to manipulate its genome are readily available and the resulting phenotypes can be studied in a time-efficient manner.

The first aim of this dissertation was to determine the cellular localization of KCNL-2. Transgenic lines that harbor extrachromosomal arrays of the KCNL-2 gene that was tagged with GFP at the amino or carboxy termini were imaged using widefield or confocal fluorescence microscopy systems. Additionally, transgenic lines that express a KCNL-2 promoter-GFP construct were imaged. This process revealed that the channel is predominantly expressed in the nervous system of the worm. KCNL-2 is expressed in cell bodies and processes in the nerve ring, in neurons that project to the tip of the nose, the pharyngeal nervous system, the ventral nerve cord and in tail ganglia. This process also revealed that GFP-tagged KCNL-2 is highly

expressed in neuronal processes that innervate the vulva and by the egg-laying neurons VC4 and VC5. Promoter-GFP expression also showed that various isoforms of KCNL-2 may be expressed in the vulval muscles, although to a lesser degree since this is not visualized when the full-length channel is expressed. The second aim of this dissertation was to identify the physiological functions of KCNL-2 based on the anatomical expression profile. Phenotypic analysis of a KCNL-2 null strain, *kcnl-2(tm1885)*, and of transgenic lines that overexpress KCNL-2 was carried out. I found that *kcnl-2(tm1885)* demonstrates a mild egg-laying defective phenotype and that KCNL-2-overexpression transgenic lines demonstrate a strong egg-laying constitutive phenotype. I undertook strategies to identify the minimal neuronal circuit in which KCNL-2 function to regulate the rate of egg-laying, but these mechanisms remain to be fully elucidated. This is the first in depth investigation of an SK channel homologue in *C. elegans*. The expression of KCNL-2 in various neurons, including the pharyngeal nervous system and the egg-laying neurons, offers the opportunity to further investigate SK channel function in minimal neuronal circuits in the context of an *in vivo* system.

2.0 A SMALL CONDUCTANCE CALCIUM-ACTIVATED K^+ CHANNEL IN *C. ELEGANS*, KCNL-2, PLAYS A ROLE IN THE REGULATION OF THE RATE OF EGG-LAYING

2.1 INTRODUCTION

In mammals, four KCNN genes that encode the small- ($K_{Ca}2.1$, $K_{Ca}2.2$, $K_{Ca}2.3$) and intermediate-conductance ($K_{Ca}3.1$) Ca^{2+}-activated potassium channels have been cloned (Ishii et al., 1997; Joiner et al., 1997; Kohler et al., 1996). SK channels have a diverse expression profile and function to hyperpolarize cells in which they are expressed. In the nervous system, the SK channel family functions to generate a component of the afterhyperpolarization (AHP) that follows action potentials (Adelman et al., 2012). This AHP is the rate-limiting step in preserving precision and frequency of pacemaker activity in neurons. SK channels have been shown to regulate the excitability of Purkinje cells, hippocampal pyramidal neurons and dopaminergic neurons, and as a result SK channels have been implicated in a wide array of neurological disorders including episodic ataxia type 2, epilepsy and schizophrenia (Empson and Jefferys, 2001; Fernandez de Sevilla et al., 2006; Shakkottai et al., 2004; Walter et al., 2006; Wolfart et al., 2001). The biological functions of SK channels have been widely investigated using mouse models. A $K_{Ca}2.2$ deletion mutant, the frissonant mouse model, displays altered AHPs that result in irregular action potential firing frequency leading to rapid tremor and locomotor instability

(Szatanik et al., 2008). Another mouse model in which $K_{Ca}2.1$ and $K_{Ca}2.2$ channel expression was specifically knocked down in the deep cerebellar nuclei showed phenotypes reminiscent of cerebellar ataxia deficits, such as postural instability, defective motor learning and severe incoordination (Shakkottai et al., 2004). However, despite the evidence that shows the role of SK channels in the CNS, as demonstrated in transgenic mouse lines, the correlation of SK channel function to the described neurological disorders has not been ascertained.

In addition to its role in the nervous system, SK channels are a potential pharmacological target for hypertension and incontinence due to their functions in regulating the contractility of vascular and urinary bladder smooth muscle cells, respectively (Brahler et al., 2009; Herrera et al., 2003; Taylor et al., 2003; Thorneloe et al., 2008). Additionally, $K_{Ca}2.3$-overexpression in mice has been shown to hinder uterine contractions during labor resulting in the death of the parent and pups, while suppression of $K_{Ca}2.3$ did not result in phenotypic consequences (Bond et al., 2000).

C. elegans is a particularly advantageous model organism to study SK channel function due to its molecular and genetic tractability as well as its anatomical simplicity. As the cuticle and embryo eggshell are transparent, cellular processes can be visualized *in vivo* by widefield and confocal microscopy. The nervous system of *C. elegans* has been mapped from its early developmental stages throughout adulthood and this information can afford the study of SK channel function in isolated neuronal circuits (White et al., 1986a). Mutations that render the channel as inactive or hyperactive often result in opposing phenotypes and therefore study of the behavior of *C. elegans* can yield physiological knowledge of SK channels. In *C. elegans* there are four genes, F08A10.1, B0399.1, C03F11.1 and C53A5.5, that encode SK channel homologues. Herein, we demonstrate the biological significance of the KCNL-2 protein, which

is encoded by the F08A10.1 gene. We show that KCNL-2 is predominantly expressed in the nervous system of *C. elegans* where it plays a novel role in the regulation of the rate of egg-laying.

2.2 RESULTS

2.2.1 Essential Structural Domains of Mammalian SK Channels are Conserved in KCNL-2

The *C. elegans* genome contains 80 potassium channel-encoding genes whose products serve to regulate the excitability of cells and their residing organ systems (Bargmann, 1998). Of these, four genes, F08A10.1, B0399.1, C03F11.1 and C53A5.5, encode channels that are homologous to human SK channels. Up to eight splice variants (KCNL-2-a through –h) of KCNL-2 have been predicted based on expressed sequence tag (EST) data (http://www.wormbase.org, WS231, 07.12.2012). The splice variants KCNL-2-f, -g and –h (accession numbers NM_001263764, NM_001263763 & NM_001263765, respectively) were identified more recently and their analysis remains outside the scope of this study since they were not encoded by the WRM063DE08 fosmid (*C. elegans* Reverse Genetics Core Facility, Canada) that was used for our investigation of KCNL-2. We sequenced and analyzed the yk1015a02, yk1103e07, yk1295d10 and yk1401h05 cDNA clones (obtained from Yuji Kohara, National Institute of Genetics of Japan) encoding transcripts of KCNL-2. Sequencing of yk1295d10 shows a full-length clone of KCNL-2b (accession number NM_181991) that is incompletely spliced, while the sequence of yk1401h05 reveals an alternative isoform of KCNL-2a (accession number

NM_059833), which we termed KCNL-2aii (accession number JX455834). yk1103e07 and yk1015a02 encode partial transcripts of KCNL-2c and –d, respectively (accession numbers NM_181991 & NM_181992). In this study, we analyzed the expression of the first five splice variants of KCNL-2 encoded by the fosmid in addition to the newly identified KCNL-2aii isoform as depicted in Figure 2.1A. The a, aii, d, and e splice variants share the same initiation site, are 98% identical and their open reading frames span ~12.5 kb, while the b and c splice variants have the same initiation site, are 98% identical, but their exons span ~3 kb (Figure 2.1A). Additionally, as shown by Figure 2.1A, the a, b, d and e splice variants share a common stop codon, while the aii and c splice variants are alternatively spliced and share a second stop codon. Alignments of the peptide sequences of the KCNL-2 splice variants show that the worm orthologue bears 37% identity to $K_{Ca}2.2$ (Figure 2.1B), and 35% identity to the $K_{Ca}2.1$, $K_{Ca}2.3$ and $K_{Ca}3.1$ channels. The greatest degree of homology occurs in the core of the channel (~50% identity) where the six transmembrane domains (Figure 2.1B, solid lines), the potassium selective pore (Figure 2.1B, dotted line) and the calmodulin-binding domain (Figure 2.1B, dashed line) are conserved. There is little homology between the amino and carboxy termini of KCNL-2 and mammalian SK channels. Hydrophobicity scores of the primary sequence of KCNL-2a reveal seven highly hydrophobic regions corresponding to the S1-S6 transmembrane domains and the pore motif (Figure 2.1D) (Kyte and Doolittle, 1982). Since the structural domains that are known to be important in mammalian SK channels are conserved, this suggests that KCNL-2 would have similar biological functions to its mammalian homologues. A KCNL-2 deletion mutant, *kcnl-2(tm1885)*, was generated by the National Bioresource Project (Japan). As shown by Figure 2.1C, the *kcnl-2(tm1885)* mutation results in a frameshift that leads to a

premature stop codon upstream of the first transmembrane domain of all isoforms of KCNL-2. Therefore, the *kcnl-2(tm1885)* mutation likely results in a null channel.

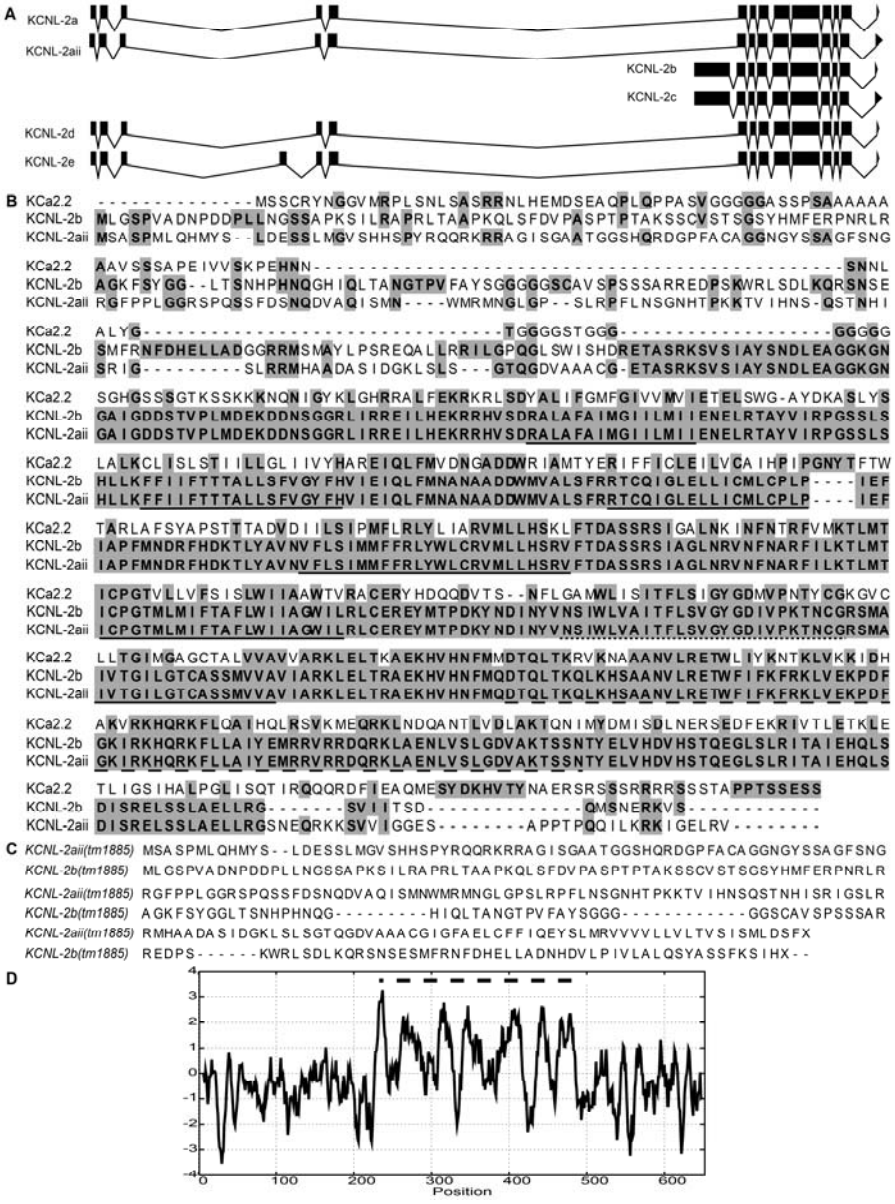

Figure 2.1. Structural Analysis of KCNL-2 Isoforms.
A) The WRM063DE08 fosmid encodes six isoforms of KCNL-2, which vary in their amino and carboxy termini of the predicted protein structure. The exon structures show that there are two initiation sites that are 9.5 kb apart and two stop codons that are 68 bp apart. B) KCNL-2 isoforms have 37% identity with $K_{Ca}2.2$, while KCNL-2aii and -b are 71% identical. The greatest degree of conservation occurs in the core of the channel where the S1-S6 transmembrane domains (underlined solid), the potassium selective pore filter (underlined dotted), and the

calmodulin binding domain (underlined dashed) are encoded. C) *kcnl-2(tm1885)*, a 962 bp deletion, results in a premature stop codon before the first TMD of KCNL-2-aii and -b. D) Kyte-Doolittle hydropathy plot of the KCNL-2a isoform showing seven domains that are highly hydrophobic, which represent the 6 TMDs and the pore motif (dashed line).

2.2.2 Phenotypic Analysis of KCNL-2

Given the structural similarity of KCNL-2 to mammalian SK channels and the well-defined anatomy of *C. elegans*, we propose that using *C. elegans* would serve as a practical model system to further understand the physiology of SK channels. In order to investigate possible functions of KCNL-2, we carried out phenotypic assays on *kcnl-2(tm1885)* and KCNL-2-overexpressing transgenic lines at 20^{o}C. The *kcnl-2(tm1885)* strain was outcrossed 8 times to remove extraneous mutations that resulted from TMP treatment. To monitor the overall health of these organisms that lacked the KCNL-2 channel, we assayed the survival of a population of late L4 animals from the described worm strains. Figure 2.2A shows the Kaplan-Meier survival curves of N2 and *kcnl-2(tm1885)* worms. Based on a Logrank test, the longevities of N2 and *kcnl-2(tm1885)* organisms are not significantly different suggesting that the KCNL-2 channel is not required for survival of the adult animals. To examine possible functions of KCNL-2 in reproduction, we measured the brood size of *kcnl-2(tm1885)* animals. The brood size of *kcnl-2(tm1885)* organisms was assessed by counting the number of progeny after 48 hrs of development at 20^{o}C. As shown by Figure 2.2B, the brood size of *kcnl-2(tm1885)* organisms is significantly smaller than that of N2 animals. This smaller brood size of *kcnl-2(tm1885)* animals can be attributed to a population of the progeny undergoing larval arrest and eventual death due to a post embryonic developmental delay (Figure 2.3A). Although loss of KCNL-2 led to larval

arrest and slow growth, transformation of *kcnl-2(tm1885)* organisms with KCNL-2 (tagged and untagged) did not rescue these phenotypes. The lack of rescue may be due to extraneous mutations elsewhere in the *kcnl-2(tm1885)* genome, but this possibility was not investigated further.

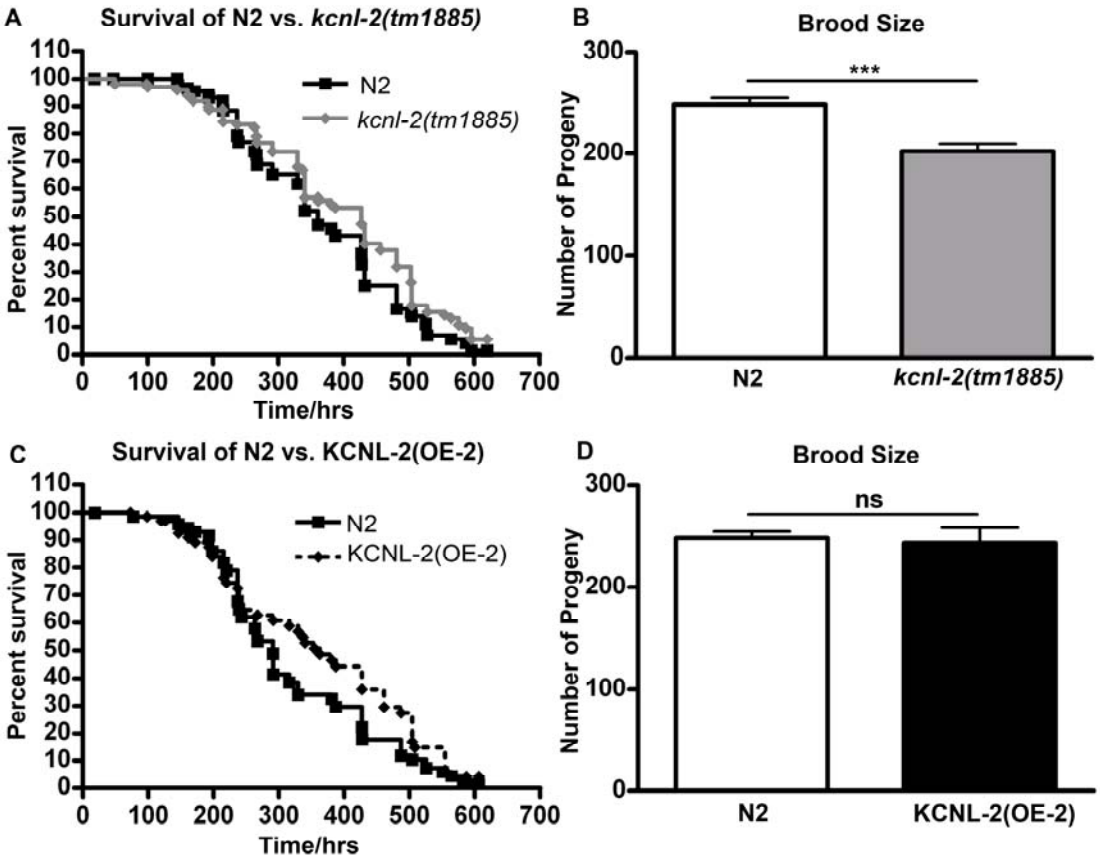

Figure 2.2. Phenotypic analysis of *kcnl-2(tm1885)* and KCNL-2(OE), a transgenic line that overexpresses $P_{kcnl\text{-}2}$*kcnl-2(taa2)::gfp* in the N2 background.
A,C) Kaplan-Meier Survival Curves showing the longevities of N2 vs. *kcnl-2(tm1885)* (n=80; p=0.06, Logrank test) or N2 vs. KCNL-2(OE-2) (n=50; p=0.12, Logrank test). B,D) Brood size of N2 vs. *kcnl-2(tm1885)* (n≥17; p<0.001, Student's *t*-test) or N2 vs KCNL-2(OE-2) (n≥13; p=0.77, Student's *t*-test).

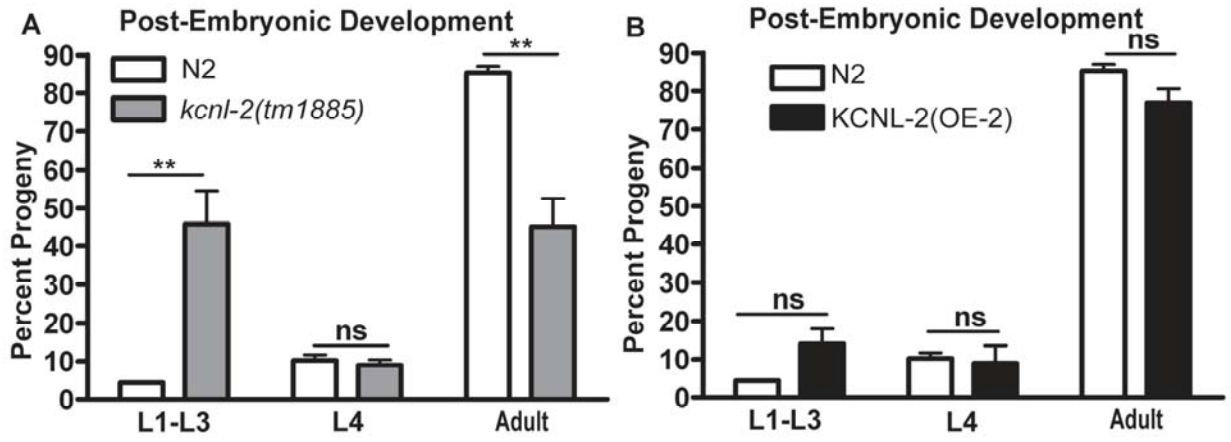

Figure 2.3. Post-embryonic Developmental Analysis
of A) *kcnl-2(tm1885) vs. N2* (n=3; adults: $p<0.05$; L4: $p>0.05$; L1-L3 larvae: $p<0.05$, Kruskal-Wallis *H* test) or B) N2 vs. KCNL-2(OE-2) (n=3; adults, L4, L1-L3 larvae: $p>0.05$ *;* Kruskal-Wallis *H* test).

Since the *kcnl-2(tm1885)* animals did not yield an overt phenotype that could be rescued by transforming the null organisms with the KCNL-2 gene and phenotypic anomalies are often observed in SK knockout mouse models, we sought to determine if overexpression of the KCNL-2 gene in *C. elegans* would yield an overt phenotype. Transgenic lines overexpressing $P_{kcnl\text{-}2}$*kcnl-2(taa2)::gfp* (line 2), KCNL-2(OE-2), were assayed for longevity and brood size. Overexpression of the KCNL-2 gene did not result in observable differences in longevity (Figure 2.2C) and brood size (Figure 2.2D) when compared to N2 animals. Also, as shown by Figure 2.3B, no observable differences were seen in the post embryonic development of KCNL-2(OE-2) animals relative to N2 worms. These results demonstrate that overexpression of KCNL-2 did not result in deleterious effects on survival of the organisms or produce defects in gametogenesis and fertilization.

2.2.3 KCNL-2 is Expressed in the Nervous System

To aid in the identification of the biological functions of KCNL-2, we sought to determine its localization. KCNL-2 was fused to GFP so that it was effectively tagged at the amino termini ($P_{kcnl\text{-}2}$*gfp::kcnl-2*) or at the carboxy termini ($P_{kcnl\text{-}2}$*kcnl-2::gfp*). As shown by Figure 2.1A, the coding sequences for splice variants a, aii, d and e share the same initiation site (atg1), while that of splice variants b and c occurs ~9.5 kb downstream of the first initiation site (atg2). Similarly, splice variants a, b, d, and e end at a stop codon (taa1) that is 68 bp upstream of the stop codon of splice variants aii and c (taa2). Therefore, four constructs were made where GFP was fused to either initiation site or stop codon in order to determine if the splice variants are differentially expressed. Expression of the transformation vectors was driven under 1,951 bp of the KCNL-2 endogenous promoter. Confocal fluorescent imaging of transgenic lines expressing these constructs showed a neuronal expression pattern (Figure 2.4). Figure 2.4A shows the expression of KCNL-2 when tagged at the latter stop codon ($P_{kcnl\text{-}2}$*kcnl-2(taa2)::gfp*). As shown in Figure 2.4A, KCNL-2 is expressed in head neurons, the nerve ring (NR), motor neurons of the ventral nerve cord (VNC), the dorsal cord (DC) and tail ganglia. Figures 2.4B-D show magnified images of $P_{kcnl\text{-}2}$*kcnl-2(taa2)::gfp*, while Figures 2.4E-G show magnified images of $P_{kcnl\text{-}2}$*gfp::(atg2)kcnl-2*. It is noteworthy to mention that $P_{kcnl\text{-}2}$*kcnl-2(taa2)::gfp* was expressed in many neuronal processes innervating the vulva (Figure 2.4C), while $P_{kcnl\text{-}2}$*gfp::(atg2)kcnl-2* shows expression in the VC4 and VC5 neurons (arrows) of the egg-laying apparatus in addition to other neuronal processes innervating the vulva (Figure 2.4F). This absolute neuronal expression profile suggests that KCNL-2 in *C. elegans* functions similarly to mammalian SK channels in regulating the excitability of neurons.

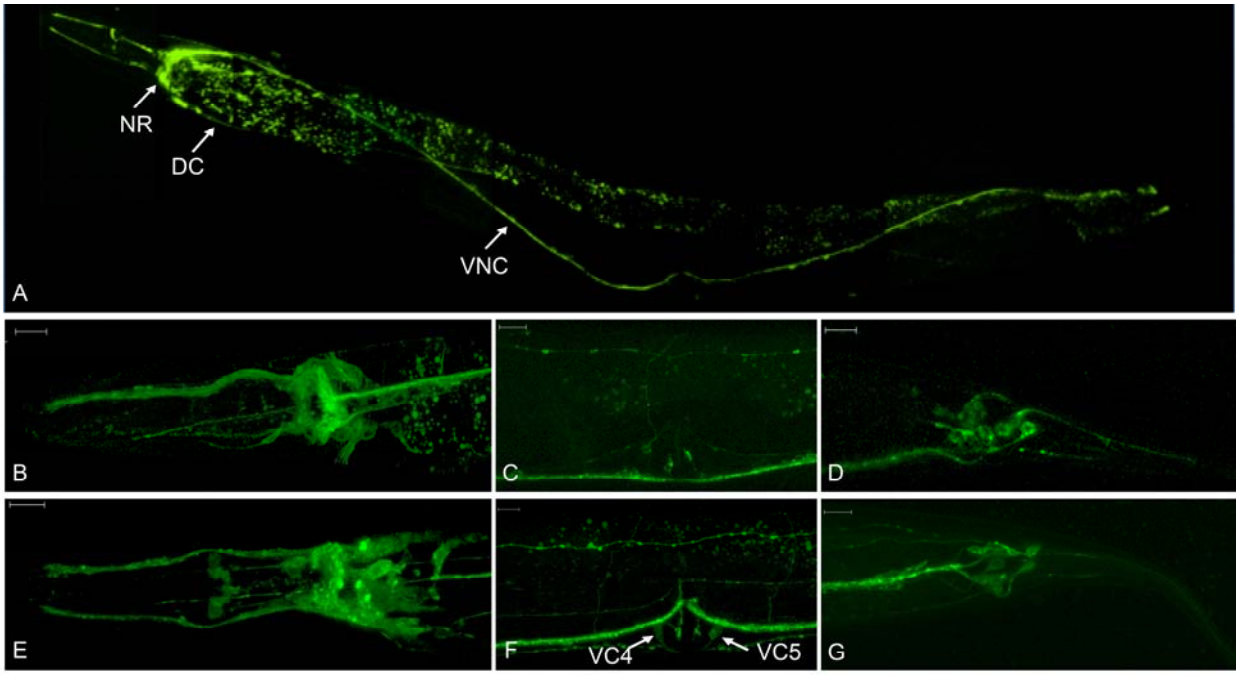

Figure 2.4. Expression pattern of KCNL-2.
A) The F08A10.1 gene was amplified from the WRM063DE08 fosmid and GFP was fused to the latter stop codon to produce a translational gene fusion that tagged the channel at the carboxy terminus. $P_{kcnl\text{-}2}$*kcnl-2(taa2)::GFP* localized to the neurons of the head, the NR, motor neurons of the VNC, the DC, the pharyngeal nervous system, and to tail ganglia (widefield fluorescent image). B-G. Magnified confocal images of $P_{kcnl\text{-}2}$*kcnl-2(taa2)::GFP* (B-D) and $P_{kcnl\text{-}2}$*gfp::(atg2)kcnl-2* (E-G) when expressed in the N2 background (Scale bar=10 μm). B,E. Neurons of the head, the pharyngeal nervous system, and cell bodies of the nerve ring. C) Neuronal processes innervating the vulva. F. Neuronal processes at the vulva, including the VC4 &VC5 cell bodies (arrows). D,G) Tail ganglia. Images were taken and processed by Cliff J. Luke.

Faint protein expression in tissues can be difficult to visualize. Since GFP diffuses freely throughout the cytoplasm of cells in which it is expressed, we made two constructs to drive GFP expression under the KCNL-2 promoter to aid in determining the complete expression profile of KCNL-2 that may be masked in transgenic lines that express GFP-tagged KCNL-2. The first construct, $P_{kcnl\text{-}2}$*(atg1)gfp*, encompassed the coding sequence of GFP which was expressed downstream of the promoter of KCNL-2 (1,951 bp upstream of atg1). The second construct,

$P_{kcnl\text{-}2}$*(atg2)gfp*, expressed GFP at the second initiation site where the coding sequences for KCNL-2-b and –c were deleted. As shown by Figure 2.5A-C, $P_{kcnl\text{-}2}$*(atg1)gfp* showed a neuronal expression profile with additional GFP-expression in the vulval muscles. As shown by Figure 2.5D-F, $P_{kcnl\text{-}2}$*(atg2)gfp* showed a strict neuronal expression profile that complemented the expression profile of the $P_{kcnl\text{-}2}$*kcnl-2::gfp* constructs. $P_{kcnl\text{-}2}$*(atg2)gfp* readily labels the VC4 and VC5 neurons and displays a highly innervated vulva, a feature that is lacking in the expression profile of $P_{kcnl\text{-}2}$*(atg1)gfp*. Ultimately, since both $P_{kcnl\text{-}2}$*(atg1)gfp* and $P_{kcnl\text{-}2}$*(atg2)gfp* are expressed in different neurons, this suggests that the various isoforms of KCNL-2 may have differing neuronal expression profiles.

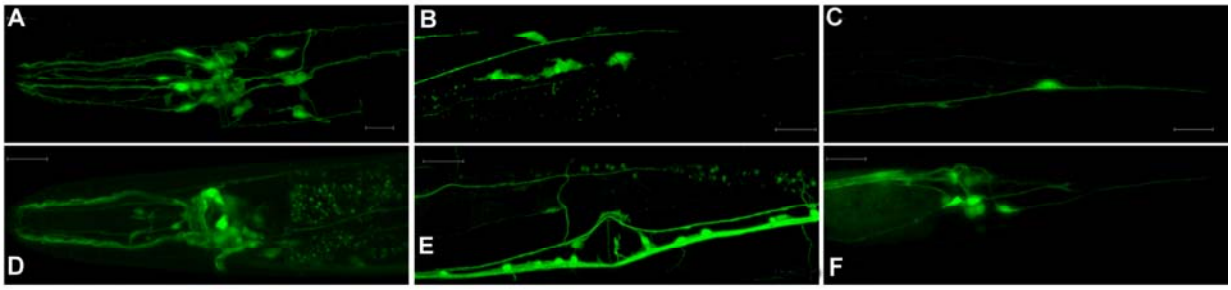

Figure 2.5. Confocal fluorescent images showing the expression pattern of the KCNL-2 promoter-GFP constructs.
A-C. $P_{kcnl\text{-}2}$*(atg1)gfp* is expressed in neurons of the head and NR (A), the vulval muscles (B), and in a cell body in the tail (C). D-F. $P_{kcnl\text{-}2}$*(atg2)gfp* is expressed in head neurons and NR (D); VNC, VC4 & VC5, and DC (E); and tail ganglia (F). Images were taken and processed by Cliff J. Luke.

2.2.4 Overexpression of KCNL-2 Causes a Hyperactive Egg-Laying Phenotype

The expression of KCNL-2 in neurons that innervate the vulva may implicate KCNL-2 in the regulation of the rate of egg-laying. To investigate this phenomenon, we carried out unlaid egg assays and egg-staging assays as described previously (Koelle and Horvitz, 1996). Hyperactive egg-laying mutants are characterized as having fewer eggs *in utero* and as laying a greater percent of early-stage eggs relative to wild type animals, while egg-laying defective (Egl) mutants expel their eggs less efficiently and retain a greater number of eggs *in utero* (Koelle and Horvitz, 1996; Mendel et al., 1995; Segalat et al., 1995). A fertilized egg develops *in utero* for approximately 2.5 to 3 hours in wild-type animals, at which point it has greater than 100 cells under normal developmental conditions. Behavioral assays were conducted on the non-integrated transgenic lines that overexpressed $P_{kcnl\text{-}2}$*kcnl-2(taa1)::gfp* and $P_{kcnl\text{-}2}$*kcnl-2(taa2)::gfp* in the N2 background, abbreviated KCNL-2(OE-1) and KCNL-2(OE-2) for overexpression lines 1 and 2, respectively. Egg-counting *in utero* or egg-staging assays were conducted on gravid adult hermaphrodites 36 hours after the late larval L4 stage at 20^{o}C. As shown in Figure 2.6A and 2.6B, the KCNL-2 overexpressing transgenic lines have a significantly fewer number of eggs *in utero*, whereas the *kcnl-2(tm1885)* animals have a significantly higher number of eggs *in utero* when compared to N2 animals. This phenomenon of fewer eggs retained *in utero* at the adult stage was demonstrated by eight independent transgenic lines and is suggestive of a hyperactive egg-laying phenotype. In both KCNL-2(OE-1) and KCNL-2(OE-2) strains, approximately 50% of the population of animals from 4 transgenic lines had fewer than or equal to 7 eggs retained *in utero* per worm. Egg-staging assays revealed that the proportion of young eggs from KCNL-2(OE-1) (54.8±4.4%) and KCNL-2(OE-2) (60.6±7.2%) was significantly

greater than those of N2 animals (2.8±2.8%). Taken together these data suggest that KCNL-2-overexpressing transgenic lines demonstrate a hyperactive egg-laying phenotype.

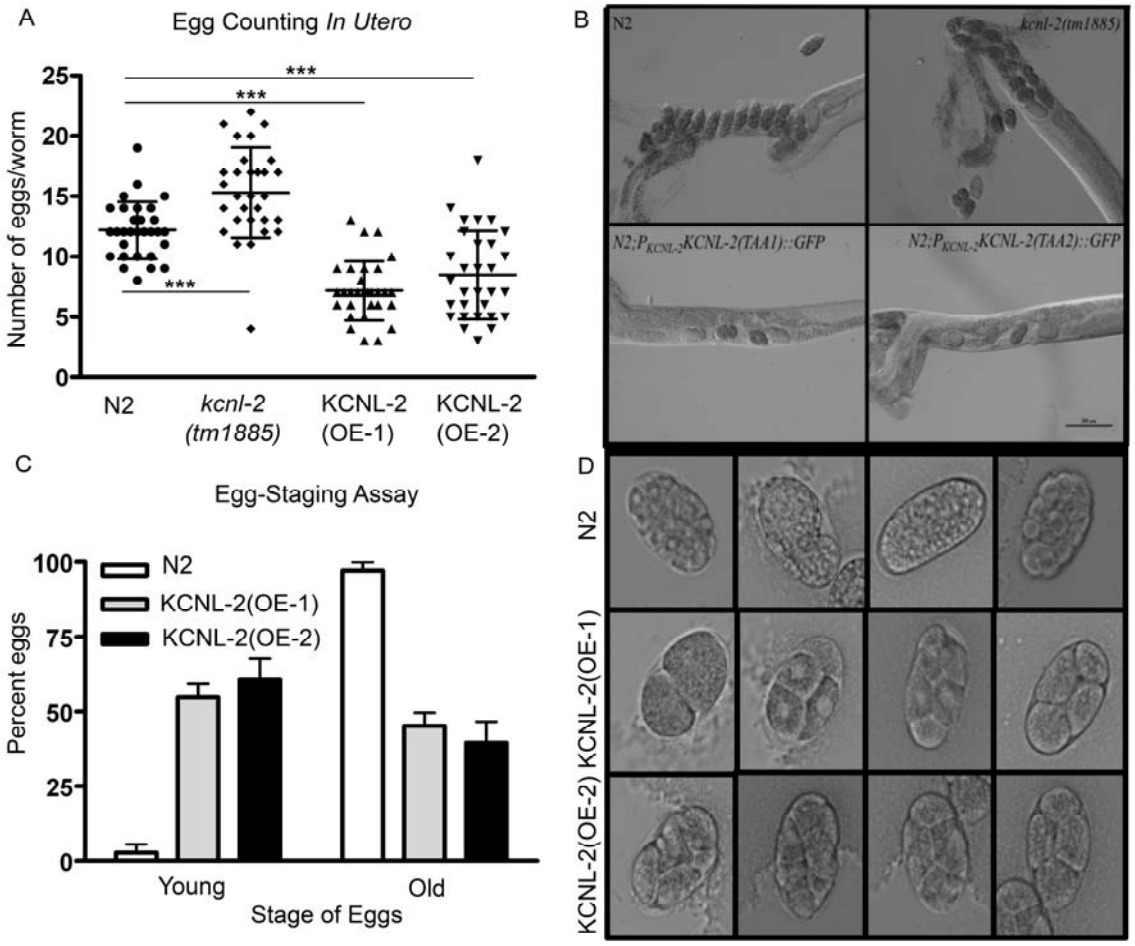

Figure 2.6. Overexpression of KCNL-2 in the N2 background causes a Hyperactive Egg-Laying Phenotype.
A) An unlaid egg assay was carried out by dissolving the cuticle of adult worms in 1.8% sodium hypochlorite and shows that the number of eggs *in utero* in transgenic lines that overexpress KCNL-2 are significantly less than the number of eggs retained *in utero* in N2 and *kcnl-2(tm1885)* strains ($p<0.001$), while *kcnl-2(tm1885)* has a significantly increased number of eggs retained *in utero* relative to N2 worms ($p<0.001$). B) Representative images of worms from each strain. C) Egg-staging assays reveal that the proportion of young eggs from KCNL-2(OE-1) (54.82±7.65%) and KCNL-2(OE-2) (60.57±12.48%) was significantly greater than those of N2 worms (2.78±4.81%) (n=3, $p<0.05$; Kruskal-Wallis *H* test).

To determine the role of KCNL-2 in the Egl phenotype seen in *kcnl-2(tm1885)* animals, we crossed *kcnl-2(tm1885)* worms with N2 males to create heterozygotes that were assayed for the number of eggs retained *in utero*. As shown in Figure 2.7A, *kcnl-2(tm1885)* animals consistently showed an increased number of eggs retained *in utero* relative to N2 animals. Heterozygotes retained an average number of eggs that was significantly greater than that of N2 animals, but significantly less than the average number of eggs found in the null strain. Therefore, the mild Egl phenotype demonstrated by *kcnl-2(tm1885)* animals was partially rescued in the heterozygotes. Additionally, we transformed the null strain with 1 ng/µl, 10 ng/µl or 90 ng/µl of $P_{kcnl\text{-}2}$*kcnl-2(taa2)::gfp* to generate lines KCNL-2(OE-3), KCNL-2(OE-4), and KCNL-2(OE-5), respectively (Figure 2.7). As shown in Figure 2.7B, the average number of eggs retained *in utero* by KCNL-2(OE-3) was not significantly different from the N2 animals, but was significantly different from the *kcnl-2(tm1885)* organisms. These results show that transformation of the null strain with 1 ng/µl KCNL-2 or crossing the null strain with N2 males rescued the Egl phenotype and supports our hypothesis that the Egl phenotype seen in *kcnl-2(tm1885)* organisms occurs specifically due to the loss of KCNL-2. Additionally, transgenic lines created with concentrations as low as 10 ng/µl $P_{kcnl\text{-}2}$*kcnl-2(taa2)::gfp* into the *kcnl-2(tm1885)* background (KCNL-2(OE-4)) produced the hyperactive egg-laying phenotype where the animals retained fewer eggs *in utero* than the wild-type and *kcnl-2(tm1885)* animals. Transformation of 90 ng/µl $P_{kcnl\text{-}2}$*kcnl-2(taa2)::gfp* into the *kcnl-2(tm1885)* background (KCNL-2(OE-5)) created a distribution that is not different from KCNL-2(OE-2). Additionally, KCNL-2(OE-4) and KCNL-2(OE-5) organisms lay a significantly greater proportion of early-stage eggs relative to N2 organisms and therefore these organisms hyperactively lay their eggs (Figure 2.7C). Generation of two opposing phenotypes, an Egl phenotype in the KCNL-2 null strain and

a hyperactive egg-laying phenotype in transgenic lines that overexpress KCNL-2, supports a specific role of KCNL-2 in the regulation of the rate of egg-laying.

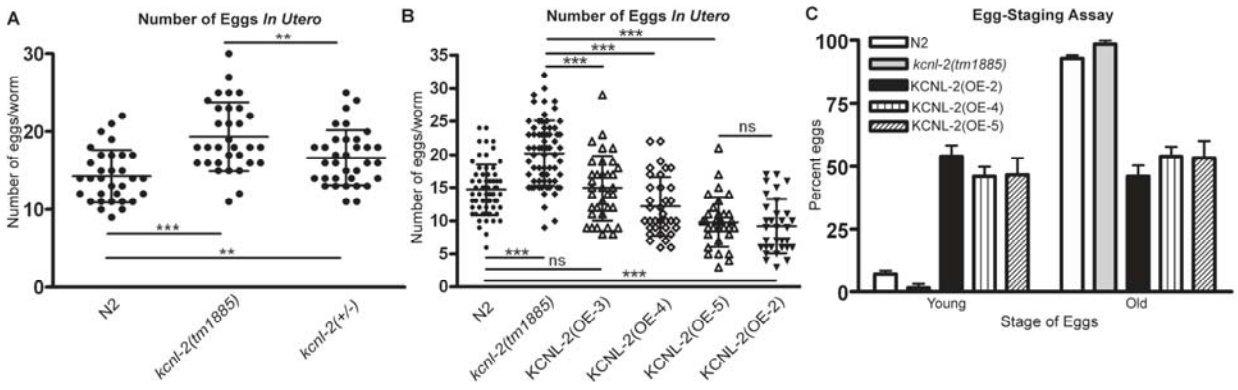

Figure 2.7. Rescue of the mild Egl phenotype shown by *kcnl-2(tm1885)* worms.
A) *kcnl-2(tm1885)* animals retain a significantly greater number of eggs *in utero* relative to N2 animals (P<0.0001). The number of eggs *in utero* in heterozygotes (*kcnl-2(-/+))* is significantly greater than that of the N2 animals (p=0.007), but significantly less than the average number of eggs found in *kcnl-2(tm1885)* animals (p=0.008). B) Transformation of *kcnl-2(tm1885)* with 1 ng/µl, 10 ng/µl or 90 ng/µl of $P_{kcnl\text{-}2}$*kcnl-2(taa2)::gfp* gives the transgenic lines KCNL-2(OE-3), KCNL-2(OE-4) and KCNL-2(OE-5), respectively. The average number of eggs retained *in utero* by KCNL-2(OE-3) was not significantly different from the N2 animals (P=0.8) but was significantly different from the *kcnl-2(tm1885)* organisms (p<0.0001). KCNL-2(OE-4) and KCNL-2(OE-5) retain fewer eggs *in utero* than N2 animals (p<0.005; p<0.0001, respectively) and *kcnl-2(tm1885)* animals (p<0.0001) (Student's *t* test). C) Egg-staging assays show that the proportions of young eggs from KCNL-2(OE-2) (54.0±4.3%), KCNL-2(OE-4) (46.0±3.9%), and KCNL-2(OE-5) (46.6±6.7%) are significantly greater than those of N2 (7.2±1.3%) & *kcnl-2(tm1885)* worms (1.6±1.6%) ((p<0.05; n=3, Kruskal-Wallis *H* test).

2.3 DISCUSSION

The human KCNN gene family has been linked to several neurological disorders, but the anatomical complexity of the mammalian nervous system limits studies of these channels in these model organisms. All 302 neurons in the *C. elegans* hermaphrodite have been identified and their development have been traced from the embryo to the adult stage (White et al., 1986a). Therefore, isolated neuronal circuits can be potentially teased apart from a larger network and the functions of its resident proteins can be studied in minimal circuits. *C. elegans* can therefore serve as a practical *in vivo* model to study the physiology of SK channels.

Utilizing a reverse genetics approach, we investigated the functions of KCNL-2 in a putative null strain, *kcnl-2(tm1885)*, and in transgenic strains that overexpress the channel. The *tm1885* mutation leads to the formation of a null channel since it results in a premature stop codon before the first transmembrane domain of the channel. These organisms are developmentally delayed and undergo larval arrest (Figure 2.3A). However, transformation of *kcnl-2(tm1885)* organisms with the KCNL-2 gene does not rescue this phenotype. Several explanations may account for this. It has been demonstrated that a truncated $K_{Ca}2.3$ isoform (SKCa3Δ) yields the amino terminus of the channel due to a premature stop codon before the first transmembrane domain and has a dominant negative effect on $K_{Ca}2.2$ currents (Miller et al., 2001). Similarly, expression of the amino terminal fragment of human $K_{Ca}2.2$ in Jurkat cells abolishes $K_{Ca}2.2$ currents (Fanger et al., 2001). Therefore, the expression of the amino terminus of KCNL-2 in *kcnl-2(tm1885)* mutants could conceivably suppress other natively expressed SK homologues that show an overlapping expression profile in *C. elegans*. In this case, the

phenotype would still be KCNL-2-specific, but cannot necessarily be attributed only to the loss of KCNL-2. More recently, sequences of additional splice variants of KCNL-2 have been deposited on Wormbase which suggests that the gene is 31, 227 base pairs in length and encodes several splice variants other than the ones described in this study (http://www.wormbase.org, WS231, 07.12.2012). All splice variants retain the same channel core but have differing amino and carboxy termini. Upon analysis of these sequences, the *tm1885* mutation would still result in null channels. However, the construct used for overexpression and rescue of knockout phenotypes spanned 12, 427 base pairs and did not encode the newly described splice variants. Therefore, rescue of the developmental delay and larval arrest seen in *kcnl-2(tm1885)* mutants may require all isoforms, but we did not investigate the function of these additional splice variants. Additionally, there remains a possibility that despite backcrossing the *kcnl-2(tm1885)* organisms with N2 worms eight times, extraneous mutations from TMP treatment may have remained in the *kcnl-2(tm1885)* genome. However, we did not further investigate this possibility.

Here we provide evidence that KCNL-2, an SK channel homologue, plays a role in regulating the rate of egg-laying. As shown by Figure 2.6A, *kcnl-2(tm1885)* mutants retain a significantly greater number of eggs *in utero* than N2 animals, however, this phenotype is relatively mild. This result is not surprising since mechanisms may exist to compensate for the loss of KCNL-2 by upregulating other potassium channel family members that show overlapping expression. Additionally, we show that the Egl phenotype displayed by *kcnl-2(tm1885)* organisms can be rescued by transformation of low DNA concentrations of KCNL-2 and by crossing with N2 males to produce heterozygotes, thereby further supporting the hypothesis that this phenotype occurs specifically due to the loss of KCNL-2. Approximately 50% of each

KCNL-2-overexpressing line showed two phenotypes characteristic of hyperactive egg-laying mutants: they retained fewer eggs *in utero* and greater than 50% of their newly laid eggs were early-stage eggs (Figure 2.6). The brood size of KCNL-2(OE-2) was not significantly different from that of N2 animals (Figure 2.2D), supporting the notion that there are no defects in fertility or gametogenesis otherwise.

The egg-laying apparatus consists of two HSNs, six VC neurons and sixteen egg-laying muscles, where the HSN and VC neurons are the only neurons that have been shown to synapse with the vulval muscles (White et al., 1986a). Defects in the egg laying apparatus can cause egg-laying defective or hyperactive egg-laying phenotypes. The HSNs stimulate egg-laying through the neurotransmitter serotonin by causing contraction of the 16 egg-laying muscle cells which leads to expulsion of eggs from the vulva (Koelle and Horvitz, 1996; Moresco and Koelle, 2004). However, the role of the VC neurons remains disputed as they have been shown to have dual functions of inhibition and stimulation of egg-laying (Bany et al., 2003; Kim et al., 2001; Zhang et al., 2008). Bany and colleagues showed that morphological defects and defects for the synthesis and packaging of acetylcholine in the VC neurons were the underlying basis for hyperactive egg-laying in nine mutants (Bany et al., 2003). Hyperactive egg-laying was ultimately due to the lack of inhibition of egg-laying (Bany et al., 2003). The hyperactive egg-laying phenotype observed in lines that overexpress KCNL-2 is reminiscent of that obtained when the VC4 & VC5 neurons were laser-ablated; that is, mutant animals that lacked VC4 & VC5 were shown to have a strongly hyperactive egg-laying phenotype where greater than 50% early stage eggs were laid by these organisms (Bany et al., 2003). Given that mammalian SK channel homologues function to cause the slow and medium afterhyperpolarization in neurons and that the KCNL-2-b and –c isoforms are expressed in the VC4 and VC5 neurons, we reasoned

that knockout of KCNL-2 would increase the excitability of the VC neurons, thereby increasing inhibition and slowing egg-laying (Bowden et al., 2001; Gerlach et al., 2004; Stocker et al., 1999). Conversely, overexpression would largely decrease the excitability of the VC neurons, slowing inhibition of egg-laying and ultimately leading to a hyperactive egg-laying phenotype. To define the mechanisms by which overexpression of KCNL-2 causes a constitutive egg-laying phenotype, we subcloned the KCNL-2aii cDNA and the region of the gene that encodes the KCNL-2-b and –c splice variants downstream of a VC-specific promoter, pMD64 (Bany et al., 2003). Overexpression of this construct in the VC neurons did not reproduce the hyperactive egg-laying phenotype (data not shown). Therefore, it is unlikely that the KCNL-2 channel functions in the VC neurons to produce this phenotype. Alternatively, given that $P_{kcnl\text{-}2}$*(atg1)gfp* and $P_{kcnl\text{-}2}$*(atg2)gfp* are expressed in different neurons and therefore, the KCNL-2 isoforms are very likely to be differentially expressed, it is possible that this phenotype occurs specifically due to overexpression of specific isoforms. However, this possibility was not further tested. Additionally, the $P_{kcnl\text{-}2}$*(atg1)gfp* construct shows expression in the vulval muscles. However, we postulate that KCNL-2 does not function to regulate the rate of egg-laying through the vulval muscles since overexpression of KCNL-2 would hyperpolarize the vulval muscles, decrease the contractility and cause an egg-laying defective phenotype, the opposite of the egg-laying constitutive phenotype seen in the KCNL-2-overexpressing lines. Additionally, none of the KCNL-2-GFP fusion constructs show observable expression in the vulval muscles, suggesting a negligible role in regulating the rate of egg-laying through expression in the vulval muscles.

In a genetic screen, KCNL-2 was identified as a modifier gene of the *C. elegans* survival of motor neuron (SMN) protein (Dimitriadi et al., 2010). KCNL-2 was shown to affect two of the resulting phenotypes from SMN loss of function (*Cesmn-1*) organisms (Dimitriadi et al.,

2010). Knockdown of KCNL-2 by RNAi in *Cesmn-1* mutants proved to enhance growth defects and to decrease pharyngeal pumping defects (Dimitriadi et al., 2010). As shown by Figure 2.4B and 2.4E, KCNL-2 is expressed in the somatic and pharyngeal nervous systems of *C. elegans* and therefore a function for KCNL-2 in pharyngeal pumping is highly conceivable. However, our attempts at RNAi knockdown of KCNL-2 were unsuccessful as RNAi treatment did not result in diminished $P_{kcnl\text{-}2}$*kcnl-2::gfp* expression in the neurons. The disparity in the RNAi results may have occurred since Dimitriadi *et al.* used strains that had wild-type copies of the channel, while we measured RNAi knockdown in transgenic lines that overexpressed the KCNL-2 channel (Dimitriadi et al., 2010). As noted by other investigators, RNAi-sensitive *C. elegans* mutant strains often exhibit abnormalities in their behavior. For example, the *rrf-3* strain has a decreased brood size which could hinder our studies of the egg-laying defects that occur as a function of KCNL-2 expression (Simmer et al., 2002). Alternatively, the $P_{unc\text{-}119}$*SID1* strain was transformed with $P_{kcnl\text{-}2}$*kcnl-2::gfp*, but we found that we did not get efficient RNAi knockdown in these transgenic strains (Calixto et al., 2010). Since RNAi in neurons is known to be inefficient and since loss of KCNL-2 leads to an Egl phenotype, while overexpression of KCNL-2 causes an Egl-C phenotype, we did not further pursue RNAi experiments.

As delineated by White and colleagues, in addition to the VC neurons, the posterior touch receptor (PLM) neurons and the PVNR form chemical synapses with the HSNs (White et al., 1986a). Inhibition of egg-laying occurs through the ALM and PLM touch receptor neurons which alter the activity of the HSNs (Sawin, 1996; Zhang et al., 2008). Additionally, neuropeptides released by the BAG neurons have been shown to inhibit egg-laying by stimulating EGL-6 which is expressed in the HSNs (Ringstad and Horvitz, 2008). Therefore, regulation of the rate of egg-laying is multi-faceted and can be limited by neurons outside the

perimeter of the egg-laying circuitry. Given the function of SK channels to regulate the excitability of cells and that KCNL-2 is vastly expressed in neuronal processes that innervate the vulva of the worm, our data supports a role of KCNL-2 in regulating the rate of egg-laying through its expression in neurons that inhibit egg-laying. However, the identity of these neurons remains to be determined.

3.0 CONCLUSION AND FUTURE DIRECTIONS

K^+ channels function to regulate the excitability of cells in which they are expressed and disruption of this function often links K^+ channels to diseases of the nervous and muscular systems. Members of the K_v, SK and BK channel families function to regulate neuronal firing frequency and maintenance of this pacemaker activity is crucial for the proper functioning of the nervous system. As a result, K^+ channels from different families or within the same family often contribute to overlapping functions within the nervous system. Due to the complexity of the mammalian nervous system and the existence of numerous redundant mechanisms to compensate for the loss of function of any particular K^+ channel, simpler model organisms are sought to study the physiological functions of K^+ channels. As detailed in the Introduction, knowledge about the roles of K^+ channels in diseases and compounds that inhibit/activate K^+ channel function have been gained through the study of K^+ channels in model organisms.

Since the hierarchy of K^+ channels found in mammals is conserved in *C. elegans*, the study of K^+ channels in this organism has allowed the characterization of mutations that often have parallel biophysical and physiological roles of their mammalian orthologues (Salkoff et al., 2005). Both the *Shaker* and EAG channels were first identified in *Drosophila* due to an overt leg-shaking phenotype of mutants on exposure to ether (Papazian et al., 1987). These discoveries led to the identification of other voltage-gated K^+ channels within the same family in *Drosophila* such as the *Shab*, *Shaw* and *Shal* channels (Butler et al., 1989). These K_v channels

were subsequently cloned in mammals. Similarly, the use of *C. elegans* as a model organism has also allowed the identification of novel mutations in K^+ channels that cause behavioral abnormalities in the worm. For example, EXP-2 is a K_v channel in *C. elegans* that is functionally similar to HERG channels in determining the shape and duration of pharyngeal and cardiac action potentials, respectively (Davis et al., 1999). Study of this channel in *C. elegans* allowed the identification of a gain-of-function mutation in EXP-2 (C480Y) that favors the open conformation of the channel and alters the shape and duration of pharyngeal action potentials (Davis et al., 1999). Pharyngeal actions potentials are a model for cardiac action potentials and drugs that target K^+ channels or their β-subunits that are involved in arrhythmia are being investigated in *C. elegans*. For example, it was demonstrated that EGL-2 in *C. elegans*, an EAG K^+ channel homologue, was inhibited by the antidepressant imipramine, which can induce arrhythmia in humans (Weinshenker et al., 1999). Prior to this, it was unknown that an EAG channel homologue is a target of imipramine and this investigation therefore provided a feasible mechanism by which imipramine could induce arrhythmia in humans. *C. elegans* is therefore an invaluable model organism to study K^+ channel function.

Through the generation of the medium component of the AHP in the CNS, SK channels are implicated in controlling the firing patterns of neurons of the hippocampal pyramidal neurons, DA midbrain neurons, Purkinje cells, and the DCN and as a result, SK channels are linked to diseases of the CNS such as episodic ataxia type 2, epilepsy, Parkinson's disease and Schizophrenia (Pedarzani and Stocker, 2008). Expression of SK2 in the hippocampal CA1 pyramidal neurons also implicates the channel in learning and memory functions (Lin et al., 2008; Ngo-Anh et al., 2005). The use of mouse models has allowed the study and confirmation of the physiological roles for SK channels in the CNS. A mouse model for cerebellar ataxia was

developed where SK channel function was disrupted in the CNS by expressing a truncated SK3 transcript, SK3-1B-GFP, that has a dominant negative effect on other SK channels (Shakkottai et al., 2004). Expression of SK3-1B-GFP in the DCN of the cerebellum in mice resulted in the defining phenotypes of cerebellar ataxia (Shakkottai et al., 2004). These mouse models demonstrate the importance of SK channels in the generation of the AHP, disruption of which leads to diseases of the CNS. Therefore SK channels are pharmacological targets to regulate neuronal pacemaker activity for the treatment of various neurological disorders. Disparities in mammalian models are observed due to the complexity of their nervous systems, the existence of redundant mechanisms to compensate for the loss of SK channels and because the expression of an incomplete channel can lead to a dominant negative effect on other SK channels instead of simple knockout of channel function. For example, in the *frissonant* mouse model the first and second coding exons of the KCNN2 gene are disrupted which leads to the formation of two abnormal transcripts that were identified in the brain of heterozygous and homozygous mice (Szatanik et al., 2008). This mutation resulted in elimination of the AHP in the MVN neurons and in severe neurological phenotypes (Szatanik et al., 2008). Alternatively, overt behavioral deficits were not reported for a KCNN2 knockout mouse model (Bond et al., 2004). The abnormal transcripts that were identified in the *frissonant* mouse model may in turn exert a dominant negative effect on other SK channel homologues expressed in the CNS and this may account for the differences in behaviors observed between this model and the mouse model described by Adelman and colleagues (Bond et al., 2004; Szatanik et al., 2008).

There are four SK channel homologues in *C. elegans*: KCNL-1 (Clone B0399.1), KCNL-2 (Clone F08A10.1), KCNL-3 (Clone C03F11.1), and KCNL-4 (Clone C53A5.5). In this thesis, I characterized the expression pattern and functions of KCNL-2. The KCNL-2 isoforms are less

than 30% identical to the KCNL-1, -3 and -4 genes, with the most noticeable homology being in the pore domain. Limited studies have been done on KCNL-1 and KCNL-3 and have been reported in *International Worm Meeting* abstracts. It was reported that a transcriptional GFP fusion to the KCNL-1c splice variant results in expression in the vulval muscles, anal depressor muscle and in unidentified neurons (Frokjar-Jensen et al., 2007). An unidentified gain-of-function mutation in KCNL-1 was reported to result in defective egg laying and enteric muscle contraction (Frokjar-Jensen et al., 2007). Based on the expression profile of a $P_{kcnl\text{-}3}$*gfp* construct, it was reported that KCNL-3 is expressed in the amphid neurons, ventral cord motor neurons, and tail ganglia (Buechner et al., 2007). This SK channel homologue was also reported to be bound to calmodulin and to evoke apamin-sensitive currents (Buechner et al., 2007). Based on these reports, it is likely that the KCNL channels function similarly to mammalian SK channels to regulate the excitability of cells in which they are expressed. As described in the Introduction, there are numerous advantages to using *C. elegans* as a model organism and it would therefore serve as a valuable system to gain further insight into the regulation of SK channel activity and the physiological functions of SK channels.

3.1 LOCALIZATION OF KCNL-2

The first aim of my thesis research was to investigate the expression profile of KCNL-2. As described previously, the KCNL-2 coding sequence used in this project spans 12, 500 bp and encodes up to six splice variants (KCNL-2a through e, Figure 2.1). In this study, I used the unspliced KCNL-2 gene for all experiments unless otherwise noted. The organisms were transformed with constructs of KCNL-2 fused with GFP at either the amino or carboxy terminus.

Tagging the channel at the carboxy termini, $P_{kcnl\text{-}2}$*kcnl-2(taa1)::gfp* or $P_{kcnl\text{-}2}$*kcnl-2(taa2)::gfp*, did not distinguish between the splice variants that spanned the entire coding sequence (a, aii, d, and e) versus the splice variants that spanned the last 3 kb of the gene (b and c). However, tagging the channel at the amino termini, $P_{kcnl\text{-}2}$*gfp::(atg1)kcnl-2* or $P_{kcnl\text{-}2}$*gfp::(atg2)kcnl-2*, distinguished between these splice variants. As shown by Figure 2.4, KCNL-2 is expressed throughout the nervous system and more specifically, KCNL-2 localizes to neurons of the nerve ring, pharyngeal nervous system, VNC, dorsal cord, processes innervating the vulva, and tail ganglia. $P_{kcnl\text{-}2}$*kcnl-2(taa2)::gfp* has a different expression profile from $P_{kcnl\text{-}2}$*gfp::(atg2)kcnl-2*. As is shown by the magnified images in Figures 2.4B-G, the most notable difference occurs at the vulva where $P_{kcnl\text{-}2}$*gfp::(atg2)kcnl-2* is expressed in the VC4 and VC5 neurons and in other neuronal processes innervating the vulva, while $P_{kcnl\text{-}2}$*kcnl-2(taa2)::gfp* occurs only in unidentified processes innervating the vulva. This suggests that various isoforms of KCNL-2 are differentially expressed. Greater insight into the differential expression of the KCNL-2 isoforms was obtained by observing the expression patterns of the KCNL-2 promoter-GFP constructs as described in detail below. While KCNL-2 is expressed in the major ganglia of the worm, the channel is not expressed in the entire nervous system. For example, KCNL-2 expression is clearly absent from the HSNs whose cell bodies occur at the vulva and processes extend to the nerve ring (Garriga et al., 1993). Additionally, the described KCNL-2 constructs are not expressed in the GABA nervous system of *C. elegans* (Schuske et al., 2004).

In order to determine the physiological functions of KCNL-2 in *C. elegans*, it was necessary to identify specific neurons in which the gene is expressed. Since KCNL-2 is expressed in multiple motor neurons along the VNC and in the nerve ring, identification of individual neurons based on cell body location proved to be difficult. Since GFP diffuses freely throughout the

cytoplasm of cells in which it is expressed and can aid in the identification of cells in which KCNL-2 is faintly expressed, two constructs were made to drive GFP expression under the KCNL-2 promoter. $P_{kcnl\text{-}2}$*(atg1)gfp* encompassed 1,951 bp upstream of atg1 and the coding sequence of GFP and in the $P_{kcnl\text{-}2}$*(atg2)gfp* construct, GFP was subcloned upstream of atg2 without disturbing the upstream coding sequence of KCNL-2. As shown by Figure 2.5, $P_{kcnl\text{-}2}$*(atg1)gfp* and $P_{kcnl\text{-}2}$*(atg2)gfp* do not show an overlapping expression profile. That is, $P_{kcnl\text{-}2}$*(atg1)gfp* (Figure 2.5A) is expressed in unidentified neurons of the head that are different from those in which $P_{kcnl\text{-}2}$*(atg2)gfp* is expressed (Figure 2.5D). Additionally, $P_{kcnl\text{-}2}$*(atg1)gfp* is expressed in neurons that resemble the touch receptor neurons described as the anterior lateral microtubule cells (ALM neurons) (Figure 2.5B) and the posterior lateral microtubule cells (PLM neurons) with a conspicuous ciliated cell body in the tail region (Figure 2.5C). Figure 2.5B also shows that the $P_{kcnl\text{-}2}$*(atg1)gfp* construct is also expressed in the vulval muscles, while $P_{kcnl\text{-}2}$*(atg2)gfp* is clearly absent from all muscle cells (Figure 2.5E). The expression profile of $P_{kcnl\text{-}2}$*(atg2)gfp* is vastly different from that of $P_{kcnl\text{-}2}$*(atg1)gfp* since expression of the latter construct is only visible in one neuron running along the VNC, while $P_{kcnl\text{-}2}$*(atg2)gfp* expression is observed in multiple neuronal processes and cell bodies along the VNC (Figure 2.5E) and in as many as eight cell bodies in the lumbar ganglia (Figure 2.5F). Additionally, $P_{kcnl\text{-}2}$*(atg2)gfp* is expressed in the VC4 and VC5 neurons and in additional neuronal processes that innervate the vulva (Figure 2.5E). Interestingly, $P_{kcnl\text{-}2}$*gfp::(atg1)kcnl-2* expression was observed in the nervous system but not in the egg-laying neurons or the vulval muscles (data not shown), while $P_{kcnl\text{-}2}$*gfp::(atg2)kcnl-2* was expressed throughout the nervous system and in VC4 and VC5 (Figure 2.4E-G). This data suggests that the isoforms of KCNL-2 are differentially expressed and that there are localization signals within the introns of KCNL-2 that may be pertinent to

KCNL-2 function. In the splice variants that span the entire coding sequence of the gene used in this investigation (KCNL-2-a, -aii, -d and –e), two longer introns occur after the first three exons (~3kb and ~6 kb, respectively). Images of $P_{kcnl\text{-}2}$*(atg1)gfp* and $P_{kcnl\text{-}2}$*(atg2)gfp* shown in Figure 2.5 supports the hypothesis that localization signals are encoded by these intronic expanses since deletion of the KCNL-2 coding sequence in the $P_{kcnl\text{-}2}$*(atg1)gfp* construct drives protein expression in a different subset of neurons from those identified in transgenic organisms expressing $P_{kcnl\text{-}2}$*(atg2)gfp*. A necessary future direction would be to define the location of other neuronal cell bodies in which KCNL-2 is expressed through microscopy to facilitate the identification of physiological functions based on the expression profile.

3.2 KCNL-2-NULL ORGANISMS EXHIBIT A POST-EMBRYONIC DEVELOPMENTAL DELAY

The second aim of my thesis was to characterize the phenotypes of a KCNL-2-null strain, *kcnl-2(tm1885)*, and of transgenic lines that overexpress KCNL-2, KCNL-2(OE-1) and KCNL-2(OE-2). A phenotypic anomaly was observed when investigating the brood size of *kcnl-2(tm1885)* organisms. That is, the brood size of *kcnl-2(tm1885)* organisms is significantly smaller than that of N2 animals (Figure 2.2B). Further analysis of *kcnl-2(tm1885)* animals showed the knockout worms are developmentally delayed and that this developmental delay is mostly attributed to larval arrest of a large population of the knockout worms (Figure 2.3 and Figure A.1). That is, 88.1 ± 3.0% of N2 worms and 47.9 ± 6.9% of knockout worms developed normally, 8.8 ± 1.9% of N2 worms and 19.2 ± 3.7% of knockout worms developed slowly, and 3.7 ±1.4% of N2

worms and 32.9 ± 6.1% of knockout worms were arrested at the L1-L3 larval stage. Loss of this population of the progeny due to larval arrest accounts for the smaller brood size of *kcnl-2(tm1885)* organisms. However, transformation of *kcnl-2(tm1885)* organisms with the KCNL-2 gene did not rescue these phenotypes. The reasons for the lack of rescue have been discussed in greater detail in Chapter 2. The *tm1885* mutation can potentially lead to the expression of the amino terminus of the KCNL-2 channel since a premature stop codon occurs before the first transmembrane domain (Figure 2.1C). As discussed previously, it has been demonstrated that the amino termini of mammalian $K_{Ca}2.2$ and $K_{Ca}2.3$ have a dominant negative effect on $K_{Ca}2.2$ currents (Miller et al., 2001; Fanger et al., 2001). Expression of the amino terminus of KCNL-2 in *kcnl-2(tm1885)* mutants could therefore have a dominant negative effect on the other SK channel homologues that show an overlapping expression profile. A future experiment in order to test this possibility would be to generate transgenic lines that express an equivalent amino terminus of KCNL-2 and to subsequently analyze the post-embryonic development of the organisms. As discussed previously, sequences of additional splice variants of KCNL-2 (-f, -g, and -h) have recently been identified which suggests that the gene is 31, 227 base pairs in length (http://www.wormbase.org, WS231, 07.12.2012). However, the KCNL-2 gene that was amplified from the WRM063DE08 fosmid spanned 12, 427 base pairs and encodes splice variants KCNL-2-a through -e. Therefore, the alternative splice variants of KCNL-2 could be required for rescue of the developmental delay and larval arrest seen in *kcnl-2(tm1885)* mutants. Future studies would require cloning the full-length KCNL-2 gene that encodes all splice variants from genomic DNA and transforming the *kcnl-2(tm1885)* organisms with the full length gene to investigate the possibility of rescuing these developmental defects. And finally, extraneous mutations from TMP treatment may not have been removed from the *kcnl-2(tm1885)*

genome via backcrossing with the N2 animals. To correct for this possibility, the *kcnl-2(tm1885)* organisms were backcrossed eight times with N2 organisms to remove greater than 99.6% spurious mutations, however the developmental delay still persists after these crosses. Mutations that are in close proximity to the *kcnl-2(tm1885)* mutation would be more difficult to eliminate via outcrossing, so there still remains a possibility that the developmental delay is not specific to *kcnl-2(tm1885)*.

A role for KCNL-2 in the embryonic development of *C. elegans* is supported by Anne Hart and colleagues who showed that knockdown of KCNL-2 by RNAi in *Cesmn-1* (*C. elegans* survival of motor neuron (SMN) protein) mutants intensified their growth defects (Dimitriadi et al., 2010). One explanation for this observed phenotype could be that the pre-existing growth defects of *Cesmn-1* mutants are exacerbated since *kcnl-2(tm1885)* animals are developmentally delayed. While Hart and colleagues were successful in observing phenotypes as a result of RNAi knockdown of KCNL-2 in the wild-type background, I could not confirm the developmental delay observed in *kcnl-2(tm1885)* organisms by RNAi since RNAi treatment did not result in diminished $P_{kcnl\text{-}2}$*kcnl-2(taa2)::gfp* expression in the neurons when using a clone from the Ahringer library (Figure A.2) (Kamath, 2003). This result was not surprising as it is a well-accepted fact that neurons in *C. elegans* are refractory to RNAi because of their lack of expression of SID-1 (Calixto et al., 2010). Hence, I obtained a strain of worms in which SID1 was expressed under a pan neuronal marker, UNC-119, and I transformed the $P_{unc\text{-}119}$SID1 worms with $P_{kcnl\text{-}2}$*kcnl-2::gfp* and subjected these organisms to RNAi-treatment. The KCNL-2 channel expression was not efficiently knocked down in these organisms. Various strains have been engineered that are more susceptible to RNAi in the nervous system, however they may

present alternative disadvantages as discussed in Chapter 2. Therefore, RNAi experiments were not included in this investigation.

3.3 KCNL-2 PLAYS A ROLE IN THE REGULATION OF THE RATE OF EGG-LAYING

Analysis of the rate of egg-laying in KCNL-2 mutant worms also revealed atypical behavior. That is, the *kcnl-2(tm1885)* animals are mildly egg-laying defective (Egl), while eight independent transgenic lines that overexpress KCNL-2 are egg-laying constitutive (Egl-C) (Figure 2.6). Additionally the Egl phenotype of *kcnl-2(tm1885)* organisms was rescued in a dose-dependent manner, supporting that this phenotype is KCNL-2-specific (Figure 2.7). Transformation of 90 ng/µl $P_{kcnl\text{-}2}$*kcnl-2(taa2)::gfp* into the *kcnl-2(tm1885)* or N2 background produces a hyperactive egg-laying phenotype. As shown in Figure A.3, a specific role for KCNL-2 in the regulation of the rate of egg-laying is demonstrated by the Egl-C phenotype shown in two independent transgenic lines that overexpress the KCNL-2aii coding sequence under its endogenous promoter. The $P_{kcnl\text{-}2}$*gfp::kcnl-2aii* construct is expressed in two pairs of unidentified neurons in the head and in one cell body occurring in the tail (Figure A.3 A-E). The transgenic lines *KCNL-2aii-1 and -2* have significantly fewer eggs *in utero* per adult worm relative to N2 worms ($P<0.0001$), while the average number of eggs *in utero* per worm in these transgenic lines is not significantly different from that of KCNL-2(OE-2) ($P>0.5$). This data suggests that KCNL-2 plays a role in the regulation of the rate of egg-laying in neurons outside the described egg-laying circuitry, although these neurons remain to be identified. Generation of two opposing phenotypes, an Egl phenotype in the KCNL-2 null strain and a hyperactive egg-

laying phenotype in transgenic lines that overexpress KCNL-2, supports a specific role of KCNL-2 in the regulation of the rate of egg-laying.

As discussed in the Introduction, EGL-36 is a K_v channel in *C. elegans* that functions in the regulation of the rate of egg-laying through its expression in the vulval muscles. Gain-of-function mutations in EGL-36 (*egl-36(gf)*) cause an Egl phenotype, while a dominant negative mutation in the *egl-36(gf)* background rescued the Egl phenotype and produced an Egl-C phenotype (Elkes et al., 1997; Johnstone et al., 1997). It is important to note that loss-of-function mutations in EGL-36 did not alter the rate of egg-laying (Johnstone et al., 1997). So to, the mild egg-retentive phenotype observed in *kcnl-2(tm1885)* organisms is not surprising since alternative K^+ channels could be upregulated to compensate for the loss of KCNL-2. Based on this principle, I hypothesized that overt phenotypes would be more readily visible through overexpression of KCNL-2, which would hyperpolarize neurons in which they are expressed. In agreement with this, the Egl-C phenotype in transgenic lines KCNL-2(OE-1) and KCNL-2(OE-2) resulted in approximately 50% young eggs being laid by adults, characteristic of a strong hyperactive egg-laying phenotype.

When assaying egg-laying in KCNL-2(OE1) and KCNL-2(OE2), I used an *N2;*P_{kcnl-2}*(atg1)gfp* transgenic line as a control. As shown in Figure A.4, I found that expression of GFP under the endogenous promoter caused lethality of these worms. That is, the median survival of N2 worms was 291.5 hrs and that of *N2;*P_{kcnl-2}*(atg1)gfp* was 220 hrs, while the longevities of KCNL-2(OE1) and KCNL-2(OE2) were not significantly different from that of the N2 organisms. A percentage of the *N2;*P_{kcnl-2}*(atg1)gfp* worms showed a severe egg-laying defective phenotype where the embryos hatched within the adult worm, the opposite phenotype observed in KCNL-2-overexpressing lines. Since *N2;*P_{kcnl-2}*(atg1)gfp* is expressed in the vulval muscles, it

is possible that the strong Egl phenotype seen in these worms are due to toxicity induced by GFP overexpression in these cells. As discussed previously, the KCNL-2 gene is complex with unusually large introns and multiple splice variants and it remains a possibility that the *N2;P$_{kcnl-2}$(atg1)gfp* construct contains transcriptional factors that may contribute to this phenotype. Therefore, the *N2;P$_{kcnl-2}$(atg1)gfp* strain was not found to be an optimal control. Based on these experiments, I exclude the possibility that overexpression of KCNL-2 causes a non-specific phenotype as seen in the *N2;P$_{kcnl-2}$(atg1)gfp* organisms.

Based on the observed phenotypes, I sought to identify the mechanism by which knockout or overexpression of KCNL-2 would alter the rate of egg-laying. The literature supports a role for the VC neurons in the inhibition of egg-laying. Defects that affect the function of the VC neurons have been shown to cause hyperactive egg-laying in several mutants due to the lack of inhibition of egg-laying (Bany et al., 2003). Additionally, in *egl-1(n986)* mutants and in *lin-39(n709)* mutants, the HSNs and the VC neurons undergo premature cell death, respectively. In *egl-1(n986)* mutants the VCs remain largely inactive, while in *lin-39(n709)* mutants the HSNs become hyperactive, supporting an interdependence between these two subsets of neurons (Zhang et al., 2008). Calcium transients in both sets of neurons are coupled to egg-laying events, suggesting that the HSNs and the VCs act synergistically to control the rate of egg-laying events in *C. elegans* (Zhang et al., 2008). The pMD64 promoter drives expression of genes specifically in the ventral type C neurons (1-6) and in vulval muscles (Bany et al., 2003). In an effort to determine if KCNL-2 regulates the rate of egg-laying through its expression in the VC neurons, I expressed the channel downstream of the pMD64 promoter while deleting the KCNL-2 promoter region (Bany et al., 2003). As shown in Figure A.5, expression of *pMD64kcnl-2(taa2)::gfp* was not limited to the VC neurons and vulval cells as described**,** suggesting that regulatory elements

within the introns of KCNL-2 dictate expression of the channel in the nervous system of the worm. As discussed previously, the KCNL-2b and –c isoforms localize to the VC4 and 5 neurons and based on this expression pattern, worms were transformed with the KCNL-2 gene encoding the -b and –c isoforms downstream of the pMD64 promoter (Figure A.6). These transgenic worms did not demonstrate a hyperactive egg-laying phenotype. Additionally, expression of KCNL-2-a, -aii, and –b cDNA clones downstream of the pMD64 promoter showed a faint and mosaic expression pattern and did not give a consistent hyperactive egg-laying phenotype. Therefore, the data did not support a role for KCNL-2 in the regulation of the rate of egg-laying through its expression in the VC neurons.

An alternative neuronal pathway that is involved in the regulation of the rate of egg-laying involves the ALM and PLM mechanosensory neurons (Sawin, 1996). In the dissertation research of Sawin, inhibition of egg-laying occurred due to mechanical stimulation through vibration (Sawin, 1996). The ALM and PLM touch receptor neurons chemically innervate the HSNs and alter their activity (Sawin, 1996; Zhang et al., 2008). When stimulated by vibration, mutant animals in which the ALM and PLM neurons were laser-ablated laid eggs at a rate that was not different from the control animals that were not stimulated by vibration, while ablation of either the ALM or PLM neuron still led to sensitivity to vibration. Interestingly, KCNL-2 a, aii, d and e isoforms are expressed in these mechanosensory neurons, however its role exclusively in these neurons has not been tested (Figure 2.5). In addition to the mechanosensory and VC neurons, neuropeptides released by the BAG neurons have been shown to inhibit egg-laying by stimulating EGL-6 which is expressed in the HSNs (Ringstad and Horvitz, 2008). KCNL-2 is expressed in many unidentified neurons of the head, but its role in regulating the role

of egg-laying through its expression in the BAG neurons is doubtful since ablation of these neurons does not result in a hyperactive egg-laying phenotype (Ringstad and Horvitz, 2008).

In summary, I have shown that knockout of KCNL-2 causes an Egl phenotype that is rescued in transgenic lines where *kcnl-2(tm1885)* organisms were transformed with 1ng/ul KCNL-2. I have also shown that overexpression of KCNL-2 consistently causes an Egl-C phenotype in multiple independent transgenic lines. KCNL-2 is highly expressed in multiple neuronal pathways that innervate the vulva. Given the function of SK channels to regulate the excitability of neurons in which they are expressed, I propose that loss of function of KCNL-2 increases the excitability of a neuronal pathway that inhibits egg-laying by acting on the vulval muscles thereby causing an Egl phenotype. Conversely, I propose that overexpression of KCNL-2 hyperpolarizes this undefined inhibitory neuronal pathway, thereby decreasing its action potential firing frequency and causing a hyperactive egg-laying phenotype. It remains to be defined what the mechanism is by which KCNL-2 regulates the rate of egg laying. The availability of promoter constructs to drive the expression of KCNL-2 in isolated neuronal pathways offers the opportunity to further study KCNL-2 and its physiological functions in *C. elegans*.

3.4 BIOPHYSICAL PROPERTIES OF KCNL-2

A previous aim of this dissertation research was to study the electrophysiological properties of the splice variants of KCNL-2 in a heterologous expression system. I carried out preliminary experiments to establish this system. I tagged the KCNL-2-a and –c splice variants at the amino terminus with a V5 epitope and carried out western blots of transiently transfected HEK293 cells

using the V5 mouse monoclonal antibody. As shown by Figure A.7, the molecular weight of the isolated protein was ~75 KDa as expected for these splice variants. I transiently transfected HEK293 cells with the KCNL-2-a, -aii, -b, or -c cDNA constructs that were tagged at the carboxy terminus with YFP. Each splice variant appeared to be mostly trapped intracellularly as determined by widefield fluorescence microscopy (Figure A.8). In addition, I was unable to record currents from stable HEK293 cell lines expressing the KCNL-2 cDNA clones using excised patch clamp techniques. These results are not surprising since mammalian cells may not encode the necessary machinery required for folding, assembly or trafficking of the channel to the plasma membrane. For example, the KCa3.1c isoform is expressed at the cell surface only in the presence of a BK channel β-subunit (Barmeyer et al., 2010). I propose cell surface biotinylation experiments of cell lines expressing the KCNL-2a-V5 and KCNL-2c-V5 constructs. If these experiments confirm the expression of the KCNL-2 splice variants at the cell surface membrane, whole cell patch clamp can be employed on the stable HEK293 cell lines described in the methods to study the biophysical properties of these channels.

An alternative strategy would be to study the biophysical properties of KCNL-2 in cultured *C. elegans* cells. *C. elegans* embryonic cells undergo morphological differentiation in cell culture to form cell types found in L1 larvae, which are mostly neuronal and muscular cells (Christensen et al. 2002). Expression of KCNL-2 would be determined by visualizing the expression of GFP-tagged constructs. The caveat of this protocol would be to distinguish between the biophysical properties of KCNL-2 and its homologues, which are expressed in muscle and neurons as well, since the biophysical properties of these channels are not characterized. It would therefore be necessary to obtain a strain of *C. elegans* in which the KCNL-1, -3 and -4 channels are knocked out, however the survival of such organisms may be

affected due to the loss of these channels. Another major disadvantage of this protocol is the inability to distinguish between the specific splice variants. It would be essential to understand the biophysical properties of KCNL-2 in order to study the effects of mutations and/or to study the effects of pharmacological inhibitors/activators in neuronal circuits.

3.5 THE STUDY OF SK CHANNEL TRAFFICKING

Given the role of SK channels in regulating neuronal function, these channels are valuable pharmacological targets for the treatment of various diseases of the CNS. Since the number of ion channels expressed at the plasma membrane determines the cumulative physiological effects of a particular ion channel, trafficking of SK channels is a pertinent field of study which could lead to the development of new therapeutic options (Balut et al., 2012). In *C. elegans*, members of the endocytosis and recycling machinery have conserved functions with their mammalian counterparts and as a result, *C. elegans* have been established as a model organism to study protein trafficking (Grant and Donaldson, 2009; Grant and Sato, 2006). For example, the endocytic Rab proteins and the receptor-mediated endocytosis (rme) genes are functionally conserved in *C. elegans* (Grant and Sato, 2006). Since KCNL-2 is naturally expressed in the nervous system of the worm, trafficking of the channel can be studied in the neurons. Additionally, I would drive expression of KCNL-2 in the intestinal cells using the NHX-2 promoter since this organ system allows biochemical methods such as western blots and co-immunoprecipitation assays that are otherwise difficult in neurons (Nehrke and Melvin, 2002).

3.6 CONCLUSION

The ultimate goal of this dissertation research was to establish a pathophysiological model system to study the phenotypes that result from altering SK channel activity *in vivo*. The first aim of this thesis was to determine the cellular localization of KCNL-2. Widefield and confocal fluorescence imaging of transgenic organisms that expressed KCNL-2 under its endogenous promoter revealed that the channel is predominantly expressed in the nervous system. The second aim of my thesis was to identify the physiological functions of KCNL-2 in *C. elegans* by investigating the phenotypes of knocking out or overexpressing the channel. Phenotypic analysis of a KCNL-2 null strain and of transgenic lines that overexpress KCNL-2 strongly supports a role for KCNL-2 in the regulation of the rate of egg-laying. The KCNL-2 null strain demonstrates a mild Egl phenotype, while the transgenic lines that overexpress KCNL-2 have a strong hyperactive egg-laying phenotype. In addition to identifying the mechanisms by which KCNL-2 functions to regulate the rate of egg-laying, other pathways such as the channel's function in the pharyngeal nervous system remains to be investigated. Interestingly, differential expression of the KCNL-2 isoforms also offers the possibility of studying the function of individual isoforms in their respective neuronal circuits. This investigation is the first in depth study of an SK channel homologue in *C. elegans* and it offers the opportunity to further investigate the physiological functions of KCNL-2 and to study signaling pathways in which the channel is involved in an *in vivo* system.

4.0 MATERIALS & METHODS

4.1 KCNL-2 CONSTRUCTS

The cDNA clones yk1015a02, yk1103e07, yk1295d10 and yk1401h05 were obtained from Yuji Kohara (National Institute of Genetics of Japan). The yk1401h05 clone encodes the splice variant KCNL-2aii, the yk1295d10 clone encodes the KCNL-2b splice variant with an unspliced intron, and the yk1103e07 and yk1015a02 clones encode partial transcripts of KCNL-2c and KCNL-2d, respectively. The cDNA clones were digested from the parent plasmid pME18S-FL3 with EcoRI and NotI and subcloned into the pcDNA3.1 vector (Invitrogen, Carlsbad, CA). These transcripts were used to generate the KCNL-2a, b, c and d full-length coding sequences in pcDNA3.1 according to the sequences deposited on Wormbase (http://www.wormbase.org, WS231, 07.12.2012). HindIII and KpnI sites were introduced 5' and 3' into the KCNL-2a, aii, b, and c coding sequences, respectively, and the PCR products were subcloned into the pEYFP-N1 plasmid (Invitrogen) so that the channels were tagged at the carboxy termini with YFP. KCNL-2a and KCNL-2c were subcloned into the pcDNA3.1/V5-His-TOPO plasmid (Invitrogen) so that these channels were tagged at the carboxy termini with the V5 epitope. All mutations and deletions were generated using the Stratagene QuikChange site-directed mutagenesis kit (Stratagene, La Jolla, CA). PCR amplification was done using Platinum ® Taq DNA Polymerase High Fidelity (Invitrogen). All cDNAs were sequenced with the ABI 3730*xl* DNA

Analyzer (University of Pittsburgh, PA) to ensure the fidelity of the constructs and analyzed with ClustalW (Larkin et al., 2007).

4.2 NEMATODE CULTURE

Worms were cultured according to standardized protocols described by Brenner (Brenner, 1974). Worms were grown on nematode growth media (NGM) plates seeded with the OP50 strain of *E. coli* at 20^{o}C. NGM plates are composed of 3.0g/L NaCl, 20.0 g/L Bacto-Agar, 2.5 g/L Bacto-peptone, a final concentration of 0.005 mg/ml cholesterol in 95% ethanol, 0.001 M $MgSO_4$, 0.001 M $CaCl_2$, and 0.025 M KPO4 buffer (pH 6). OP50 was prepared by growing a single colony of OP50 in 3 ml LB broth overnight at 37°C with shaking (Bhatia et al., 2011). An ml of this starter culture was added to 1L LB broth, which was incubated at 37°C until an OD_{600} of 0.5 was attained. The bacteria were washed twice with M9 Buffer (42.3 mM Na_2HPO_4, 22.0 mM KH_2PO_4, 85.6 mM NaCl, 1 mM $MgSO_4$.7H2O) and concentrated to an OD_{600} of 10. The Bristol N2 strain was used as the control organism for all *in vivo* experiments.

4.3 CROSSING MUTANT ORGANISMS

A KCNL-2 mutant strain, *kcnl-2(tm1885)*, was obtained from Shohei Mitani (National Bioresource Project, Japan). The *kcnl-2(tm1885)* strain was outcrossed eight times with N2 males to remove extraneous mutations induced by 4,5',8-trimethylpsoralen (TMP) treatment. The *kcnl-2(tm1885)* mutation is a 962 base pair deletion. PCR was conducted using primers external

and internal to the deleted region to distinguish between wild-type, knockout, and heterozygous worms. For distinction between N2 and *kcnl-2(tm1885)* organisms, the external forward primer, Ext F F08A10.1, has the sequence 5' CGT GTG ATA ATC CTC CAA TC 3' and the external reverse primer, Ext R F08A10.1, has the sequence 5' GCA CTC CTA CCT GCT TAG TA 3'. For distinction between *kcnl-2(tm1885)* and heterozygotes, the forward primer, Del Int F2, has the sequence 5' GGC AGT ACT AAA TCT TTG CAT AGC 3' and the Ext R F08A10.1 primer was used.

To initiate backcrosses, wild-type males were crossed with knockout hermaphrodites. Males were generated by heat shocking the N2 organisms at 27°C for 18 hours. The eggs laid by the hermaphrodites were allowed to hatch and develop for 48 hours. Since males normally arise in 0.1% of the population, successful mating would produce an estimated 100% heterozygous male progeny. Twelve male heterozygotes were crossed with three wild-type hermaphrodites. This would yield 50% wild-type and 50% heterozygous progeny. 16 L4 worms were selected from the progeny to grow up and lay eggs on individual dishes. Single worm PCR (SWPCR) was conducted on the 16 parental worms to determine if they were heterozygotes. From positive plates, 16 L4 progeny were allowed to self-fertilize and lay eggs on individual plates. Self-fertilization of a heterozygous animal would yield 25% WT, 50% heterozygotes, and 25% knockout organisms. SWPCR was conducted on the parental worms. Homozygous knockout clones were selected for the subsequent crosses and ultimately for all *in vivo* experiments.

4.4 TRANSGENIC WORM STRAINS

The WRM063DE08 fosmid was obtained from Donald G. Moerman at the C. elegans Reverse Genetics Core Facility (Vancouver, Canada). The KCNL-2 channel (Accession number NC_003279) was amplified from this fosmid using 3 pairs of primers: 5'CTAGCG***GGTACC***ATGTCAAGCTCTGCCCCTTTC3' and 5'CGGCGTAGTGATCCAATACGAGAG3'; 5'CAAGCATAATCTCGCTAGTCC3' and 5'CGAGCGGAGTGGTTGAGATGG3'; 5'ATTCTGTTCGAACTGTCGCCCAG3' and 5'CGGATC***GCGGCCGC***ATAGATTATTAAGAACGCCTAG3' (Integrated DNA Technologies, Coralville, Iowa). The first amplified fragment was 5,770 bp in length and included 1,951 bp of the promoter region, the second fragment was 5,774 bp in length, and a third fragment of the gene was 3,294 bp in length. Fragments 1, 2 and 3 were digested with KpnI and SalI, SalI and BglII, and BglII and NotI, respectively. These restrictions sites naturally occur within the KCNL-2 gene. The KpnI and NotI sites occur within the primers (italicized and bold), while the SalI and BglII sites occur in overlapping regions between fragments 1 & 2 and fragments 2 & 3, respectively. These three fragments were sequentially subcloned into the pCR®-Blunt II-Topo® vector (Invitrogen) to re-construct the full-length gene. This strategy to reconstruct the KCNL-2 gene was undertaken since amplification of the entire coding sequence for KCNL-2 was possible, but subcloning the gene into the vector was not feasible.

The genomic DNA that encodes the KCNL-2 channel displays two initiation sites and two stop codons which allows for alternative splicing and the formation of up to 6 isoforms. GFP was PCR-amplified from the pPD95.75 vector (a gift from Andrew Fire, Stanford University). Two unique restriction sites, MluI and SacII, were introduced sequentially at the initiation or stop codons of the open reading frame of KCNL-2. GFP was subcloned between

these sites so that the channel was effectively tagged at the amino or carboxy termini. When cloned at the carboxy termini, the initiation codon was deleted from the GFP coding sequence, ensuring that GFP was not expressed independently of the channel. Additionally, two constructs were created to monitor GFP expression downstream of the KCNL-2 promoter. The GFP coding sequence was cloned downstream of the promoter region of KCNL-2, which was composed of 1,951 bp upstream of the first initiation site ($P_{kcnl\text{-}2}$*(atg1)gfp*). The GFP coding sequence was cloned at the second initiation site where the coding sequences for the KCNL-2-b and –c clones were deleted $P_{kcnl\text{-}2}$*(atg2)gfp*. A construct was also generated to drive expression of the KCNL-2aii under its natural promoter, $P_{kcnl\text{-}2}$*gfp::kcnl-2aii*. A promoter that drives VC-specific expression, pMD64, was a gift from James J. Moresco and Michael R. Koelle (Bany et al., 2003). This promoter was cloned upstream of the KCNL-2 open reading frame using KpnI and MluI restriction sites to give the *pmd64kcnl-2(taa2)::gfp* construct. pMD64 was also cloned upstream of the last 3kb of the KCNL-2 gene that encodes the –b and –c isoforms to give the *pmd64gfp::(atg2)kcnl-2* construct. Transgenic lines were created using methods described previously (Mello et al., 1991). These constructs were injected with the co-injection marker $P_{myo\text{-}2}$*mCherry* into N2 and *kcnl-2(tm1885)* worms as described in Table 1. Transgenic strains used for imaging were co-injected with the pRF4 plasmid at 50 ng/ul. The total DNA concentrations for microinjections were made up to 100 ng/µl using pBluescript II vector (Agilent Technologies, Santa Clara, CA) as filler DNA.

Table 4.1. List of trangenic strains used in this study.

Strain	Strain ID	Plasmid (ng/µl)		Co-injection Marker (ng/µl)	
N2	KCNL-2(OE-1)	P_{KCNL-2}KCNL-2(TAA1)::GFP	90	P_{myo-2} mCherry	10
N2	KCNL-2(OE-2)	P_{KCNL-2}KCNL-2(TAA2)::GFP	90	P_{myo-2} mCherry	10
kcnl-2(Δ)	KCNL-2(OE-3)	P_{KCNL-2}KCNL-2(TAA2)::GFP	1	P_{myo-2} mCherry	10
kcnl-2(Δ)	KCNL-2(OE-4)	P_{KCNL-2}KCNL-2(TAA2)::GFP	10	P_{myo-2} mCherry	10
kcnl-2(Δ)	KCNL-2(OE-5)	P_{KCNL-2}KCNL-2(TAA2)::GFP	90	P_{myo-2} mCherry	10
N2	*P_{kcnl-2}(atg1)gfp*	$P_{KCNL-2(ATG1)}$GFP	50	pRF4	50
N2	*P_{kcnl-2}(atg2)gfp*	$P_{KCNL-2(ATG2)}$GFP	50	pRF4	50
N2	*P_{kcnl-2}gfp::kcnl-2aii*	P_{KCNL-2}GFP::KCNL-2aii	90	P_{myo-2} mCherry	10
N2	*p_{kcnl-2}gfp::(atg2)kcnl-2*	P_{KCNL-2}GFP::(ATG2)KCNL-2	50	pRF4	50
N2	*pmd64kcnl-2(taa2)::gfp*	pMD64KCNL-2(TAA2)::GFP	90	P_{myo-2} mCherry	10
N2	*pmd64gfp::(atg2)kcnl-2*	pMD64GFP::(ATG2)KCNL-2	90	P_{myo-2} mCherry	10

4.5 BEHAVIORAL ASSAYS

All values were reported as Mean ± SEM and if $p<0.05$, then the data sets were interpreted as being significantly different. Longevity assays were performed as described previously (Klass, 1977). In each Longevity assay (n=3), a population of 25 L4 worms was placed onto individual NGM plates at 20^{o}C. For each worm strain, the percentage survival of the population of worms was monitored and recorded daily until all organisms died. The data was plotted on Kaplan-Meier survival curves and analyzed using a Logrank test. The brood size assay was performed as described previously by Singson and colleagues (Singson et al., 1998). For each assay (n=3), ten late L4 worms were placed onto individual NGM plates on sequential days until the fertility period came to an end. The number of eggs laid over a five day period by a single subject was measured. The data was analyzed using a Student's *t*-test. For post-embryonic development (PED) assays (n=3), a population of 25 young adult worms (24 hrs post late L4 stage) was allowed to lay eggs for 2 hours, after which the adults were removed and the developmental stage of the progeny was scored after 72 hrs (Larsen et al., 1995). Normalized values were analyzed using a Kruskal-Wallis *H* test.

4.6 EGG-LAYING ASSAYS

Koelle & Horvitz have described two methods to assay the rate of egg-laying (Koelle and Horvitz, 1996). The first determines the number of unlaid eggs retained *in utero* per adult animal and the second determines the developmental stage of newly laid eggs. For both egg-laying assays, late L4 animals were grown for 36 hours at 20^{o}C to yield a synchronized population of

adults. To count the number of eggs *in utero*, a total of 30 animals were analyzed. Individual animals were dissolved in 1.8% sodium hypochlorite in a Nunc 384 well plate (ThermoScientific, Rochester, NY) and the number of eggs *in utero* was counted after the cuticle dissolved using an inverted microscope. Given that the transgenic KCNL-2-overexpressing lines were not integrated, these strains do not constitute a homogenous population due to the loss of extrachromosomal arrays or genetic mosaicism. Therefore for each experiment, 50% of a synchronized population of adult animals with single rows of eggs (n=25) were selected using a high power dissecting scope. These animals were allowed to lay eggs for 30 minutes on NGM plates with OP50 as the food source and the eggs were scored as early if they were composed of eight cells or less or late if they had greater than eight cells (Ringstad and Horvitz, 2008).

4.7 CELL CULTURE

Human embryonic kidney (HEK293) cells (American Type Culture Collection, Manassas, VA) were transfected with the described constructs using LipofectAMINE 2000 (Invitrogen) according to the manufacturer's recommended protocol. HEK293 cells were cultured in Dulbecco's Modified Eagle's Medium (Invitrogen) supplemented with 10% fetal bovine serum in a humidified 5% CO2, 95% O2 chamber at 37^{o}C. HEK293 cells were grown on poly-L-lysine-coated glass coverslips (Sigma, St. Louis, MO) and transiently transfected with KCNL-2a-YFP, KCNL-2aii-YFP, KCNL-2c-YFP, or KCNL-2d-YFP constructs. The cells were fixed and permeabilized with 2% paraformaldehyde plus 0.1% Triton-X-100 and the nuclei were labeled with Hoechst 33258 (Sigma). Cells were imaged using an Olympus IX-81 widefield fluorescence microscope.

4.8 BIOCHEMISTRY

HEK293 cells were transiently transfected in 60-mm dishes using LipofectAMINE 2000 and 5 µg of the KCNL-2a-V5 or KCNL-2c-V5 constructs. Cells were lysed in lysis buffer (50mM HEPES, pH 7.4, 150 mM NaCl, 1% v/v Triton X-100, 1 mM EDTA containing CompleteTM EDTA-free protease inhibitor mixture mix, RocheApplied Science). The protein concentrations were measured, normalized and re-suspended in Laemmli sample buffer to achieve equivalent loading concentrations. Individual proteins samples were resolved by SDS-PAGE (8% gel) and transferred to nitrocellulose. Blots were blocked for 1 h at room temperature using Tris-buffered saline blocking solution containing 5% (w/v) milk powder, 0.1% (v/v) Tween 20, and incubated with the primary anti-V5 Ab (1:1000 dilution) (Invitrogen) and subsequently with the secondary goat anti-mouse IgG (1:10,000 dilution). West Pico chemiluminescent substrate (Pierce) was used for protein detection.

4.9 IMAGING OF *C. ELEGANS* STRAINS

Transgenic and mutant animals were immobilized using 6 µl 0.05mM sodium azide in 35 mm optical glass bottomed dishes (MatTek Corporation, Ashland, MA). Widefield images were collected using a standard fluorescence inverted microscope over 40 Z-planes using a 20x 0.75 NA or a 60x 1.4 NA oil Apochromat objective. Epifluorescence was captured using FITC (Ex 488 nm; Em 512 nm) filter sets (Chroma) with a Coolsnap HQ2 CCD camera (Photometrics). Confocal images were collected using a Leica TCS SP8 microscope. GFP fluorescence was illuminated using a 488nm argon laser line with a 63x 1.4NA oil Apochromat CS2 objective.

Fluorescence was captured using a spectral HyD detector over ~100 Z-planes. Both widefield and confocal images were visualized, rendered and analyzed using Volocity Visualization Software (v5.4, Perkin Elmer).

APPENDIX

My goal in this thesis was to establish *C. elegans* as a model organism to study the biochemical, biophysical and physiological properties of KCNL-2, an SK channel homologue. To accomplish this goal, I studied the phenotypes associated with knockout of KCNL-2 in *kcnl-2(tm1885)* organisms or overexpression of KCNL-2 in transgenic lines. The first overt phenotype observed in the *kcnl-2(tm1885)* organisms was a post-embryonic developmental delay. As shown in Figure A.1, I assessed the underlying basis of this developmental delay and found that a population of the *kcnl-2(tm1885)* organisms were slowly developing or underwent larval arrest relative to N2 organisms. Since this phenotype could not be rescued by transforming *kcnl-2(tm1885)* organisms with KCNL-2, it remains a possibility that this phenotype is not specifically due to the loss of KCNL-2. Transgenic lines that overexpress KCNL-2 demonstrate a strong Egl-C phenotype and this implicates KCNL-2 in the regulation of the rate of egg-laying. As a means to demonstrate that this Egl-C phenotype was specifically due to overexpression of KCNL-2, I employed RNAi methods to knockdown KCNL-2 expression in these lines (Figure A.2). As has been found in other studies, RNAi in neurons of *C. elegans* is inefficient and since KCNL-2 is expressed in the nervous system of the worm, I was unable to demonstrate a role for KCNL-2 in regulating the rate of egg-laying through RNAi. However, as shown in Figure A.3, a specific role for KCNL-2 in the regulation of the rate of egg-laying is supported by the Egl-C phenotype shown in transgenic lines that overexpress the KCNL-2aii isoform under the KCNL-2

promoter, while expression of GFP under the KCNL-2 promoter causes lethality of these worms and a severe egg-laying defective phenotype (Figure A.4), further supporting the hypothesis that KCNL-2 specifically plays a role in regulating the rate of egg-laying. Based on a study by Koelle and colleagues, the VC neurons were strongly implicated in the inhibition of egg-laying and since the results show that the KCNL-2b and c isoforms are expressed in VC4 and VC5, I hypothesized that KCNL-2 regulates the rate of egg-laying through its expression in the VC neurons (Bany et al., 2003). Expression of KCNL-2 under the pMD64 promoter did not limit expression of KCNL-2 to the VC neurons and vulval cells as described**,** demonstrating the complexity of this gene and suggesting that localization signals are encoded by the introns (Figure A.5). Expression of the KCNL-2 gene encoding the -b and –c isoforms downstream of the pMD64 promoter did limit expression of the channel to the VC neurons further supporting this concept (Figure A.6). The summation of the data does not support that KCNL-2 is acting in the VC neurons to regulate the rate of egg-laying.

In order to assess the biophysical properties of KCNL-2, steps were taken to establish a heterologous expression system using HEK293 cells. The molecular weight of the isolated protein from cell lines expressing the KCNL-2a and c isoforms as determined by immunoblot was equivalent to the calculated molecular weight of the proteins (Figure A.7). Additionally, KCNL-2-a, -aii, -b, or -c cDNA constructs that were tagged at the carboxy terminus with YFP were expressed in cells, but did not traffic efficiently to the cell surface membrane as determined by widefield fluorescent microscopy (Figure A.8). Therefore, there was no further progress in this aspect of the thesis.

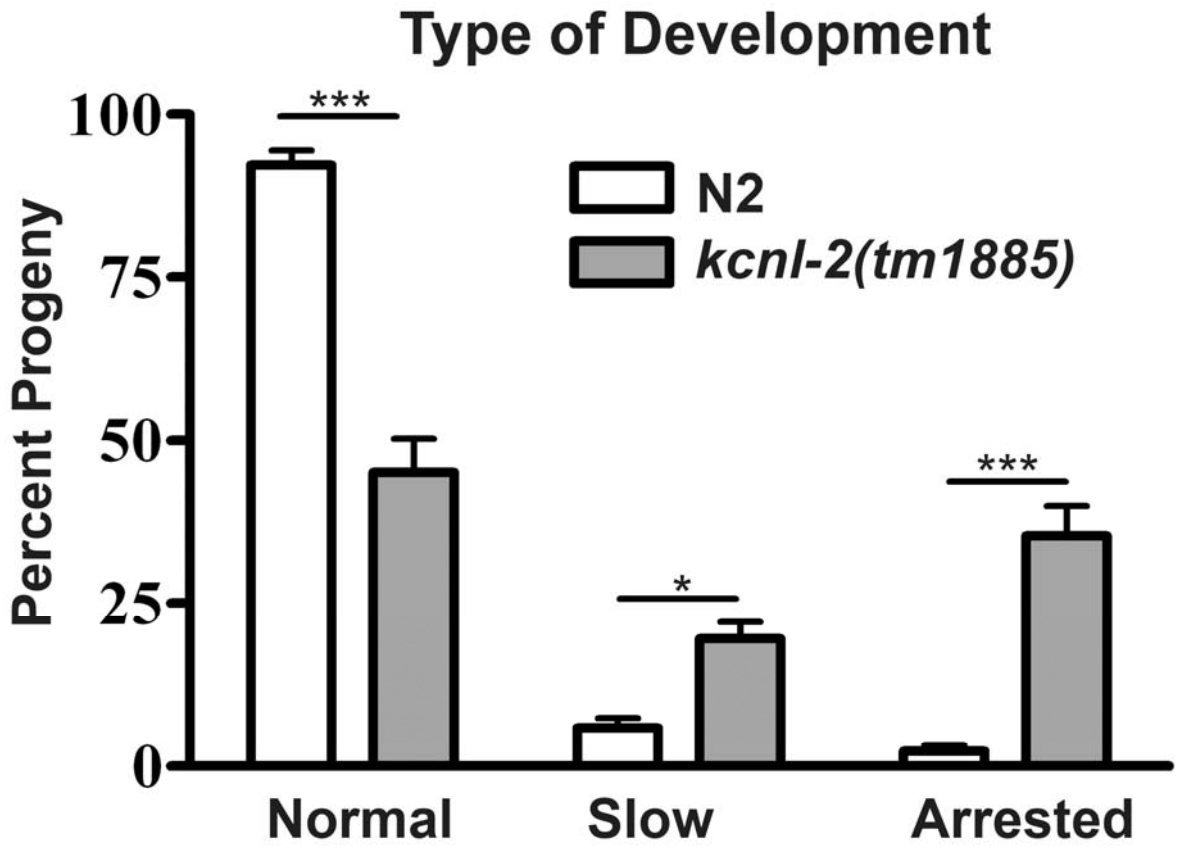

Figure A.1 Analysis of the post-embryonic development of N2 and *kcnl-2(tm1885)* animals. Organisms that developed to L4 or adult animals within 3 or 7 days were scored as normally or slowly developing, respectively. Organisms that did not develop further than the L1-L3 stage after 7 days were scored as arrested as larvae. 88.1 ± 3.0% of N2 worms and 47.9 ± 6.9% of *kcnl-2(tm1885)* worms developed normally, 8.8 ± 1.9% of N2 worms and 19.2 ± 3.7% of *kcnl-2(tm1885)* worms developed slowly, and 3.7 ±1.4% of N2 worms and 32.9 ± 6.1% of *kcnl-2(tm1885)* worms were arrested at the larval stage.

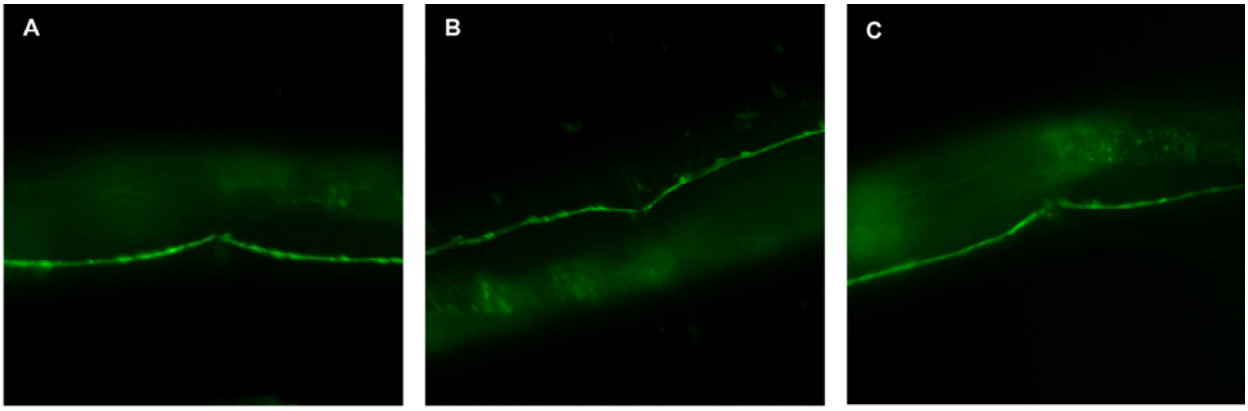

Figure A.2 Expression of $P_{kcnl\text{-}2}$*kcnl-2(taa2)::gfp* after RNAi treatment for 24 hours as monitored by widefield fluorescence microscopy.
The exposure was held constant for all strains at 390 ms. The RNAi clones were isolated from the Ahringer Library. A. L4440 vector RNAi-treatment. B. GFP RNAi-treatment. C. KCNL-2 RNAi-treatment.

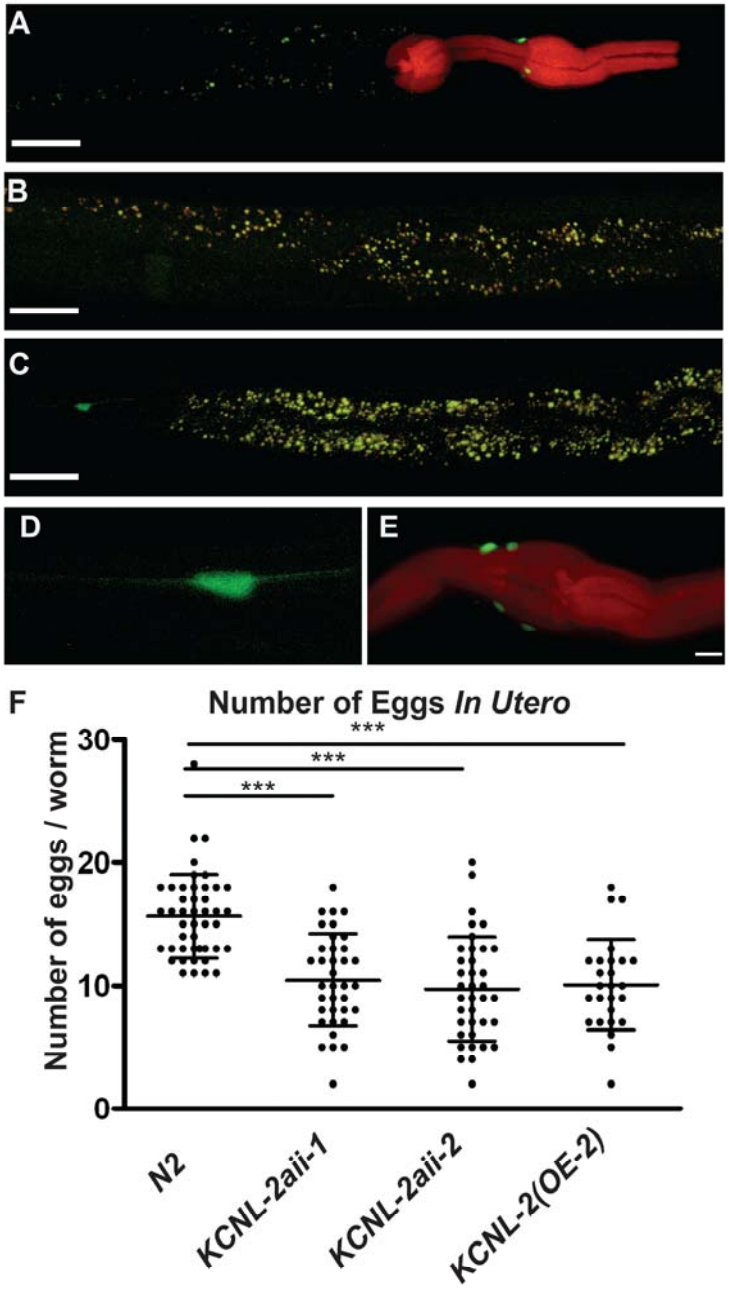

Figure A.3 Overexpression of $P_{kcnl\text{-}2}$*gfp::kcnl-2aii* in the N2 background causes a hyperactive egg-laying phenotype.
Two independent transgenic lines expressing $P_{kcnl\text{-}2}$*gfp::kcnl-2aii* (KCNL-2aii-1 and -2) have a significantly less number of eggs *in utero* relative to N2 worms (Student's *t* test, P<0.0001). The number of eggs *in utero* per worm in these transgenic lines are not significantly different from that of KCNL-2(OE-2) (P>0.5).

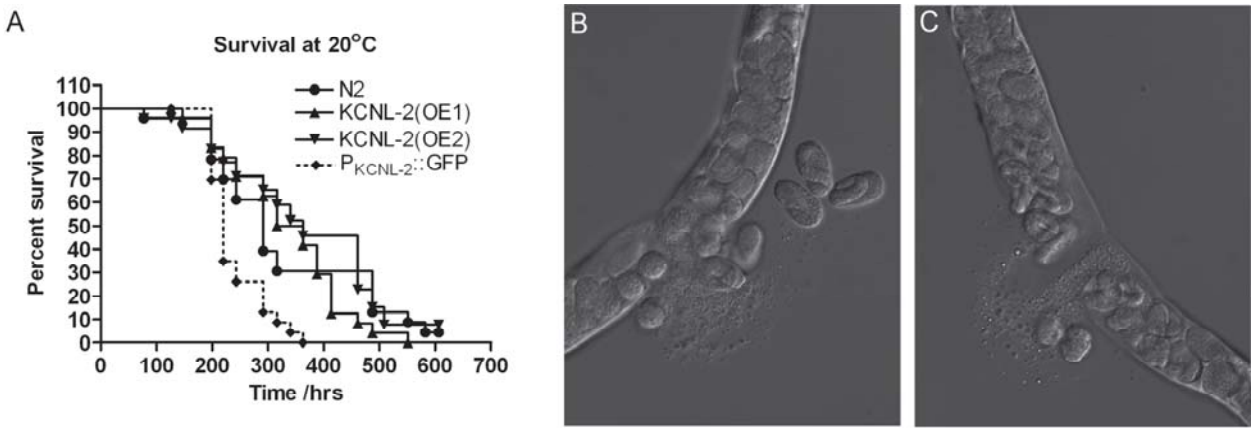

Figure A.4 Kaplan-Meier Survival Curves showing the longevities of N2, KCNL-2(OE1), KCNL-2(OE2), and $P_{KCNL\text{-}2}$GFP

(Median survival: 291.5 h, 339.3 h, 362.5 h, and 220 h, respectively). The longevity of N2 vs. KCNL-2(OE1) or KCNL-2(OE) was not significantly different (p=0.6, Logrank test). The longevity of N2 vs. *N2;*$P_{kcnl\text{-}2}$*(atg1)gfp* ($P_{KCNL\text{-}2}$GFP) was significantly different (p=0.0048, Logrank test). B-C. Representative images of transgenic animals expressing $P_{kcnl\text{-}2}$*(atg1)gfp* in the N2 background.

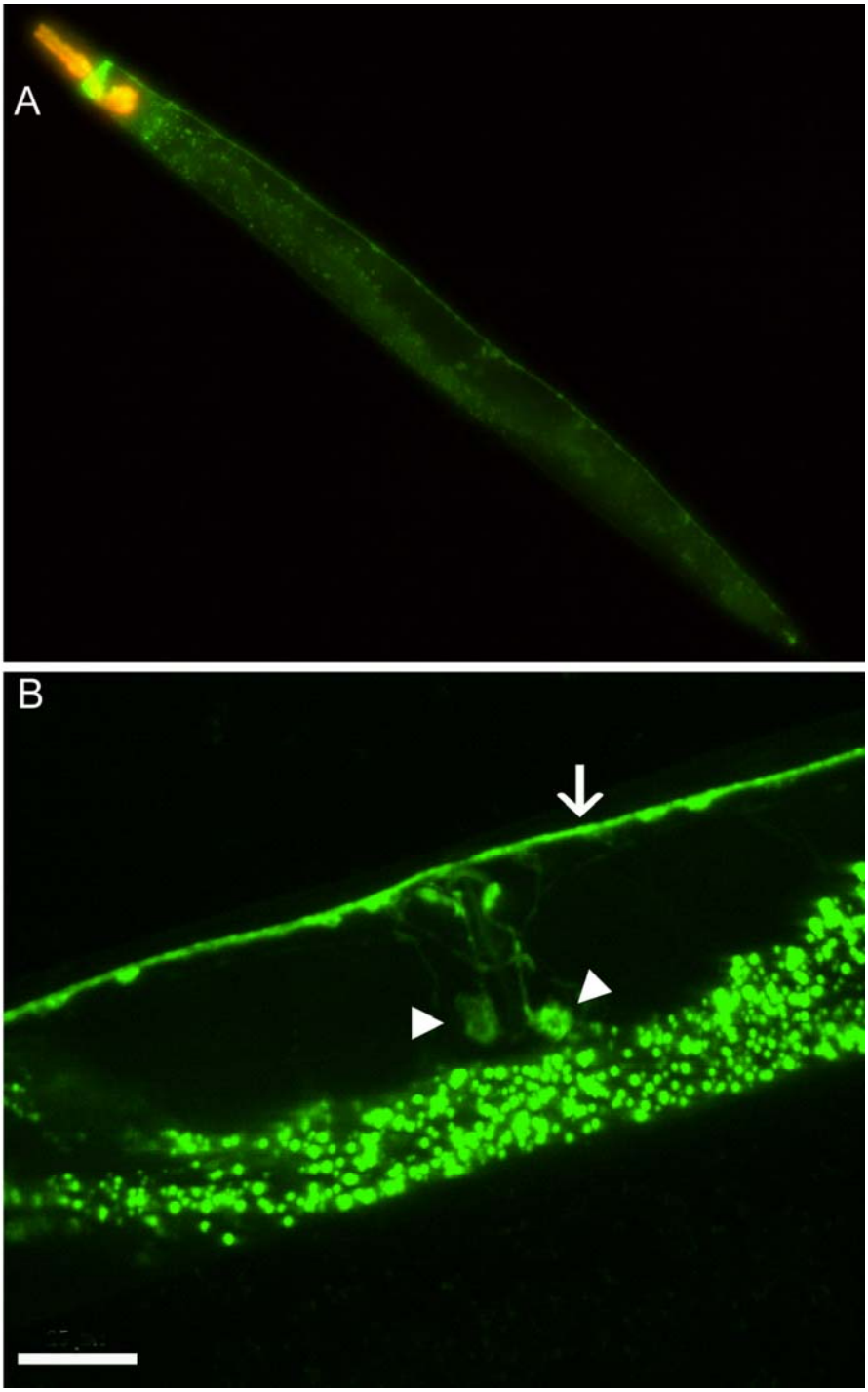

Figure A.5 Expression pattern of *pmd64kcnl-2(taa2)::gfp*.
A) The pMD64 promoter did not limit expression of the KCNL-2 channel to the VC neurons since it was still expressed in neurons along the VNC and the NR. B) A magnified image of the vulva shows expression of the channel in the VNC (arrow) and the vulval cells (arrow heads). Images were taken and processed by Cliff J. Luke.

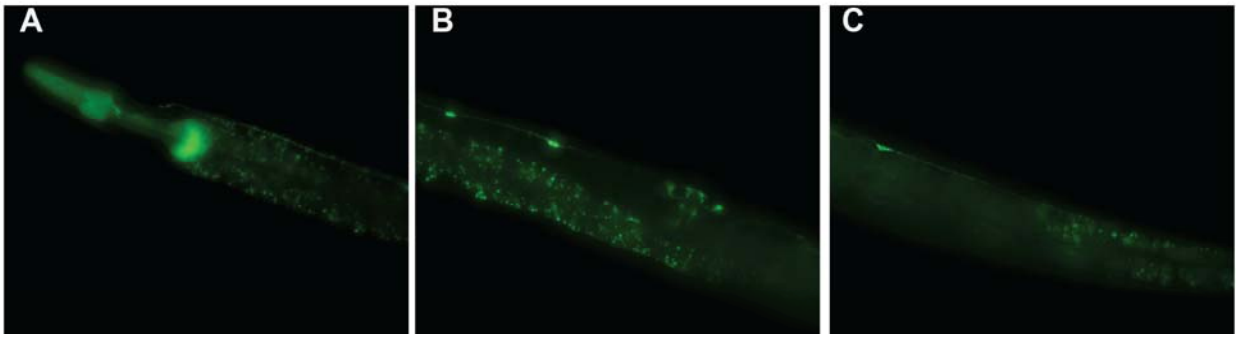

Figure A.6 Expression pattern of *pmd64kcnl-2b/c::gfp*.
The coding region of KCNL-2 that drives expression of the b and c isoforms spans ~3kb. This sequence was cloned downstream of the pMD64 promoter. A. *kcnl-2b/c::gfp* is expressed in the VC neurons that extends to the nerve ring. B. *kcnl-2b/c::gfp* expression is seen in the cell bodies of VC2, VC3, VC4 and VC5 and in the vulval cells. C. *kcnl-2b/c::gfp* expression is seen in the VC6 cell body.

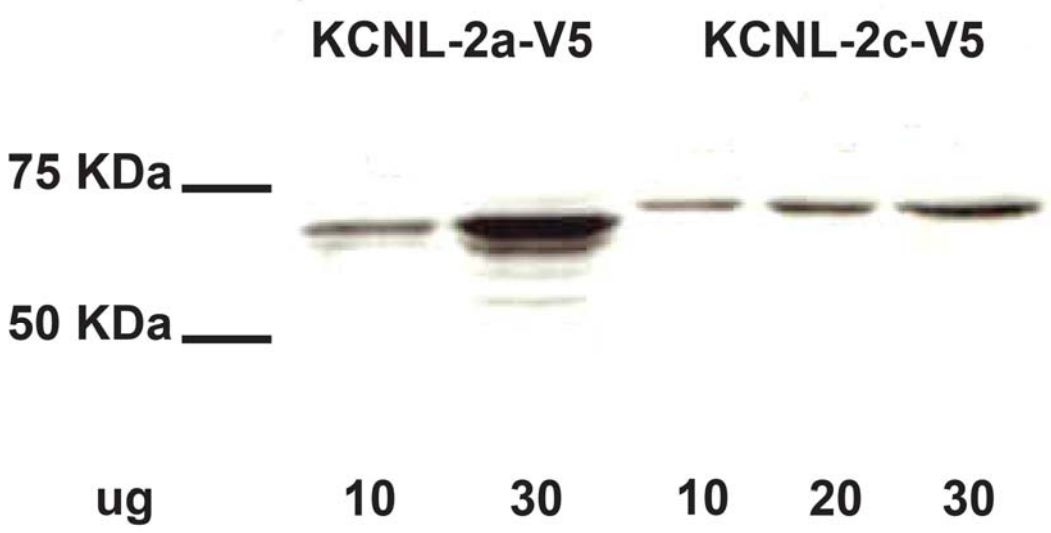

Figure A.7 Immunoblot of HEK293 cells transiently transfected with KCNL-2aii-V5 and KCNL-2c-V5 at varying concentrations.
The translated proteins are of the predicted molecular weight of ~75 KDa for the KCNL-2 isoforms.

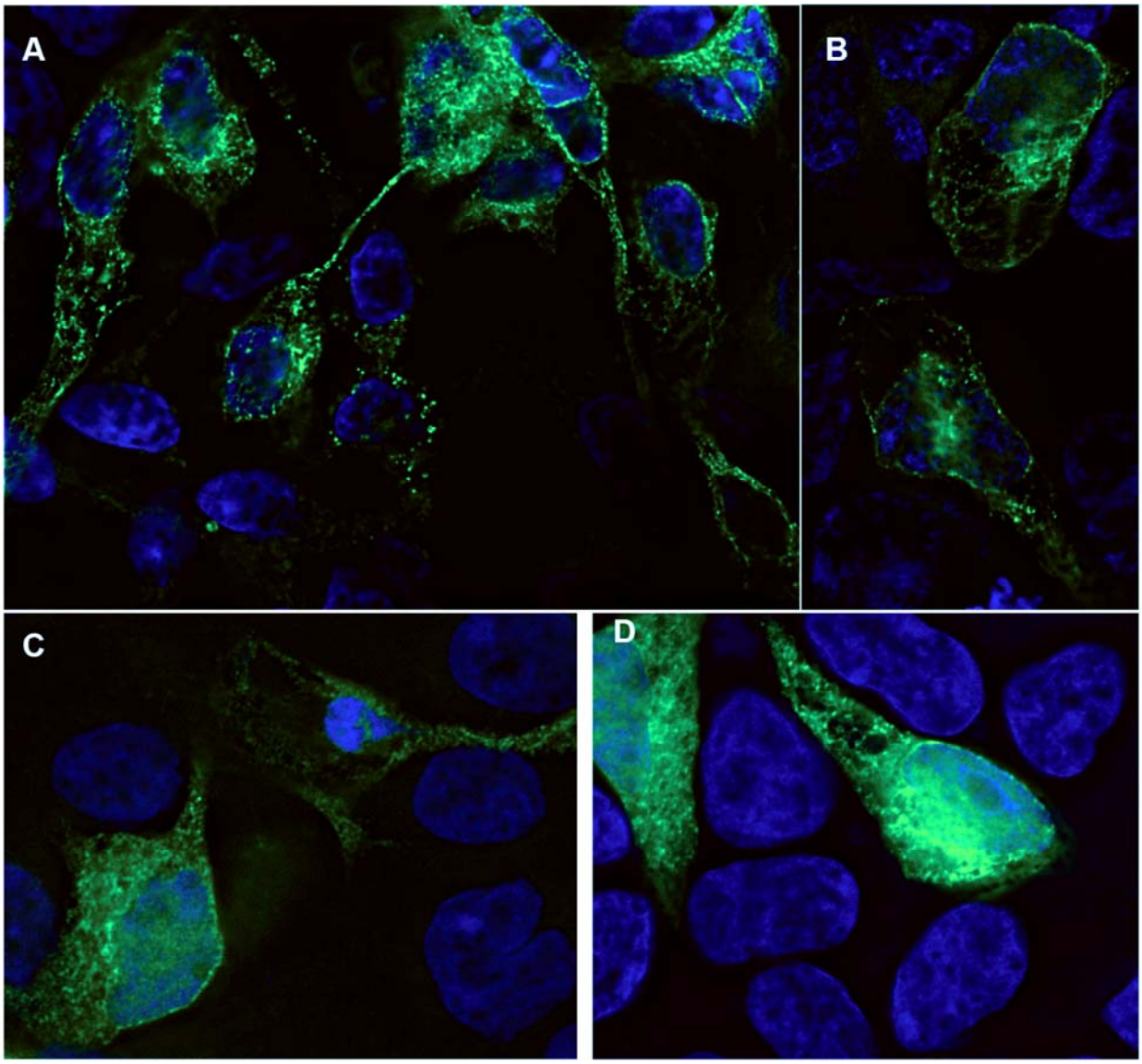

Figure A.8 HEK293 cells transiently transfected with the KCNL-2-a (A), KCNL-2-aii (B), KCNL-2-b (C), or KCNL-2–c (D) cDNA constructs that were tagged at the carboxy terminus with YFP.

BIBLIOGRAPHY

Adelman, J.P., Maylie, J., and Sah, P. (2012). Small-conductance Ca2+-activated K+ channels: form and function. Annual review of physiology *74*, 245-269.

Aggarwal, S., and Mackinnon, R. (1996). Contribution of the S4 Segment to Gating Charge in the K Channel. Neuron *16*, 1169-1177.

Altun, Z.F., and Hall, D.H. (2008). Handbook of C. elegans Anatomy.

Ashcroft, F.M., and Rorsman, P. (1989). Electrophysiology of the pancreatic β-cell. Progress in Biophysics and Molecular Biology *54*, 87-143.

Asher, V., Sowter, H., Shaw, R., Bali, A., and Khan, R. (2010). Eag and HERG potassium channels as novel therapeutic targets in cancer. World J Surg Oncol *8*, 113.

Avery, L., and Horvitz, H.R. (1989). Pharyngeal pumping continues after laser killing of the pharyngeal nervous system of C. elegans. Neuron *3*, 473-485.

Babu, Y.S., Sack, J.S., Greenhough, T.J., Bugg, C.E., Means, A.R., and Cook, W.J. (1985). Three-dimensional structure of calmodulin. Nature *315*.

Balut, C.M., Hamilton, K.L., and Devor, D.C. (2012). Trafficking of intermediate (KCa3.1) and small (KCa2.x) conductance, Ca(2+)-activated K(+) channels: a novel target for medicinal chemistry efforts? ChemMedChem *7*, 1741-1755.

Bany, I.A., Dong, M., and Koelle, M.R. (2003). Genetic and cellular basis for acetylcholine inhibition of Caenorhaditis elegans egg-laying behavior. J Neurosci *23*, 10.

Bargmann, C.I. (1998). Neurobiology of the Caenorhabditis elegans Genome. Science *282*, 2028-2033.

Barmeyer, C., Rahner, C., Yang, Y., Sigworth, F.J., Binder, H.J., and Rajendran, V.M. (2010). Cloning and identification of tissue-specific expression of KCNN4 splice variants in rat colon. Am J Physiol Cell Physiol *299*, C251-263.

Berkefeld, H., Fakler, B., and Schulte, U. (2010). Ca2+-activated K+ channels: from protein complexes to function. Physiol Rev *90*, 1437-1459.

Bhatia, S.R., Miedel, M.T., Chotoo, C.K., Graf, N.J., Hood, B.L., Conrads, T.P., Silverman, G.A., and Luke, C.J. (2011). Using C. elegans to identify the protease targets of serpins in vivo. Methods Enzymol *499*, 283-299.

Bianchi, L., Kwok, S.M., Driscoll, M., and Sesti, F. (2003). A potassium channel-MiRP complex controls neurosensory function in Caenorhabditis elegans. The Journal of biological chemistry *278*, 12415-12424.

Bond, C.T., Herson, P.S., Strassmaier, T., Hammond, R., Stackman, R., Maylie, J., and Adelman, J.P. (2004). Small conductance Ca2+-activated K+ channel knock-out mice reveal the identity of calcium-dependent afterhyperpolarization currents. The Journal of neuroscience : the official journal of the Society for Neuroscience *24*, 5301-5306.

Bond, C.T., Sprengel, R., Bissonnette, J.M., Kaufmann, W.A., Pribnow, D., Neelands, T., Storck, T., Baetscher, M., Jerecic, J., Maylie, J.*, et al.* (2000). Respiration and parturition affected by conditional overexpression of the Ca2+-activated K+ channel subunit, SK3. Science *289*.

Bowden, S.E., Fletcher, S., Loane, D.J., and Marrion, N.V. (2001). Somatic colocalization of rat SK1 and D class (Ca(v)1.2) L-type calcium channels in rat CA1 hippocampal pyramidal neurons. The Journal of neuroscience : the official journal of the Society for Neuroscience *21*, RC175.

Brahler, S., Kaistha, A., Schmidt, V.J., Wolfle, S.E., Busch, C., Kaistha, B.P., Kacik, M., Hasenau, A.L., Grgic, I., Si, H.*, et al.* (2009). Genetic deficit of SK3 and IK1 channels disrupts the endothelium-derived hyperpolarizing factor vasodilator pathway and causes hypertension. Circulation *119*, 2323-2332.

Brenner, S. (1974). The genetics of Caenorhabditis elegans. Genetics *77*, 71-94.

Brundage, L., Avery, L., Katz, A., Kim, U., Mendel, J., Sternberg, P., and Simon, M. (1996). Mutations in a C. elegans G? Gene Disrupt Movement, Egg Laying, and Viability. Neuron *16*, 999-1009.

Buechner, M., Hoynowski, S., Leming, M., Tong, X., and Mitchell, K. (2007). Genetic and electrophysiological characterization of the nematode SK3 potassium channel. International Worm Meeting.

Butler, A., Wei, A., Baker, K., and Salkoff, L. (1989). A family of putative potassium channel genes in Drosophila. Science *243*, 943-947.

Calixto, A., Chelur, D., Topalidou, I., Chen, X., and Chalfie, M. (2010). Enhanced neuronal RNAi in C. elegans using SID-1. Nature methods *7*, 554-559.

Chandy, K.G., DeCoursey, T.E., Cahalan, M.D., McLaughlin, C., and Gupta, S. (1984). Voltage-gated potassium channels are required for human T lymphocyte activation. J Exp Med *160*, 369-385.

Coetzee, W.A., and Rudy, B. (2006). Potassium Channels.

Consortium, C.e.S. (1998). Genome sequence of the nematode C. elegans: a platform for investigating biology. Science *282*, 2012-2018.

Davis, M.W., Fleischhauer, R., Dent, J.A., Joho, R.H., and Avery, L. (1999). A mutation in the C. elegans EXP-2 potassium channel that alters feeding behavior. Science *286*.

Desai, C., and Horvitz, H.R. (1989). Caenorhabditis elegans Mutants Defective in the Functioning of the Motor Neurons Responsible for Egg Laying. Genetics *121*.

Deutsch, C. (2002). Potassium channel ontogeny. Annual review of physiology *64*, 19-46.

Dias Da Silva, M.R., Cerutti, J.M., Arnaldi, L.A., and Maciel, R.M. (2002). A mutation in the KCNE3 potassium channel gene is associated with susceptibility to thyrotoxic hypokalemic periodic paralysis. J Clin Endocrinol Metab *87*.

Dimitriadi, M., Sleigh, J.N., Walker, A., Chang, H.C., Sen, A., Kalloo, G., Harris, J., Barsby, T., Walsh, M.B., Satterlee, J.S.*, et al.* (2010). Conserved genes act as modifiers of invertebrate SMN loss of function defects. PLoS genetics *6*, e1001172.

Elkes, D.A., Cardozo, D.L., Madison, J., and Kaplan, J.M. (1997). EGL-36 Shaw channels regulate C. elegans egg-laying muscle activity. Neuron *19*, 165-174.

Empson, R.M., and Jefferys, J.G.R. (2001). Ca2+ entry through l-type Ca2+ channels helps terminate epileptiform activity by activation of a Ca2+ dependent afterhyperpolarisation in hippocampal CA3. Neuroscience *102*, 297-306.

Faber, E.S., and Sah, P. (2007). Functions of SK channels in central neurons. Clin Exp Pharmacol Physiol *34*, 1077-1083.

Fanger, C.M., Ghanshani, S., Logsdon, N.J., Rauer, H., Kalman, K., Zhou, J., Beckingham□, K., Chandy, K.G., Cahalan, M.D., and Aiyar, J. (1999). Calmodulin Mediates Calcium-dependent Activation of the Intermediate Conductance KCa Channel,IKCa1. JBC *274*.

Fanger, C.M., Rauer, H., Neben, A.L., Miller, M.J., Wulff, H., Rosa, J.C., Ganellin, C.R., Chandy, K.G., and Cahalan, M.D. (2001). Calcium-activated potassium channels sustain calcium signaling in T lymphocytes. Selective blockers and manipulated channel expression levels. The Journal of biological chemistry *276*, 12249-12256.

Fernandez de Sevilla, D., Garduno, J., Galvan, E., and Buno, W. (2006). Calcium-activated afterhyperpolarizations regulate synchronization and timing of epileptiform bursts in hippocampal CA3 pyramidal neurons. Journal of neurophysiology *96*, 3028-3041.

Fire, A., Xu, S., Montgomery, M.K., Kostas, S.A., Driver, S.E., and Mello, C.C. (1998). Potent and specific genetic interference by double-stranded RNA in Caenorhabditis elegans. Nature *391*, 806-811.

Fleischhauer, R., Davis, W., Dzhura, I., Neely, A., Avery, L., and Joho, R. (2000). Ultra-fast inactivation causes inward rectification in a voltage-gated K+ channel from C. elegans. J Neurosci *20*.

Frokjar-Jensen, C., Baban, B., Jorgensen, E.M., Salkoff, L., Olesen, S., and Grunnet, M. (2007). Exp-3 encodes a small conductance calcium-activated K+ channel. . International Worm Meeting.

Ganetzky, B., and Wu, C.F. (1983). Neurogenetic analysis of potassium currents in Drosophila: synergistic effects on neuromuscular transmission in double mutants. J Neurogenet *1*, 17.

Gao, Y., Chotoo, C.K., Balut, C.M., Sun, F., Bailey, M.A., and Devor, D.C. (2008). Role of S3 and S4 transmembrane domain charged amino acids in channel biogenesis and gating of KCa2.3 and KCa3.1. The Journal of biological chemistry *283*, 9049-9059.

Garriga, G., Desai, C., and Horvitz, H.R. (1993). Cell interactions control the direction of outgrowth, branching and fasciculation of the HSN axons of Caenorhabditis elegans. Development *117*, 1071-1087.

Gerlach, A.C., Maylie, J., and Adelman, J.P. (2004). Activation kinetics of the slow afterhyperpolarization in hippocampal CA1 neurons. Pflugers Archiv : European journal of physiology *448*, 187-196.

Ghanshani, S., Wulff, H., Miller, M.J., Rohm, H., Neben, A., Gutman, G.A., Cahalan, M.D., and Chandy, K.G. (2000). Up-regulation of the IKCa1 potassium channel during T-cell activation. Molecular mechanism and functional consequences. The Journal of biological chemistry *275*, 37137-37149.

Ghatta, S., Nimmagadda, D., Xu, X., and O'Rourke, S.T. (2006). Large-conductance, calcium-activated potassium channels: structural and functional implications. Pharmacol Ther *110*, 103-116.

Glaudemans, B., van der Wijst, J., Scola, R.H., Lorenzoni, P.J., Heister, A., van der Kemp, A.W., Knoers, N.V., Hoenderop, J.G., and Bindels, R.J. (2009). A missense mutation in the Kv1.1 voltage-gated potassium channel-encoding gene KCNA1 is linked to human autosomal dominant hypomagnesemia. J Clin Invest *119*, 936-942.

Goldstein, S.A., Bockenhauer, D., O'Kelly, I., and Zilberberg, N. (2001). Potassium leak channels and the KCNK family of two-P-domain subunits. Nat Rev Neurosci *2*, 175-184.

Grant, B.D., and Donaldson, J.G. (2009). Pathways and mechanisms of endocytic recycling. Nat Rev Mol Cell Biol *10*, 597-608.

Grant, B.D., and Sato, M. (2006). Intracellular trafficking. WormBook, 1-9.

Heginbotham, L., Abramson, T., and Mackinnon, R. (1992). A functional connetion between the pores of distantly related ion chanels as revealed by mutant K+ channels. Science *258*.

Heginbotham, L., Lu, Z., Abramson, T., and MacKinnon, R. (1994). Mutations in the K+ channel signature sequence. Biophys J *66*, 1061-1067.

Heinemann, S.H., and Hehl, S. (2001). Voltage-gated Potassium Channels. eLS.

Herrera, G.M., Pozo, M.J., Zvara, P., Petkov, G.V., Bond, C.T., Adelman, J.P., and Nelson, M.T. (2003). Urinary bladder instability induced by selective suppression of the murine small conductance calcium-activated potassium (SK3) channel. The Journal of physiology *551*, 893-903.

Hibino, H., Inanobe, A., Furutani, K., Murakami, S., Findlay, I., and Kurachi, Y. (2010). Inwardly rectifying potassium channels: their structure, function, and physiological roles. Physiol Rev *90*, 291-366.

Hille, B., ed. (2001). Ion channels of excitable membranes, Third edn (Sunderland, MA 01375: Sinauer Associates).

Hodgkin, A.L., and Huxley, A.F. (1952). Currents carried by sodium and potassium ions through the membrane of the giant axon of Loligo. J Physiol *116*.

Ishii, T.M., Maylie, J., and Adelman, J.P. (1997). Determinants of apamin and d-tubocurarine block in SK potassium channels. The Journal of biological chemistry *272*, 23195-23200.

Ito, H., Tung, R.T., Sugimoto, T., Kobayashi, I., Takahashi, K., Katada, T., Ui, M., and Kurachi, Y. (1992). On the mechanism of G protein βγ subunit activation of the muscarinic K+ channel in guinea pig atrial cell membrane: comparison with the ATP-sensitive K+ channel. J General Physiol *99*.

Jan, L.Y., and Jan, Y.N. (1997). Cloned potassium channels from eukaryotes and prokaryotes. Annu Rev Neurosci *20*, 91-123.

Jentsch, T.J. (2000). Neuronal KCNQ potassium channels: physiology and role in disease. Nat Rev Neurosci *1*, 21-30.

Johnstone, D.B., Wei, A., Butler, A., Salkoff, L., and Thomas, J.H. (1997). Behavioral Defects in C. elegans egl-36 Mutants Result from Potassium Channels Shifted in Voltage-Dependence of Activation. Neuron *19*, 151-164.

Joiner, W.J., Wang, L.Y., Tang, M.D., and Kaczmarek, L.K. (1997). hSK4, a member of a novel subfamily of calcium-activated potassium channels. Proceedings of the National Academy of Sciences of the United States of America *94*, 11013-11018.

Kamath, R.S., Ahringer J. (2003). Genome-wide RNAi screening in Caenorhabditis elegans. Methods *30*, 313-321.

Kamath, R.S., Martinez-Campos, M., Zipperlen, P., Fraser, A.G., and Ahringer, J. (2001). Effectiveness of specific RNA-mediated interference through ingested double-stranded RNA in Caenorhabditis elegans. Genome Biol *2*, RESEARCH0002.

Keen, J.E., Khawaled, R., Farrens, D., Neelands, T., Rivard, A., Bond, C.T., Janowsky, A., Fakler, B., Adelman, J.P., and Maylie, J. (1999). Domains Responsible for Constitutive and Ca2+-Dependent Interactions between Calmodulin and Small Conductance Ca2+-Activated Potassium Channels J Neurosci *19*, 9.

Kim, J., Poole, D.S., Waggoner, L.E., Kempf, A., Ramirez, D.S., Treschow, P.A., and Schafer, W.R. (2001). Genes affecting the activity of nicotinic receptors involved in Caenorhabditis elegans egg-laying behavior. Genetics *157*, 1599-1610.

Klass, M.R. (1977). Aging in the nematode Caenorhabditis elegans: major biological and environmental factors influencing life span. Mechanisms of ageing and development *6*, 413-429.

Koefoed-Johnsen, V., and Ussing, H.H. (1958). The Nature of the Frog Skin Potential. Acta Physiologica Scandinavica *42*, 298-308.

Koelle, M.R., and Horvitz, H.R. (1996). EGL-10 regulates G protein signaling in the C. elegans nervous system and shares a conserved domain with many mammalian proteins. Cell *84*, 115-125.

Kohler, M., Hirschberg, B., Bond, C.T., Kinzie, J.M., Marrion, N.V., Maylie, J., and Adelman, J.P. (1996). Small-Conductance, Calcium-Activated Potassium Channels from Mammalian Brain. Science *273*, 1709-1714.

Kohler, R., and Hoyer, J. (2007). The endothelium-derived hyperpolarizing factor: insights from genetic animal models. Kidney Int *72*, 145-150.

Kupershmidt, S., Yang, I.C., Hayashi, K., Wei, J., Chanthaphaychith, S., Petersen, C.I., Johns, D.C., George, A.L., Jr., Roden, D.M., and Balser, J.R. (2003). The IKr drug response is modulated by KCR1 in transfected cardiac and noncardiac cell lines. FASEB J *17*, 2263-2265.

Kyte, J., and Doolittle, R.F. (1982). A simple method for displaying the hydropathic character of a protein. Journal of molecular biology *157*, 105-132.

Larkin, M.A., Blackshields, G., Brown, N.P., Chenna, R., McGettigan, P.A., McWilliam, H., Valentin, F., Wallace, I.M., Wilm, A., Lopez, R.*, et al.* (2007). Clustal W and Clustal X version 2.0. Bioinformatics *23*, 2947-2948.

Larsen, P.L., Albert, P.S., and Riddle, D.L. (1995). Genes that Regulate Both Development and Longevity in Caenorhabditis elegans. Genetics *139*.

Ledoux, J., Werner, M.E., Brayden, J.E., and Nelson, M.T. (2006). Calcium-activated potassium channels and the regulation of vascular tone. Physiology (Bethesda) *21*, 69-78.

Lin, M.T., Lujan, R., Watanabe, M., Adelman, J.P., and Maylie, J. (2008). SK2 channel plasticity contributes to LTP at Schaffer collateral-CA1 synapses. Nature neuroscience *11*, 170-177.

Littleton, J.T., and Ganetzky, B. (2000). Ion Channels and Synaptic Organization. Neuron *26*, 35-43.

Lu, Z. (2004). Mechanism of rectification in inward-rectifier K+ channels. Annual review of physiology *66*, 103-129.

Ma, Z., Lou, X.J., and Horrigan, F.T. (2006). Role of charged residues in the S1-S4 voltage sensor of BK channels. J Gen Physiol *127*, 309-328.

Mello, C., and Fire, A. (1995). DNA transformation. Methods Cell Biol *48*, 451-482.

Mello, C.C., Kramer, J.M., Stinchcomb, D., and Ambros, V. (1991). Efficient gene transfer in C.elegans: extrachromosomal maintenance and integration of transforming sequences. EMBO J *10*, 3959-3970.

Mendel, J.E., Korswagen, H.C., Liu, K.S., Hajdu-Cronin, Y.M., Simon, M.I., Plasterk, R.H., and Sternberg, P.W. (1995). Participation of the protein Go in multiple aspects of behavior in C. elegans. Science *267*, 1652-1655.

Miller, M.J., Rauer, H., Tomita, H., Gargus, J.J., Gutman, G.A., Cahalan, M.D., and Chandy, K.G. (2001). Nuclear localization and dominant-negative suppression by a mutant SKCa3 N-terminal channel fragment identified in a patient with schizophrenia. The Journal of biological chemistry *276*, 27753-27756.

Moresco, J.J., and Koelle, M.R. (2004). Activation of EGL-47, a Galpha(o)-coupled receptor, inhibits function of hermaphrodite-specific motor neurons to regulate Caenorhabditis elegans egg-laying behavior. The Journal of neuroscience : the official journal of the Society for Neuroscience *24*, 8522-8530.

Nehrke, K., and Melvin, J.E. (2002). The NHX family of Na+-H+ exchangers in Caenorhabditis elegans. The Journal of biological chemistry *277*, 29036-29044.

Ngo-Anh, T.J., Bloodgood, B.L., Lin, M., Sabatini, B.L., Maylie, J., and Adelman, J.P. (2005). SK channels and NMDA receptors form a Ca2+-mediated feedback loop in dendritic spines. Nature neuroscience *8*, 642-649.

Noble, K., Floyd, R., Shmygol, A., Shmygol, A., Mobasheri, A., and Wray, S. (2010). Distribution, expression and functional effects of small conductance Ca-activated potassium (SK) channels in rat myometrium. Cell Calcium *47*, 47-54.

Papazian, D., Schwarz, T., Tempel, B., Jan, Y., and Jan, L. (1987). Cloning of genomic and complementary DNA from Shaker, a putative potassium channel gene from Drosophila. Science *237*, 749-753.

Papazian, D.M., and Bezanilla, F. (1997). How does an ion channel sense voltage? . News Physiol Sci *12*.

Papazian, D.M., Timpe, L.C., Jan, Y.N., and Jan, L.Y. (1991). Alteration of voltage-dependence of Shaker potassium channel by mutations in the S4 sequence. Nature *349*, 305-310.

Park, K.H., and Sesti, F. (2007). An arrhythmia susceptibility gene in Caenorhabditis elegans. The Journal of biological chemistry *282*, 19799-19807.

Pedarzani, P., and Stocker, M. (2008). Molecular and cellular basis of small--and intermediate-conductance, calcium-activated potassium channel function in the brain. Cell Mol Life Sci *65*, 3196-3217.

Petersen, C.I., McFarland, T.R., Stepanovic, S.Z., Yang, P., Reiner, D.J., Hayashi, K., George, A.L., Roden, D.M., Thomas, J.H., and Balser, J.R. (2004). In vivo identification of genes that modify ether-a-go-go-related gene activity in Caenorhabditis elegans may also affect human cardiac arrhythmia. Proceedings of the National Academy of Sciences of the United States of America *101*, 11773-11778.

Ringstad, N., and Horvitz, H.R. (2008). FMRFamide neuropeptides and acetylcholine synergistically inhibit egg-laying by C. elegans. Nature neuroscience *11*, 1168-1176.

Salkoff, L., Kunkel, M.T., Wang, Z., Butler, A., Yuan, A., Nonet, M., and Wei, A. (1998). The impact of the C. elegans genome sequencing project on K+ channel biology, Vol 46 (Function Potassium Channels: Molecular Structure, and Diseases. Current Topics in Membranes).

Salkoff, L., Wei, A.D., Baban, B., Butler, A., Fawcett, G., Ferreira, G., and Santi, C.M. (2005). Potassium channels in C. elegans. WormBook, 1-15.

Sanguinetti, M.C., Curran, M.E., Zou, A., Shen, J., Spector, P.S., Atkinson, D.L., and Keating, M.T. (1996). Coassembly of K(V)LQT1 and minK (IsK) proteins to form cardiac I(Ks) potassium channel. Nature *384*, 80-83.

Sawin, E.R. (1996). Genetic and cellular analysis of modulated behaviors in Caenorhabditis elegans. PhD Thesis, Massachusetts Institute of Technology.

Schulte, U., Hahn, H., Konrad, M., Jeck, N., Derst, C., Wild, K., Weidemann, S., Ruppersberg, J.P., Fakler, B., and Ludwig, J. (1999). pH gating of ROMK (Kir1.1) channels: Control by an Arg-Lys-Arg triad disrupted in antenatal Bartter syndrome. Proceedings of the National Academy of Sciences of the United States of America *96*.

Schulte, U., Thumfart, J.O., Klocker, N., Sailer, C.A., Bildl, W., Biniossek, M., Dehn, D., Deller, T., Eble, S., Abbass, K.*, et al.* (2006). The epilepsy-linked Lgi1 protein assembles into presynaptic Kv1 channels and inhibits inactivation by Kvbeta1. Neuron *49*, 697-706.

Schumacher, M.A., Rivard, A.F., Bachinger, H.P., and Adelman, J.P. (2001). Structure of the gating domain of a Ca2+-activated K+ channel complexed with Ca2+/calmodulin. Nature *410*, 1120-1124.

Schuske, K., Beg, A.A., and Jorgensen, E.M. (2004). The GABA nervous system in C. elegans. Trends Neurosci *27*, 407-414.

Schwarz, J.R., and Bauer, C.K. (2004). Functions of erg K+channels in excitable cells. Journal of Cellular and Molecular Medicine *8*, 22-30.

Seebohm, G., Strutz-Seebohm, N., Ureche, O.N., Henrion, U., Baltaev, R., Mack, A.F., Korniychuk, G., Steinke, K., Tapken, D., Pfeufer, A.*, et al.* (2008). Long QT syndrome-

associated mutations in KCNQ1 and KCNE1 subunits disrupt normal endosomal recycling of IKs channels. Circulation research *103*, 1451-1457.

Segalat, L., Elkes, D.A., and Kaplan, J.M. (1995). Modulation of serotonin-controlled behaviors by Go in Caenorhabditis elegans. Science *267*, 1648-1651.

Shakkottai, V.G., Chou, C., Oddo, S., Sailer, C.A., Knaus, H., Gutman, G.A., Barish, M.E., LaFerla, F.M., and Chandy, K.G. (2004). Enhanced neuronal excitability in the absence of neurodegeneration induces cerebellar ataxia. Journal of Clinical Investigation *113*, 582-590.

Shieh, C.C., Coghlan, M., Sullivan, J.P., and Gopalakrishnan, M. (2000). Potassium channels: molecular defects, diseases, and therapeutic opportunities. Pharmacol Rev *52*, 557-594.

Shtonda, B., and Avery, L. (2005). CCA-1, EGL-19 and EXP-2 currents shape action potentials in the Caenorhabditis elegans pharynx. J Exp Biol *208*, 2177-2190.

Simmer, F., Tijsterman, M., Parrish, S., Koushika, S.P., Nonet, M.L., Fire, A., Ahringer, J., and Plasterk, R.H. (2002). Loss of the putative RNA-directed RNA polymerase RRF-3 makes C. elegans hypersensitive to RNAi. Current biology : CB *12*, 1317-1319.

Singh, B., Ogiwara, I., Kaneda, M., Tokonami, N., Mazaki, E., Baba, K., Matsuda, K., Inoue, Y., and Yamakawa, K. (2006). A Kv4.2 truncation mutation in a patient with temporal lobe epilepsy. Neurobiol Dis *24*, 245-253.

Singson, A., Mercer, K.B., and L'Hernault, S.W. (1998). Transmembrane Protein that Contains EGF-like Repeats and Is Required for Fertilization. Cell *93*.

Splawski, I., Shen, J., Timothy, K.W., Lehmann, M.H., Priori, S., Robinson, J.L., Moss, A.J., Schwartz, P.J., Towbin, J.A., Vincent, G.M.*, et al.* (2000). Spectrum of mutations in long-QT syndrome genes. KVLQT1, HERG, SCN5A, KCNE1, and KCNE2. Circulation *102*, 1178-1185.

Stocker, M., Hirzel, K., D'Hoedt, D., and Pedarzani, P. (2004). Matching molecules to function: neuronal Ca2+-activated K+ channels and afterhyperpolarizations. Toxicon *43*, 933-949.

Stocker, M., Krause, M., and Pedarzani, P. (1999). An apamin-sensitive Ca2+-activated K+ current in hippocampal pyramidal neurons. Proceedings of the National Academy of Sciences of the United States of America *96*, 4662-4667.

Strobaek, D., Teuber, L., Jorgensen, T.D., Ahring, P.K., Kjaer, K., Hansen, R.S., Olesen, S.P., Christophersen, P., and Skaaning-Jensen, B. (2004). Activation of human IK and SK Ca2+ -activated K+ channels by NS309 (6,7-dichloro-1H-indole-2,3-dione 3-oxime). Biochim Biophys Acta *1665*, 1-5.

Sulston, J.E., Schierenberg, E., White, J.G., and Thomson, J.N. (1983). The embryonic cell lineage of the nematode Caenorhabditis elegans. Dev Biol *100*, 64-119.

Syme, C.A., Gerlach, A.C., Singh, A.K., and Devor, D.C. (2000). Pharmacological activation of cloned intermediate- and small-conductance Ca2+-activated K+channels. Am J Physiol Cell Physiol *278*.

Szatanik, M., Vibert, N., Vassias, I., Guenet, J.L., Eugene, D., de Waele, C., and Jaubert, J. (2008). Behavioral effects of a deletion in Kcnn2, the gene encoding the SK2 subunit of small-conductance Ca2+-activated K+ channels. Neurogenetics *9*, 237-248.

Tabara, H. (1998). REVERSE GENETICS:RNAi in C. elegans: Soaking in the Genome Sequence. Science *282*, 430-431.

Taylor, M.S., Bonev, A.D., Gross, T.P., Eckman, D.M., Brayden, J.E., Bond, C.T., Adelman, J.P., and Nelson, M.T. (2003). Altered expression of small-conductance Ca2+-activated K+ (SK3) channels modulates arterial tone and blood pressure. Circulation research *93*, 124-131.

Thomas, J.H. (1990). Genetic analysis of defecation in Caenorhabditis elegans. Genetics *124*, 855-872.

Thorneloe, K.S., Knorn, A.M., Doetsch, P.E., Lashinger, E.S., Liu, A.X., Bond, C.T., Adelman, J.P., and Nelson, M.T. (2008). Small-conductance, Ca(2+) -activated K+ channel 2 is the key functional component of SK channels in mouse urinary bladder. American journal of physiology Regulatory, integrative and comparative physiology *294*, R1737-1743.

Tiwari-Woodruff, S.K., Lin, M.A., Schulteis, C.T., and Papazian, D.M. (2000). Voltage-dependent structural interactions in the Shaker K(+) channel. J Gen Physiol *115*, 123-138.

Tiwari-Woodruff, S.K., Schulteis, C.T., Mock, A.F., and Papazian, D.M. (1997). Electrostatic interactions between transmembrane segments mediate folding of Shaker K+ channel subunits. Biophys J *17*.

Tomita, H., Shakkottai, V.G., Gutman, G.A., Sun, G., Bunney, W.E., Cahalan, M.D., Chandy, K.G., and Gargus, J.J. (2003). Novel truncated isoform of SK3 potassium channel is a potent dominant-negative regulator of SK currents: implications in schizophrenia. Mol Psychiatry *8*, 524-535, 460.

Trudeau, M., Warmke, J., Ganetzky, B., and Robertson, G. (1995). HERG, a human inward rectifier in the voltage-gated potassium channel family. Science *269*, 92-95.

Walter, J.T., Alvina, K., Womack, M.D., Chevez, C., and Khodakhah, K. (2006). Decreases in the precision of Purkinje cell pacemaking cause cerebellar dysfunction and ataxia. Nature neuroscience *9*, 389-397.

Wang, Z.W., Saifee, O., Nonet, M.L., and Salkoff, L. (2001). SLO-1 potassium channels control quantal content of neurotransmitter release at the C. elegans neuromuscular junction. Neuron *32*.

Warmke, J., Drysdale, R., and Ganetzky, B. (1991). A distinct potassium channel polypeptide encoded by the Drosophila eag locus. Science *252*.

Waters, M.F., Minassian, N.A., Stevanin, G., Figueroa, K.P., Bannister, J.P., Nolte, D., Mock, A.F., Evidente, V.G., Fee, D.B., Muller, U.*, et al.* (2006). Mutations in voltage-gated potassium channel KCNC3 cause degenerative and developmental central nervous system phenotypes. Nat Genet *38*, 447-451.

Wei, A., Jegla, T., and Salkoff, L. (1996). Eight potassium channel families revealed by the C. elegans genome project. Neuropharmacology *35*, 805-829.

Wei, A.D., Butler, A., and Salkoff, L. (2005). KCNQ-like potassium channels in Caenorhabditis elegans. Conserved properties and modulation. The Journal of biological chemistry *280*, 21337-21345.

Weinshenker, D., Wei, A., Salkoff, L., and Thomas, J.H. (1999). Block of an ether-a-go-go-like K(+) channel by imipramine rescues egl-2 excitation defects in Caenorhabditis elegans. The Journal of neuroscience : the official journal of the Society for Neuroscience *19*, 9831-9840.

White, J.G., Southgate, E., Thompson, J.N., and Brenner, S. (1986a). The structure of the nervous system of the nematode Caenrhabditis elegans. Philos Trans R Soc Lond B Biol Sci *314*, 1.

White, J.G., Southgate, E., Thomson, J.N., and Brenner, S. (1986b). The structure of the nervous system of the nematode Caenorhabditis elegans. Philos Trans R Soc Lond B Biol Sci *314*, 1-340.

Wilson, G.F. (1998). Interaction of the K Channel beta Subunit, Hyperkinetic, with eag Family Members. Journal of Biological Chemistry *273*, 6389-6394.

Wolfart , J., Neuhoff, H., Franz, O., and J, R. (2001). Differential Expression of the Small-Conductance, Calcium-Activated Potassium Channel SK3 Is Critical for Pacemaker Control in Dopaminergic Midbrain Neurons. J Neurosci *21*.

Wulff, H., Castle, N.A., and Pardo, L.A. (2009). Voltage-gated potassium channels as therapeutic targets. Nat Rev Drug Discov *8*, 982-1001.

Xia, X.M., Fakler, B., Rivard, A., Wayman, G., Johnson-Pais, T., Keen, J.E., Ishii, T., Hirschberg, B., Bond, C.T., Lutsenko, S.*, et al.* (1998). Mechanism of calcium gating in small-conductance calcium-activated potassium channels. Nature *395*, 503-507.

Yuan, A., Dourado, M., Butler, A., Walton, N., Wei, A., and Salkoff, L. (2000). SLO-2, a K+ channel with an unusual Cl- dependence. Nature neuroscience *3*, 771-779.

Yuan, A., Santi, C.M., Wei, A., Wang, Z.W., Pollak, K., Nonet, M., Kaczmarek, L., Crowder, C.M., and Salkoff, L. (2003). The Sodium-Activated Potassium Channel Is Encoded by a Member of the Slo Gene Family. Neuron *37*.

Zhang, M., Chung, S.H., Fang-Yen, C., Craig, C., Kerr, R.A., Suzuki, H., Samuel, A.D., Mazur, E., and Schafer, W.R. (2008). A self-regulating feed-forward circuit controlling C. elegans egg-laying behavior. Current biology : CB *18*, 1445-1455.

Zuberi, S.M. (1999). A novel mutation in the human voltage-gated potassium channel gene (Kv1.1) associates with episodic ataxia type 1 and sometimes with partial epilepsy. Brain *122*, 817-825.